WARRIP

WESTERN AUSTRALIAN ROAD RESEARCH & INNOVATION PROGRAM

An initiative by: mainroads WESTERN AUSTRALIA NTRO

Improving pavement deflection bowl predictions from Traffic Speed Deflectometer (TSD) measured responses to load – Stage 1

Author: Atteeq Ur-Rehman, Richard Wix

June 2025

Final Report

Version Control

Report version no.	Date	Released to client by	Nature of revision
1	27/10/2025	Desiree Hamann	Final report for publication.

Summary

A Traffic Speed Deflectometer (TSD) measures pavement deflection at traffic speed. It uses doppler lasers to measure deflections indirectly based on deflection velocity. The existing pavement strength and in the future back-calculation of layer and subgrade moduli are based on deflection bowl shape parameters. It is important to compare TSD bowl shape characteristics with falling weight deflectometer (FWD).

The aim of WARRIP 2022-002 project was to develop an improved understanding of the deflection bowl predictions derived from TSD measurements using additional lasers to enable reliable estimates of pavement layer and subgrade moduli.

National Transport Research Organisation's (NTRO's) TSD iPAVE2 (old iPAVE) is fitted with seven lasers in front of rear axle with no lasers between 900 and 3500 mm. The new iPAVE3 is fitted with eleven lasers including 3 lasers in the back of rear axle and a laser at 1500 mm. This arrangement provides an opportunity to develop full bowl shape from TSD measurements. Three test sections were selected in Queensland with different pavement configurations comprising two thick asphalt surfaced granular pavements and a sprayed seal surfaced granular pavement. TSD and FWD surface deflections and pavement investigation data were collected from the sites in three episodes from April 2023 to April 2024.

The data analysis concluded that TSD deflection data indicate high level of repeatability for all 3 test sections. A comparison of iPAVE3 maximum deflection (D_0) values on the OWP and IWP show higher deflection on the IWP at on one of the three test sections which is not in line with the prevailing assumption among pavement engineers that the OWP deflections are generally higher and should be used to determine the adequacy for pavement structural strength. FWD data also show the similar trends (higher deflections on IWP). This finding highlights the need of incorporating deflections from both wheel paths (OWP& IWP) for improved pavement assessment.

Previous research findings indicate that the deflection measurements from TSD and FWD do not always show high correlation mainly due to different deflection measurement mechanisms of both devices. The data analysis as part of this project from 3 test sections indicate that the TSD maximum deflection (D_0) values are lower than the FWD deflection values. However, TSD and FWD deflection data show similar pavement strength trends. For curvature results, all sites showed a good repeatability between the individual iPAVE runs. In general, there was a high correlation between the TSD and FWD curvature values in both wheel paths at all trial sites. However, the full depth asphalt pavement (Section 1) showed much lower curvature values.

There is generally a good agreement between curvature results that were measured in April 2023 and 2024 at all 3 sites. However, the curvature values measured in December 2023 were higher on the 2 asphalt surfaced Ipswich-Rosewood Road sections possibly due to wet season during this period.

NTRO's iPAVE3 has 3 additional lasers behind the rear axle enabling it modelling the full deflection instead of assuming the zero deflection velocity directly under the load. Using the full bowl typically results in larger D_0 values which subsequently results in larger curvature values (as D_{200} is essentially the same). The comparison of curvature values calculated by using values behind the load (iPAVE3) and only forward sensors (iPAVE2) processing algorithm. In all 3 sites, curvature values with full bowl measurements were higher than the curvature values determined by excluding rear sensors. Further analysis of iPAVE3 data of this type is recommended so that a reliable method of adjusting between iPAVE3 and iPAVE2 Do values is derived.

In a nutshell, the TSD is relatively a new technology and use of TSD measured deflection data needs more improvement in its utilisation for pavement structural evaluation and rehabilitation design. Austroads (2021) highlighted future research directions for maximising the use of TSD deflection data in back-calculation of pavement layer and subgrade moduli. In Australasia, methods have been developed to predict equivalent FWD maximum deflections and implemented those in the design of granular overlays using the emperical approach (Austroads 2019b). There is a need to develop a method to estimate pavement and subgrade moduli from TSD deflections to assist in the design of a wider range of treatments.

Contents

Tables

Figures

1 Introduction

1.1 Background

Traffic Speed Deflectometer (TSD) is a commercially available device capable of measuring pavement deflection at traffic speed. The TSD uses doppler lasers to measure deflection indirectly based on deflection velocity.

The National Transport Research Organisation (NTRO) Intelligent Pavement Assessment Vehicle iPAVE2 is a TSD fitted with seven lasers (old vehicle) and the more recent iPAVE3 has eleven lasers to collect deflection data .

There are different ways of analysing velocity data measured by the TSD. As existing pavement strength and back-calculation of layer and subgrade moduli are based on bowl shape parameters, it is important to compare TSD bowl shape characteristics with those measured by traditional deflection devices (e.g. Falling Weight Deflectometer (FWD)). Recent Austroads research (e.g. AP-T350-19) highlighted that the derived iPAVE2 bowl away from the loading axle is not closely correlated with that of a FWD deflection bowl. This deviation can be attributed to the number and location of iPAVE2 measurement lasers .

1.2 Aim of the Project

The aim of the project (WARRIP 2022-002) was to develop an improved understanding of the deflection bowl predictions derived from iPAVE3 measurements due to the additional lasers . Reliable deflection bowl predictions are necessary for future methods of back-calculating pavement layer and subgrade modulus.

1.3 Structure of the Report

This report presents the findings of the investigations carried out as a part of WARRIP Project 2022-002 in relation to the pavement deflection bowl predictions from TSD measured responses to load.

The structure and contents of the report are as follows:

- Section 1 provides an overview of the project background and aim.
- Section 2 details the literature review of TSD deflection measurement and deflection bowl estimation.
- Section 3 covers the field trials data collection.
- Section 4 provides pavement and geotechnical interpretations
- Section 5 discusses the data analysis and interpretations
- Section 6 outlines the key findings and conclusions.
- Section 7 suggests future research direction.

2 Literature Review

This chapter summarises the literature review of the use of traffic speed deflectometer (TSD) data for pavement structural evaluation. It should be noted that the literature review is limited in scope to deflection bowl characteristics, TSD measurements correlation with FWD and back-calculation of pavement layer and subgrade moduli.

2.1 Pavement Surface Deflections

For many years, pavement surface deflections have been used to assess the structural adequacy of pavements and to design pavement strengthening treatments.

The shape of the deflection bowl is characterised by the deflection at various offsets along the pavement from the origin of the centre of the rear axle load. Figure 2.1shows a typical shape of pavement deflection bowl.

Figure 2.1 Pavement deflection bowl under applied load (Source: Austroads 2015)

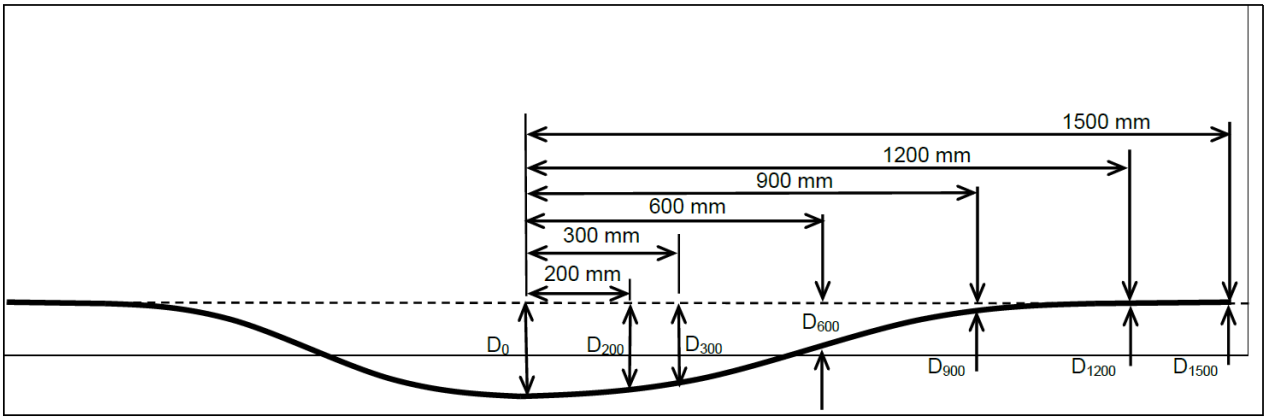

The shape of the deflection bowl is influenced by the strength of the pavement. Austroads (2013) reported that the maximum central surface deflection (D_0) has traditionally been used as an estimate of the current available pavement strength including subgrade contribution. The D_0 measurement is often compared to a design deflection value which depends on the design traffic over the design period. It is an important bowl parameter in the design of pavement rehabilitation treatments such as granular or asphalt overlays (Austroads 2019).

Deflection measurements other than D_0 can provide additional information. In Australia ($D_0 – D_{200}$) is used to measure the pavement ability to resist asphalt fatigue (Austroads 2019) and D_0, D_{200} and D_{300} are key locations required when reporting network-level strength data (Austroads 2015). In addition, SCISUB (D_{900}-D_{1500}) may be of interest as it is likely to be correlated with the modulus of the top of subgrade.

2.2 TSD Mechanism

The traffic speed deflectometer (TSD) is used to monitor the condition of the pavement in terms of deflection. It is a rolling wheel deflectometer for measuring pavement deflections at the network level.

The TSD comprises of a truck with a 10 tonne load applied on the rear, dual-tyred single axle. The downwards velocity of the deflected pavement surface under this load is measured using doppler

laser sensors aligned in a single wheel path and positioned at different offsets from the centre of the load. These lasers are mounted at an angle of ~ 2° from vertical to avoid the variable vertical suspension movement of the trailer in order to achieve a relatively constant velocity input arising from a component of the vehicle driving speed (Austroads 2012a).

The iPAVE2 is equipped with seven doppler lasers to assess the deflection in the outer wheel-path. These lasers are located in front of the rear axle of the TSD trailer. Six sensors are positioned longitudinally at 100, 200, 300, 450, 600 and 900 mm from the axis of load. The remaining sensor is located at 3500 mm from the axle load where pavement surface velocity is assumed to be zero (Austroads 2021).

Figure 2.2 shows a schematic view of the TSD with seven sensors and Figure 2.3 illustrates how TSD works.

Figure 2.2 Schematic view of the iPAVE2 (Source: Austroads 2021)

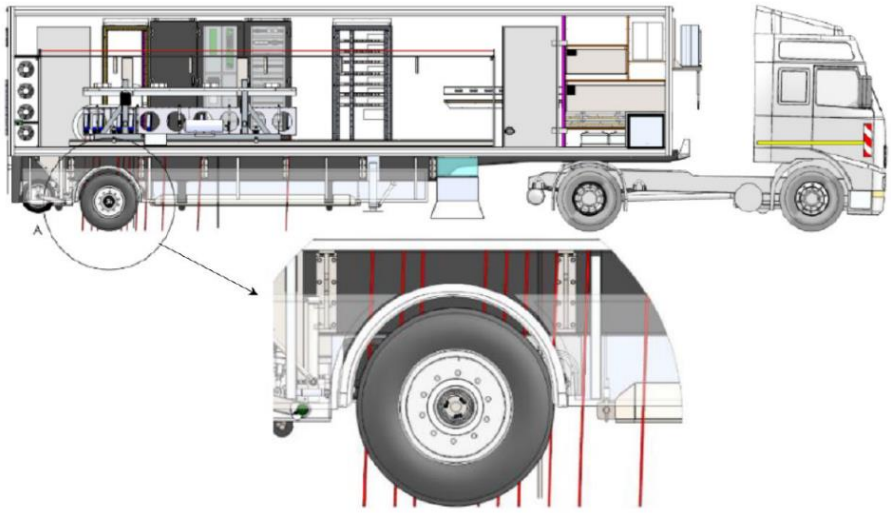

Figure 2.3 Illustration of the TSD (Source: Austroads 2012a, after Baltzer 2009)

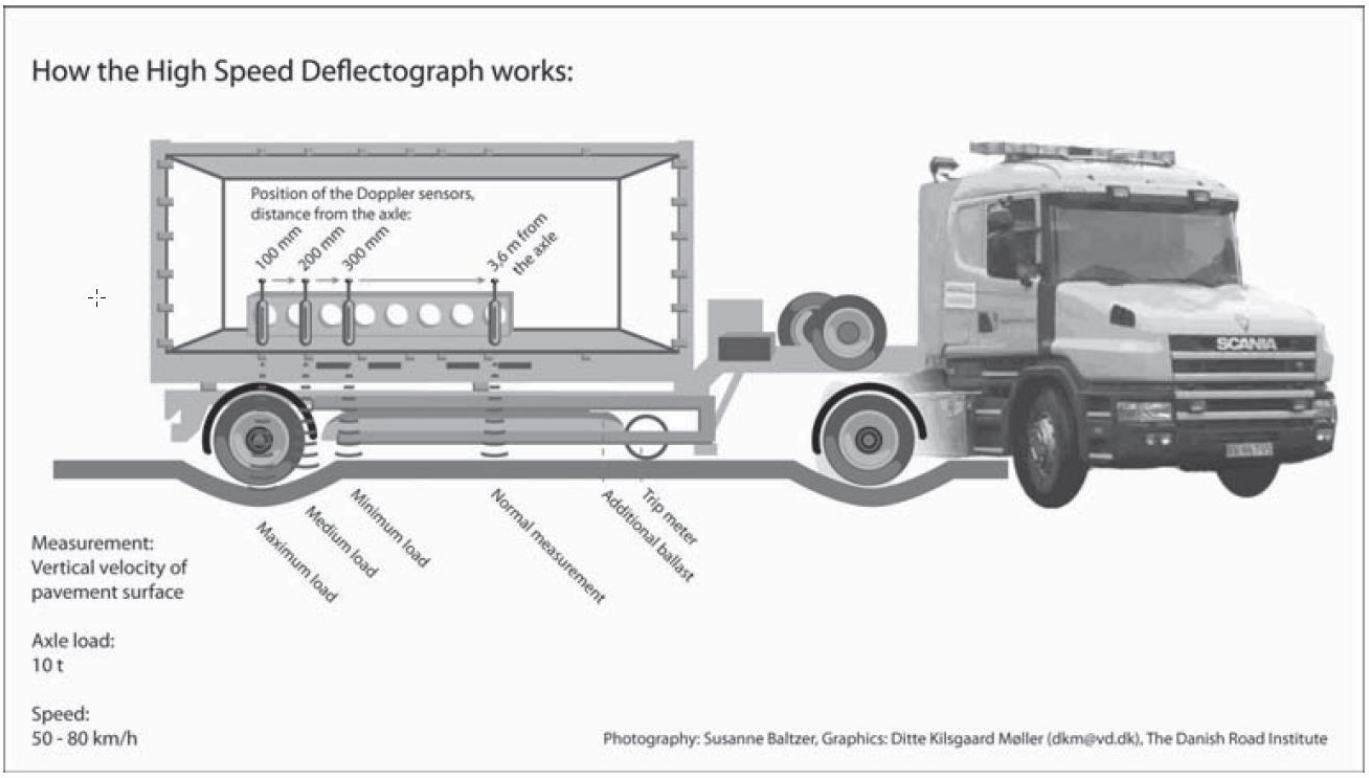

ARRB's new iPAVE3 is fitted with eleven sensors including eight doppler lasers in front of rear axle (at 110, 210, 310, 610, 910, 1160, 1510, 3060 mm) and three at the behind the rear axle (at 110, 210, 310 mm).

Besides laser systems, the TSD is equipped with an inertial unit (consisting of gyroscopes and accelerometers), an odometer (encoder), an accelerometer, temperature gauges and a GPS system. The collected data is treated in a specialised TSD post-processing software program which outputs base level data such as pavement velocity as well as processed pavement condition indicators (Austroads 2012a).

2.3 Estimating Deflection Bowls from TSD Measured Responses

In TSD measurements, pavement surface deflection is calculated from surface velocity using different methods such as:

- The processing method supplied by the manufacturer based on research by Pedersen (2013).
- Determining the deflection history at a particular location in a pavement as a function of time and employing a specific function for the slope versus sensor locations vector at each TSD measurement points (Zofka et al. 2014).
- Calculating deflection from surface velocity based on Rasmussen et al. 2008.
- In Australia, pavement deflection is calculated using integration technique developed by Muller and Roberts (2013). This technique is based on the area under the curve (AUTC). A tail-taming method was added to the original AUTC algorithm which limits the slope for the sensor at 900 mm to a maximum of two-thirds of the slope at 600 mm. This process eliminates the possibility of a flat or bulged curve (from 900 to 3500 mm) and produces a more tapered typical deflection curve all the way out to the 3500 mm position (Wix, Murnane & Moffatt 2016).

Austroads (2012a) provides details around the TSD mechanism and configuration in Australia and other TSD vehicles. These details are summarised in Table 2.1.

Table 2.1: Summary of TSD mechanism, data interpretation, testing and evaluation

Element	Details[1,2]
Configuration in Australia	
Load level	- Standard operation load is 10 tonnes - Can be reduced to 7.5 tonnes via removal of the ballast material
Sensor location	100 mm, 200 mm, 300 and 3600 mm (typical old configuration) (In UK TRL relocated 200 mm mounted laser to 750 mm in front of rear axle to explore the structural contribution from the lower pavement layer) In Australia: - iPAVE2 is equipped with seven lasers at 100, 200, 300, 450, 600, 900 and 3500 mm New iPAVE3 is equipped with eleven lasers including eight doppler lasers in front of rear axle (110, 210, 310, 610, 910, 1160, 1510, 3060 mm) and three at the behind the rear axle (110, 210, 310 mm).
Data streams	Vertical velocity (Vv), horizontal velocity (Vh) and slope (Vv/Vh) are provided for each sensor location
Laser angle	2° from vertical (to allow a constant velocity input from horizontal vehicle speed while having little effect on the vertical speed component).
Operating speed	TSD operated reliably at 80 km/h (min. operating speed 40 km/h)
Data interpretation	
Data characteristics	- Continuous data streams - For each 0.02 m travelled the system provides deflection velocity information that compares to a resolution of 5 µm - 1000 data samples are recorded per second per sensor
Surface curvature index (SCI)	- Danish use of TSD has focused on the estimation of SCI_{300} ($D_0 – D_{300}$) - Australian practice is based on curvature function (CF) ($D_0 – D_{200}$)
Slope	- Slope of the deflection bowl from TSD laser data is calculated as illustrated in the figure on the right: 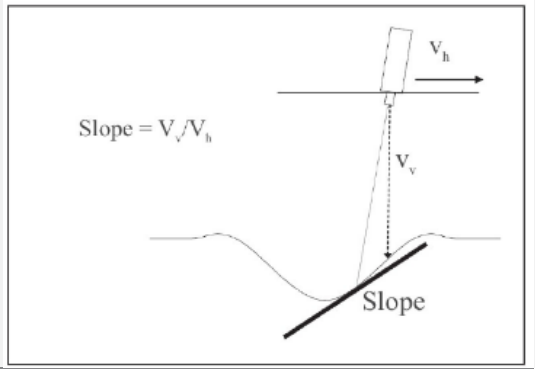
Maximum deflection (D_0)	- Traditional deflection measuring devices routinely produce a value of maximum deflection (D_0) located directly below the applied load. Unlike FWD, deflectograph and Benkelman Beam, the TSD cannot measure maximum deflection as the location at which maximum deflection occurs must have zero vertical velocity. However, with the tight array of doppler lasers near the centre of maximum deflection provides an estimate of the shape of the seat of deflection bowl. According to Baltzer (2009), TSD data from various laser positions can be interpreted to derive a very accurate shape of the seat of the deflection bowl.
Factors affecting repeatability	
Temperature	Temperature variations influence the measurement equipment and hence the measured pavement response: - At low ambient temperatures, data rate and deflection slope were found to decrease. - As lasers heated up, they were causing temperature gradient of up to 4 °C in the measurement beam which were sufficient to cause recorded differences in deflection slope by distorted the measurement beam. - Modulus of asphalt is dependent upon its temperature. Higher the temperature, the lower the modulus and higher the deflections.
Vehicle testing speed	- Early testing of UK TSD gave comparable results at different speeds (60, 70, 80 km/h)

Element	Details[1,2]
	- Asphalt modulus is dependent upon the speed of loading with the modulus increasing with loading speeds. - The effect on surface deflection caused by changes in asphalt modulus depends on thickness of the asphalt in the tested pavement. - This figure shows the pavement response variation with speed measured in the UK. 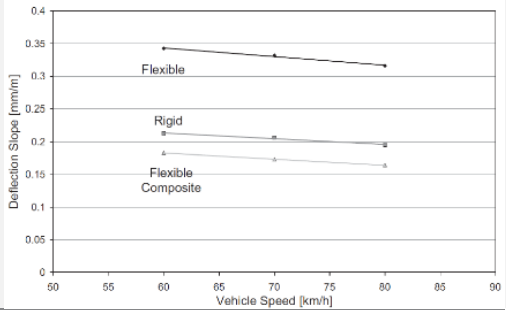
Effect of axle load	The magnitude of the load applied to the pavement is known to influence both the maximum deflection and the shape of the deflection bowl. However, there is no measured TSD data available about the influence of the load magnitude on deflection.
Pavement (strong vs weak)	Evaluation of TSD devices and studies indicate that TSD is able to differentiate between different asphalt pavement structures. It should be noted that the majority of testing has been carried out on asphalt pavements and these conclusions do not necessarily translatable to the wide range of thin bituminous surfaced granular pavements that comprise the bulk of Australian pavements.
Road surface characteristics	Performance of TSD is influenced by the road surface e.g. colour, wetness, texture and roughness: - System performs better on light coloured surfaces (e.g. concrete) and least well on new. bituminous/asphalt surfaces. - Damp roads yield lower data rate than dry surfaces.

Source: Adapted from Austroads (2012a).

Notes

1. The information presented in Table 2.1 represents the status of TSD technology as of January 2010.
2. As TSD is a newly developed technology (first prototype vehicle developed in 2004), publicly available information related to its performance and operation is limited.

Austroads (2013) also described the integration approach to TSD analysis based on numerical integration of a curve fit of TSD slope measurements versus load offset distance. Assuming that the TSD slope at the wheel load and at a point significantly distant from the load the slope are both zero, simple numerical integration of a curve fitted through the TSD measurement points between these limits, working towards the wheel load, enables the full deflection bowl to be determined. Integrating over the entire plot can accurately determine the maximum deflection (D_0). It should be noted that the precision of this technique depends on the number and position of TSD slope measurements and the type of curve fitting used. TSD deflections calculated in this way from deflections measured in Queensland (Austroads 213) were compared to approximately 600 FWD bowls collected at seven test sites in Queensland and the results looked very promising.

Muller & Roberts (2013) described the revised approach to determine the deflection measurements from the vertical pavement velocity collected by doppler lasers. The method fits a curve through a plot of surface slopes measured by the TSD versus wheel offset. However, the deflection profile is built up by numerically integrating this plot working from a fixed point at or beyond the edge of the deflection bowl towards the wheel load. The direction of integration and use of numerical methods are simple but are important departures from previous approaches because building up the deflection bowl in this way highlights the contribution of velocity measurements further from the wheel to both the shape of the deflection bowl tail and the accuracy of maximum deflection prediction.

Wix, Murnane & Moffatt (2016) also described the tail-taming process which is used to improve the quality of the TSD data. The tail of the deflection bowl is defined as being from the 900 mm laser out to where the pavement deflection velocity is assumed to be zero which is at the 3500 mm position. There are no sensors within the tail and very small fluctuations in readings can naturally occur in this area. The AUTC algorithm fits a curve through all deflection slope values and if the

900 mm result is similar or close to the 600 mm value, it will result in a flatter, less tapered curve all the way out to the 3500 mm position. Due to the relatively large distance between the 900 mm to 3500 mm lasers, a small increase in the 900 mm result can cause a significant increase in the area under the graph, and a significant variance in the resultant deflection measurement. Limiting the magnitude of the 900 mm deflection slope value to no more than two-thirds of the value at the 600 mm laser eliminates the possibility of a flat or bulged curve (from 900 mm to 3500 mm) and produces a more tapered typical deflection curve. If the difference is greater, the tail is cut off and excluded from the analysis to generate more realistic values.

2.4 Comparison of TSD with FWD Deflection Measurements

In TSD and FWD measurements, different forms of loads and pavement responses are used. FWD measures true deflection with geophones in the form of displacement of the pavement as a result of load applied through a stationary plate whereas TSD deflections are integrated from velocity with doppler lasers caused by a moving load. TSD measurements are carried out at short intervals with dynamic load and are highly representative of actual traffic loading.

Figure 2.4 shows load application principles of FWD and TSD devices.

Figure 2.4 Falling Weight Deflectometer (FWD) profile (left) and Traffic Speed Deflectometer (TSD) profile (right) (Source: NZTA 2016)

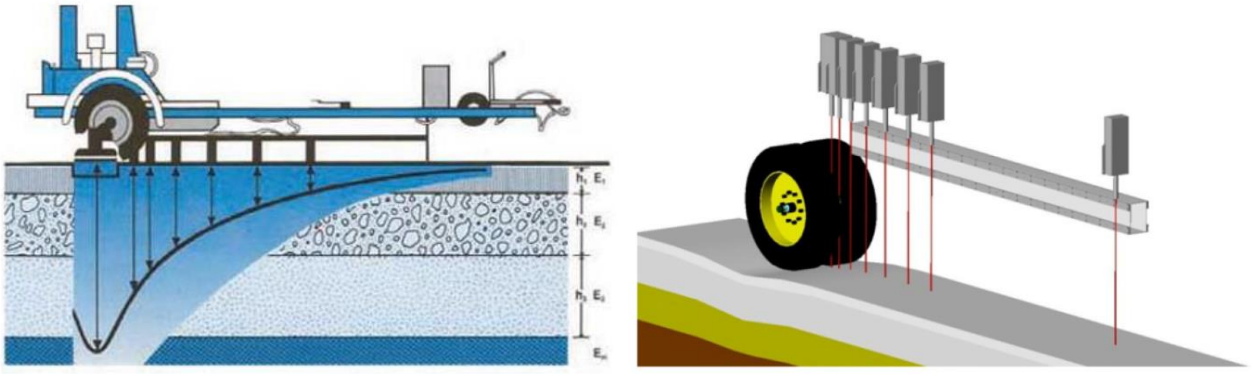

Accordingly there are two broad approaches to pavement deflection measurement

- measuring the transient vertical displacement due to rolling wheel using a test apparatus that moves along with the wheel (e.g. TSD) and
- measuring a vertical displacement at a fixed point on the ground resulting from a real or simulated wheel load (e.g. FWD).

Pseudo wheel deflection systems (e.g. FWD) do not lend themselves to travelling at traffic speed, so rolling wheel deflection systems (e.g. TSD) could be a closer simulation of heavy vehicle loading and therefore more relevant in measuring surface deflection under in-service traffic loading conditions (Austroads 2013).

Several researchers have evaluated the relationship between TSD and other deflection testing devices. Austroads (2012a) described that this comparison testing has involved direct comparison of slope (TSD) to deflection (FWD and deflectograph) and comparison of SCI_{300} (TSD) to SCI_{300} (FWD) etc. Results indicate the possibility to define a direct relationship between deflection-measuring devices that would allow TSD data to be converted into equivalent FWD/Deflectograph data (Austroads 2012a).

Figure 2.5 shows graphical presentation of results that indicate the potential of the TSD devices.

Figure 2.5 Comparison of different deflection devices – TSD deflection slope (P_{200}), FWD and deflectograph central deflection for 140 m of road (vertical scales are not related to each other) (Source: Austroads 2012a based on Ferne et al. 2009)

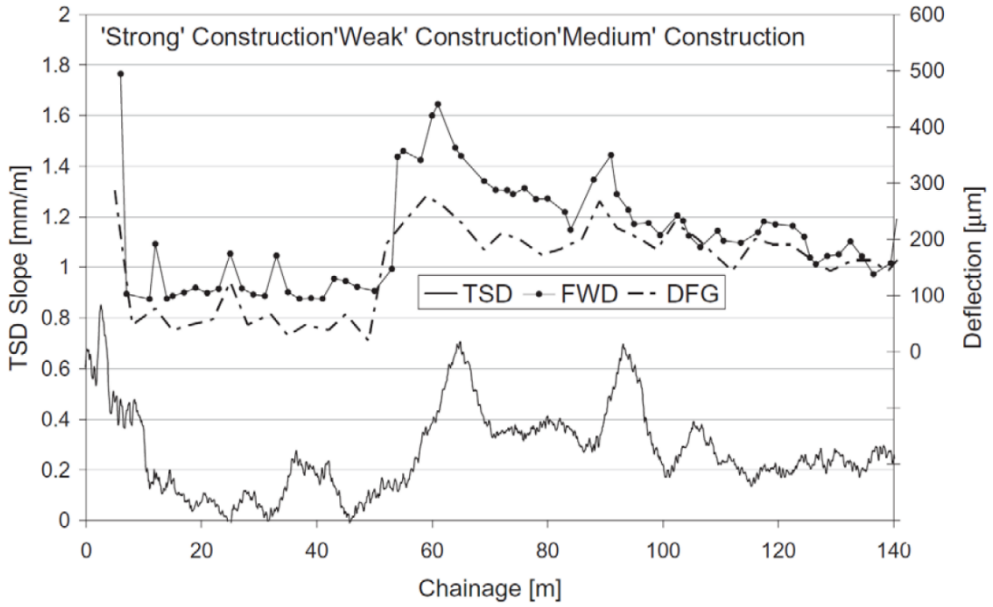

The indicated very good matches of iPAVE2 deflections with both deflectograph (DFG) and falling weight deflectometer (FWD) devices. Figure 2.6 shows comparison between the maximum deflections at Illawarra site 1 measured with DFG and FWD and estimated from TSD measurements. It can be observed that the iPAVE2 D_0 identify high and low peaks similar to the other devices.

Figure 2.6 Maximum deflection measured at Illawarra site 1, DFG, FWD and TSD at 60 km/h (Source: Austroads 2012a)

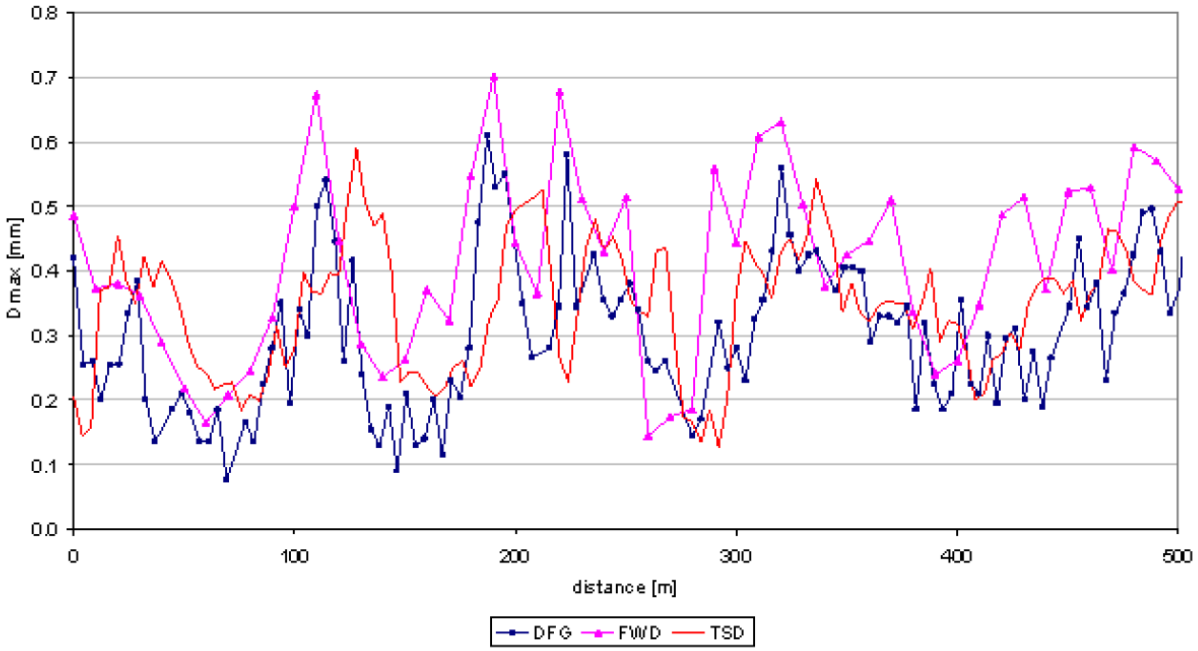

The strength of the correlation varies between devices because:

- All devices are measuring different pavement loads and responses leading to different measured responses.
- Different pavements respond differently to differently applied load.

Austroads (2012a) also reported that existing literature related to TSD, field trials and consultation with international TSD operators indicated that TSD is capable to differentiate between weak and strong pavements. Figure 2.7 shows a good correlation for a limited range of pavement strengths based on TSD, DFG and FWD data collected at the trial sites. Figure 2.8 illustrates the profile of the TSD response over a broader range of pavement types. The TSD slope measures still reflect the high and low deflections measured by the other devices.

Figure 2.7 Maximum deflection measured at Illawarra site 2, DFG, FWD and TSD at 60 km/h (Source: Austroads 2012a)

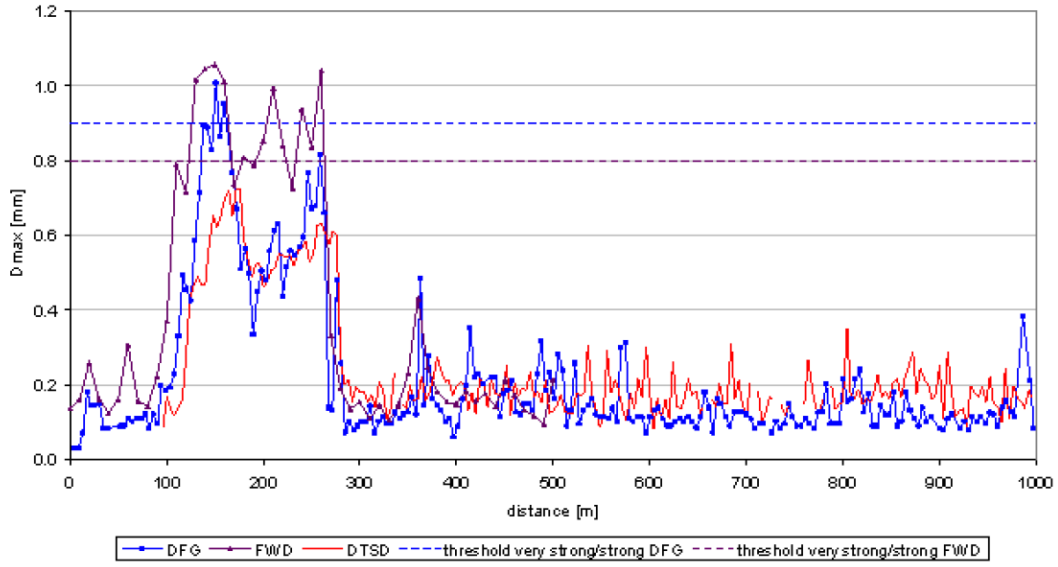

Figure 2.8 Maximum deflection (DFG & FWD) and TSD slope (S_{200}) measured at Wattamolla (Source: Austroads 2012a)

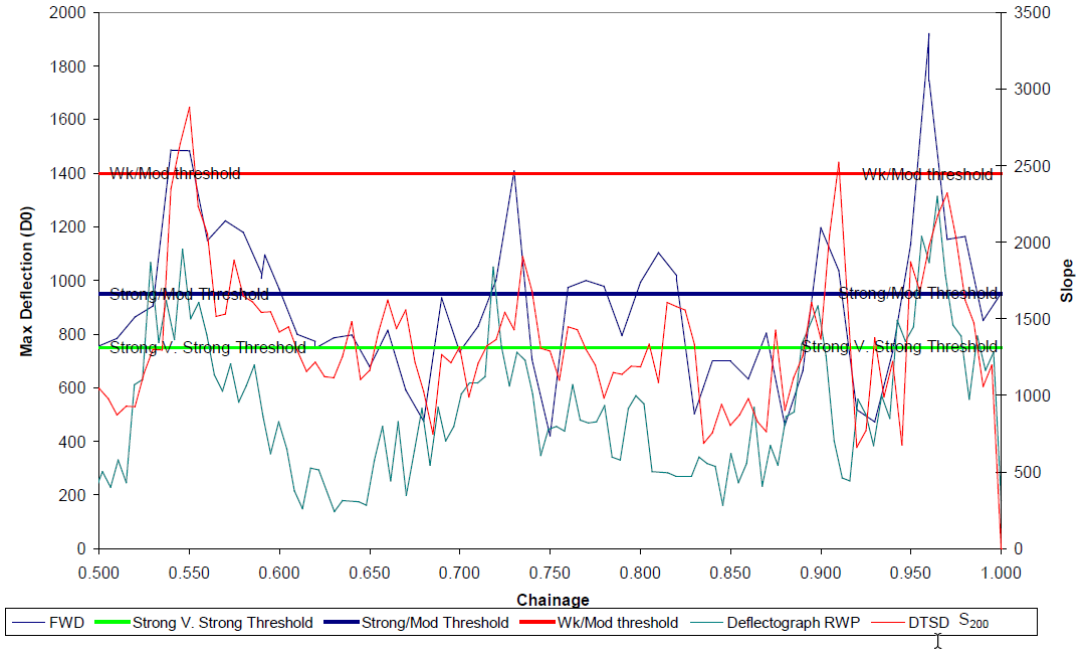

Austroads (2012b) highlighted the technical concerns to be addressed in future research including the development of a relationship between TSD and FWD deflections for a range of typical pavements in Australia and New Zealand. The proposed research also included the possible positions of doppler lasers e.g. close to the wheel load and be progressively spaced further away from the wheel load to resolve assumptions about the TSD deflection bowl.

For pavements with bound (e.g. asphalt) layers, pavement strengthening treatments maybe designed using pavement and subgrade moduli back-calculated from measured FWD deflection bowls (Austroads 2019a). As TSD and FWD deflection devices differ in loading and response measurement systems, they are not expected to measure the same deflection bowls. Regression equations have been developed to predict maximum deflection from the TSD but could not be extended to a reliable prediction of the entire deflection bowl (Austroads 2021, Austroads 2019b, Lee and Conaghan 2016).

Muller and Roberts (2013) utilised Queensland's test sites TSD and FWD data to develop an approach for predicting full TSD deflection bowls. TSD deflection bowls were validated against that of the FWD and a clear correlation was found between both methods in terms of shape and magnitude of deflection bowls.

Austroads (2014a) reported that correlation between FWD and TSD deflections based on a wide range of FWD maximum deflection values ranging from approximately 100 to 2000 microns confirmed that the TSD can differentiate between weak and strong structures for typical Australian and New Zealand pavements. The development of the AUTC method provides a basis for replacing the TSD manufacturer's analysis and outputs with fundamental estimates of vertical deflection and therefore confirms that the TSD can give reliable means for obtaining equivalent FWD data.

Austroads (2014b) reported the analysis of Polish Road and Bridge Research Institute (IBDiM) data using the AUTC numerical integration approach (Muller & Roberts 2013) for comparison against the maximum FWD deflections. For comparison, the TSD data were also analysed using the Euler-Bernoulli (EB) beam model approach. Both analysis methods were used to determine the deflection bowl at each location, from which the corresponding maximum deflection (D_0) was obtained. These results were then compared with the corresponding FWD measurements. Overall, the numerical integration approach achieved TSD deflection bowls closer and more consistent with conventional FWD bowls. This is not meant to imply that the TSD and FWD bowls should exactly match in any case, as pavement structure can affect the responses from different deflection devices. A comparison of D_0 values shows that a relationship between the TSD and FWD maximum deflections was found to have a goodness of fit (R^2) of 0.62, indicating a broadly equivalent response for FWD and TSD. Figure 2.9 shows an equivalent plot of this relationship.

Figure 2.9 Equivalent plot of maximum deflection as measured by FWD and TSD at corresponding points (Source: Austroads 2014b)

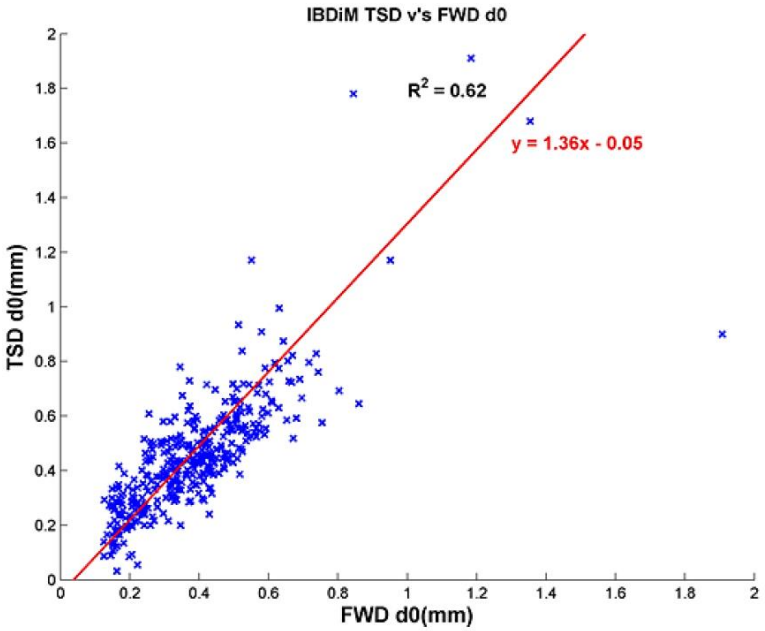

Lee and Conaghan (2016) used field trial data to derive a general equation to predict FWD D_0 deflections from measured TSD results based on linear regression. The R^2 for linear regression decreases significantly beyond an offset distance of around 400 mm. For very stiff pavements (i.e. D_0 TSD < 0.2 mm), the correlation between TSD and FWD was unclear. There was high degree of scatter in the FWD/TSD data comparison (Figure 2.10) however, most of the scatter is related to the pavement having distressed cement treated base with extensive and varied cracking observed within the test site during site inspection (road 40A). It is reasonable to expect that deflection results will vary widely.

Figure 2.10 Linear correlation of deflection measured under the load by the FWD and TSD (Source: Lee and Conaghan 2016)

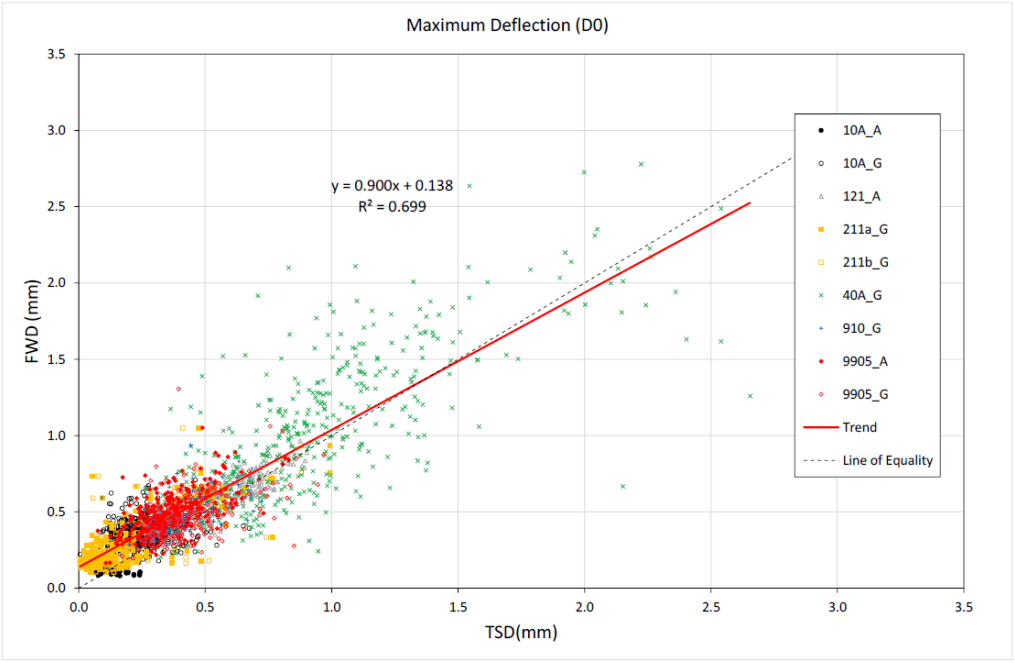

Note: G = gazettal direction and A = anti-gazettal direction in the legend

Brezina, Stryk and Grosek (2017) reported the correlation between TSD and FWD devices after applying corrections for loading force and temperature. The degree of correlation between deflection values was determined with the use of linear regression. Criteria used for establishing the relationship of two variables characterises the relationship into weak, moderate and strong with reliability coefficient R^2 values in the range of 0.1 to 0.25, 0.25 to 0.5 and 0.5 to 0.8 respectively. Based on this criteria, there was a weak relationship between TSD and FWD deflection values for the parameter SCI_{300}. Similarly, the evaluation of results for D_0 from Italy found the same trends with the increase of FWD values correlated with the increase in TSD values. Figure 2.11 and Figure 2.12 show the results of TSD and FWD measurements for parameters SCI_{300} and D_0.

Figure 2.11 Comparison of index SCI_{300} on road SS1 in Italy (Source: Brezina, Stryk & Grosek 2017)

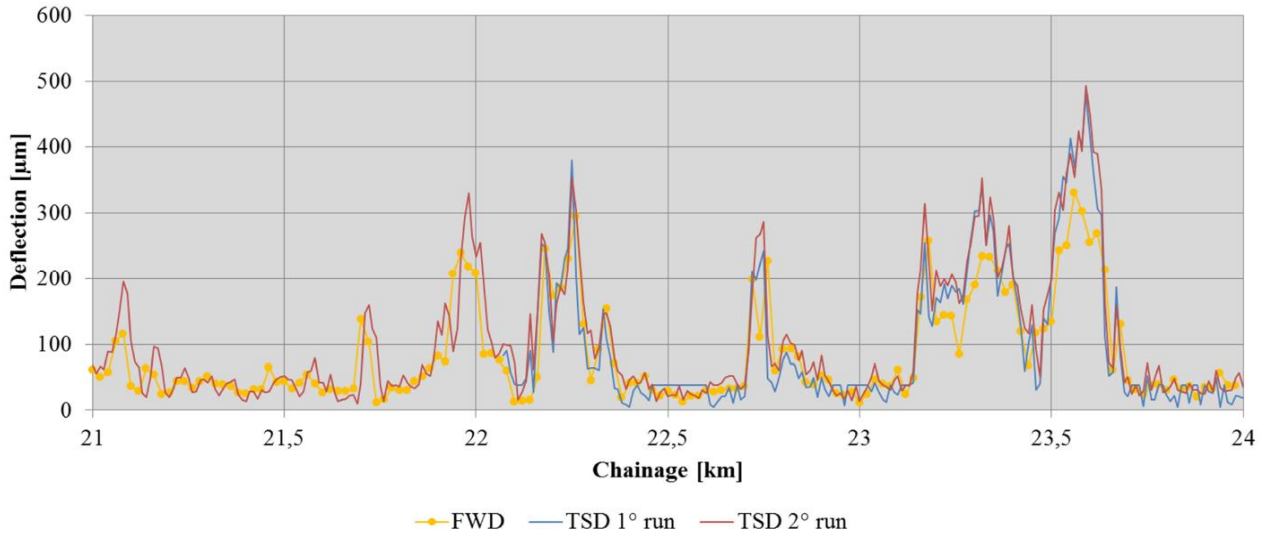

Figure 2.12 Comparison of index D_0 on road SS1 in Italy (Source: Brezina, Stryk & Grosek 2017)

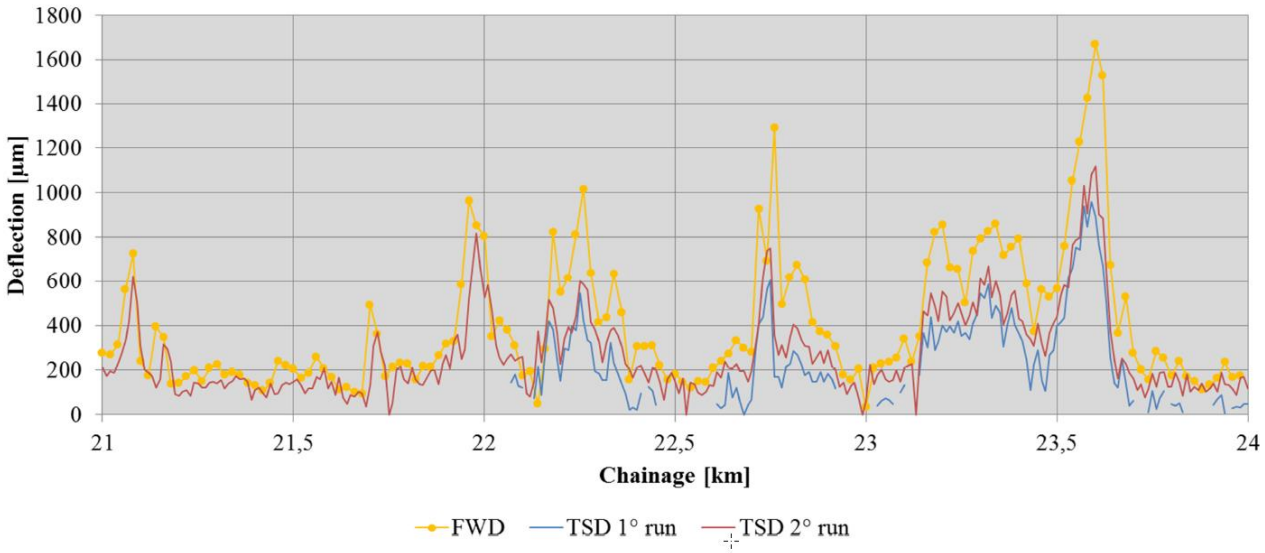

NZTA (2016) summarised the application of TSD data in New Zealand for asset management. The data used for this study contained two different deflection bowls:

- The Greenwood bowl which considers any asymmetry of bowl and extends from bowl centre to 900 mm offset. However, no deflections are calculated for the customary FWD offsets at 1200 and 1500 mm.

- The ARRB bowl which assumes all bowls are symmetrical but does determine deflections at both 1200 mm and 1500 mm offsets.

The trials with New Zealand data indicated that each of the two bowls could give more typical FWD bowl shapes in different circumstances but comparatively the ARRB bowl provided slightly more consistency. The methods examined for transforming New Zealand TSD deflection bowls into equivalent FWD deflection bowls can be placed in the order of preference as:

- Network specific individual offset method
- Route station specific method
- QMR (Queensland Main Roads) method

The network specific individual offset method provides a strong transformation from TSD recorded deflection to an equivalent FWD deflection for the given offsets whereas QMR method only calculates an equivalent FWD deflection for D_0, D_{200}, D_{300}, D_{450}, D_{600} and D_{900}. QMR method uses only central deflection from the TSD dataset and then generates a deflection bowl from only this point giving significant uncertainty on the reliability as the offset distance increases. The route station specific method has the ability to be applied across the entire range of offsets but requires a direct calibration at each offset. Figure 2.13 shows correlation of the transformation for D_0 using route station specific and individual offset methods. Both methods show good correlation with R^2 values of 0.981 and 0.980 respectively.

Figure 2.13 Transformation for D_0 using route station specific method (left) individual offset method (right) (Source: NZTA 2016)

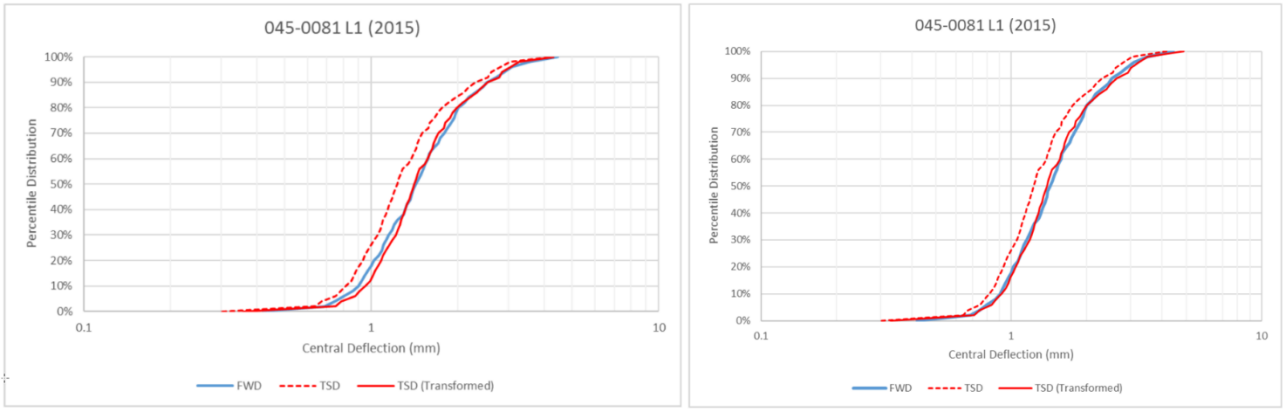

Wix, Murnane & Moffatt (2016) described the lessons learned from the trials related to operating the first TSD in Australia. TSD deflection data was validated through comparison of structural measurements from the TSD with FWD. Despite the fact that TSD and FWD are two different devices, similar results were achieved as shown in Figure 2.14. D_0 values generated by the TSD and FWD measurements over a two-year period on the Bruxner Highway near Lismore, NSW are compared.

Figure 2.14 Historic D_0 comparisons from TSD and FWD on Bruxner Highway, Lismore, NSW (Source: Wix, Murnane & Moffatt 2016)

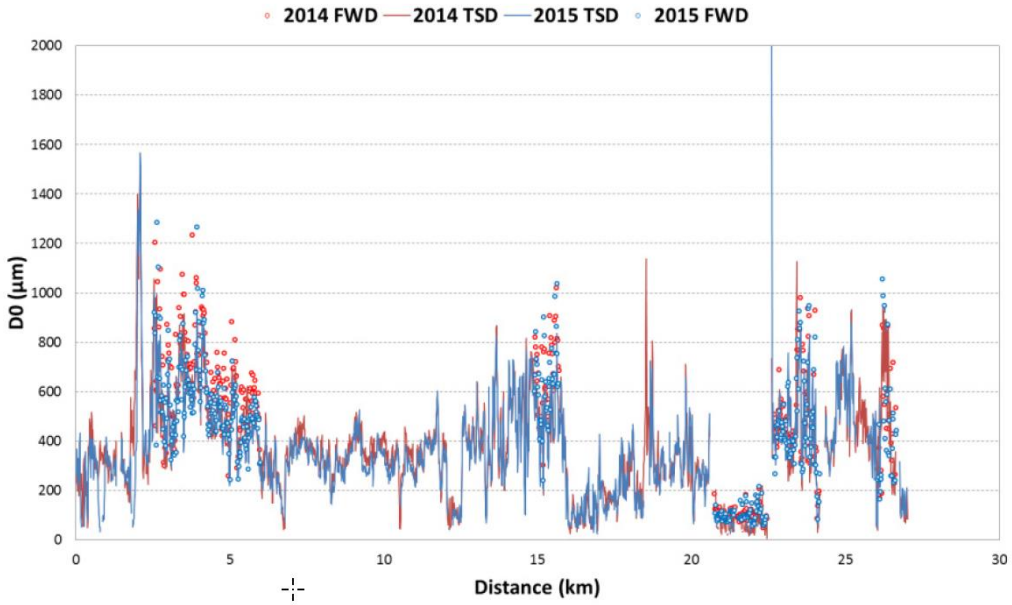

Chai et al. (2016) investigated the deflection bowls generated by the TSD on flexible pavements using the simplified deflection model (SDM). A comparison between FWD and TSD data shows a high level of correlation and a mathematical model has been established for estimation of FWD deflections using the TSD data (Figure 2.15**Error! Reference source not found.**). However, this study does not compare the SDM and AUTC technique for converting TSD data to FWD deflections. The key findings of this study can be summarised as follows:

- Relatively small deflections recorded at the D_{600} and D_{900} sensors of TSD are due to the dynamic effect of the TSD load which influence mainly the pavement materials near the impact load at the time of contact.
- Majority of $K_{2,\,900}$ parameters of the TSD deflections are less than 500 Micron/mm and the deflection bowls are said to possess moderate to high degree of subgrade nonlinearity.

Figure 2.15 TSD and FWD data collected along the test locations (Source: Chai et al. 2016)

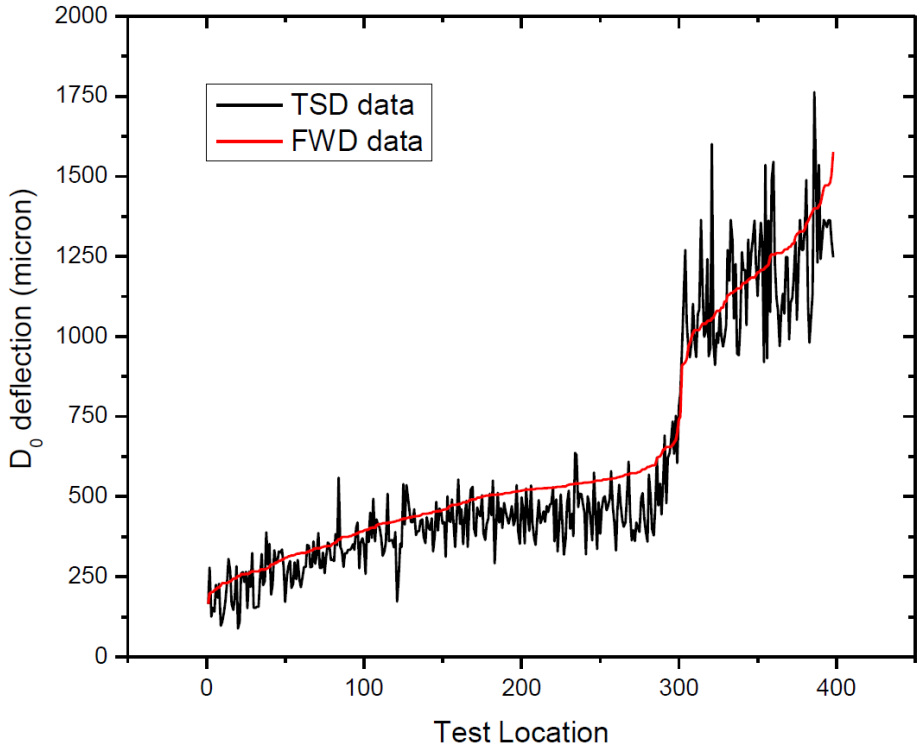

Elseifi, Zihan & Patrick (2019), in a study conducted by Louisiana Department of Transportation and Development, compared TSD and FWD measured devices and the outcome indicated a similar trend in deflections between the two devices and structural conditions along the tested road was successfully reflected in the measurements of two devices (Figure 2.16). These findings are in line with correlation between TSD and FWD deflection measurements in Australia and New Zealand.

Figure 2.16 Comparison of TSD and FWD D_0 on I81 South in Virginia (Source: Elseifi, Zihan & Patrick 2019)

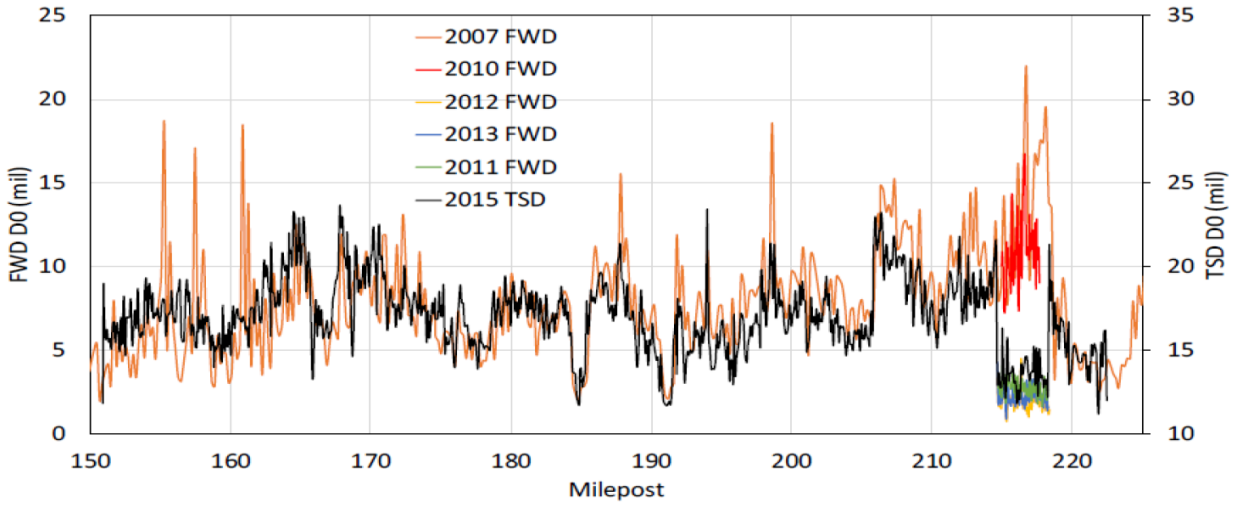

The deflection data from 2010 Australian TSD trials was re-analysed and the shape of the TSD deflection bowl and resulting predictions of D_0 and SCI_{300} were compared with FWD measurements. Moreover, TSD predictions based on this revised method (AUTC) were compared with the Danish analysis of the same data. The results illustrate a clear correlation in the shape

and magnitude of deflection bowls generated by the AUTC method compared with FWD measurements with coefficient of determination R^2 values comparing the FWD prediction and the nearest TSD prediction of 0.888 and 0.853 respectively (Figure 2.17 & Figure 2.18).

Figure 2.17 Flinders Highway (Charters Towers - Hughenden) – (a) predicted D_0 based on revised method and Danish analysis of TSD data compared with 50 kN FWD measurements and (b) corresponding SCI_{300} values (Source: Muller & Roberts 2013)

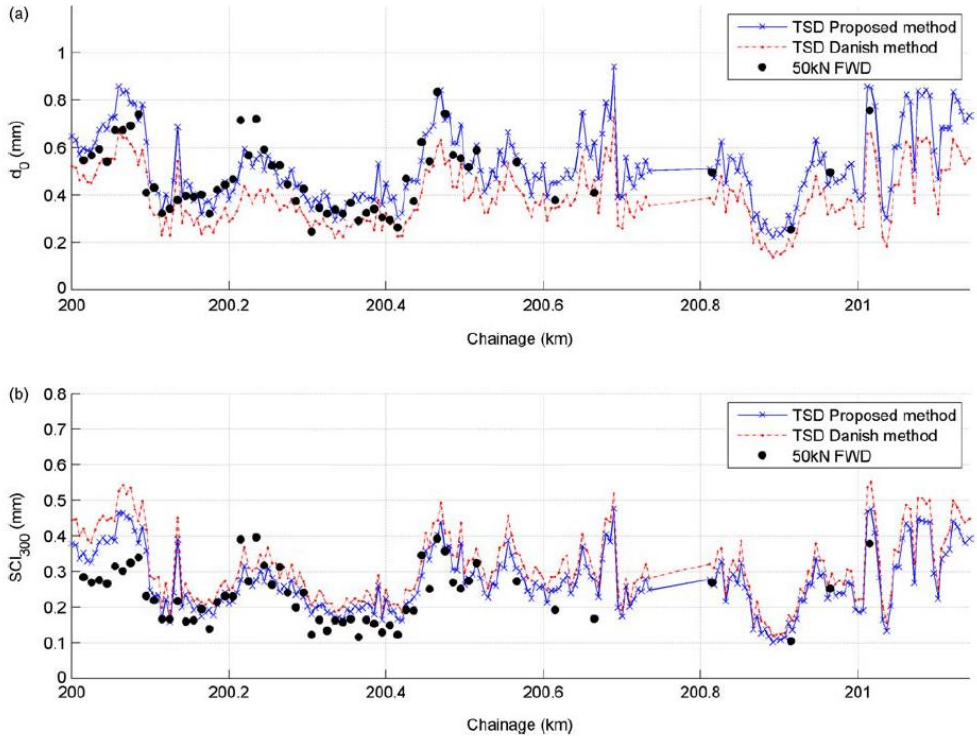

Figure 2.18 Warrego Highway (Miles - Roma) – (a) predicted D_0 based on revised method and Danish analysis of TSD data compared with 40 kN FWD measurements and (b) corresponding SCI_{300} values (Source: Muller & Roberts 2013)

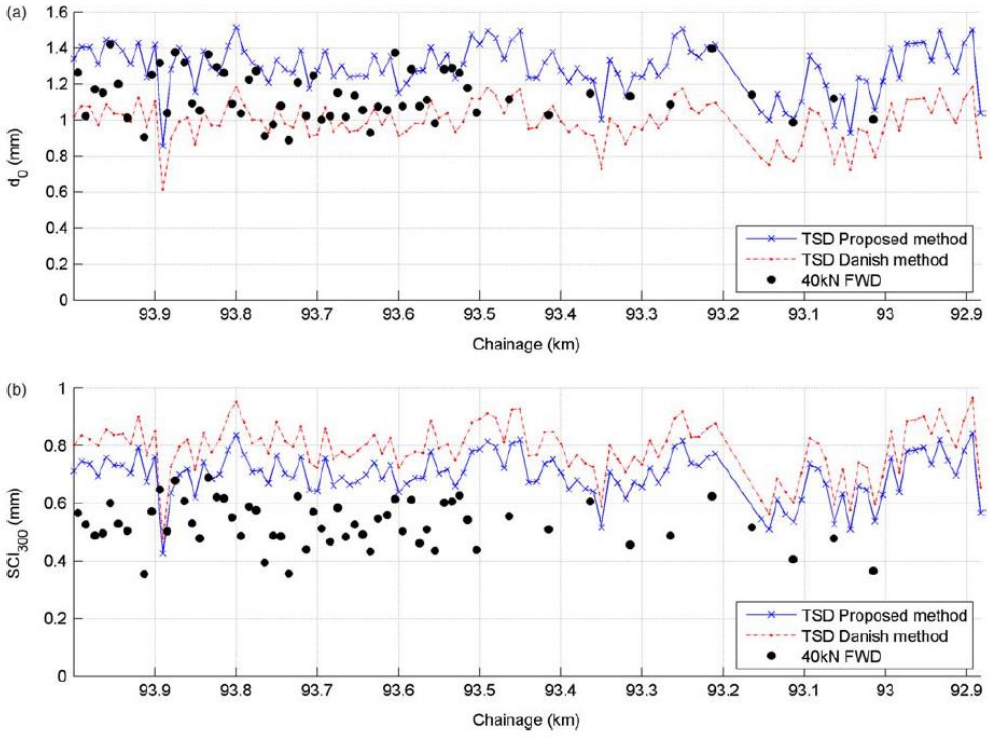

Austroads (2019b) reported that most of the research indicates that FWD and TSD measurements are linearly correlated. For further analysis, Deming regression method was used as D0 values in both datasets include measurement errors. Moreover, it was considered that each instrument presents the same variance in error. Deming regression was performed for sprayed seal surfaced granular pavements and asphalt pavements datasets.

For sprayed seal surfaced granular pavements, the linear relationship parameters for the maximum defection (D_0) is given in Table 2.2. The plots of the regression results are presented in Figure 2.19. Standard error (SE) was calculated to estimate how much the data points spread around the regression line. In this case, SE is 0.25 mm which is significant with deflections from 0.7 mm being currently considered for the empirical treatment design.

Table 2.2: Linear relationships between FWD and TSD maximum deflections for sprayed seal surfaced granular pavements

Offset	FWD vs TSD regression equation(1)	Pearson correlation coefficient R	Coefficient of Determination R^2	Standard error SE(2) mm
D_0	y = 1.06x – 0.06	0.83	0.69	0.25

1 y is the predicted 40 kN FWD value and x is representative of the 50 kN TSD data value, both in mm.
2 SE is the standard error of the estimate.
Source: Austroads 2019b.

The coefficient of R = 0.8 would indicate a very strong linear correlation using the qualitative scale. However, the coefficient of determination R^2 = 0.7 showed that around 30% of the variance of FWD measured deflection cannot be predicted from the TSD measured deflection.

Figure 2.19 Determining regression of FWD vs TSD for maximum deflection D_0 for sprayed seal surfaced granular pavements (Source: Austroads 2019b)

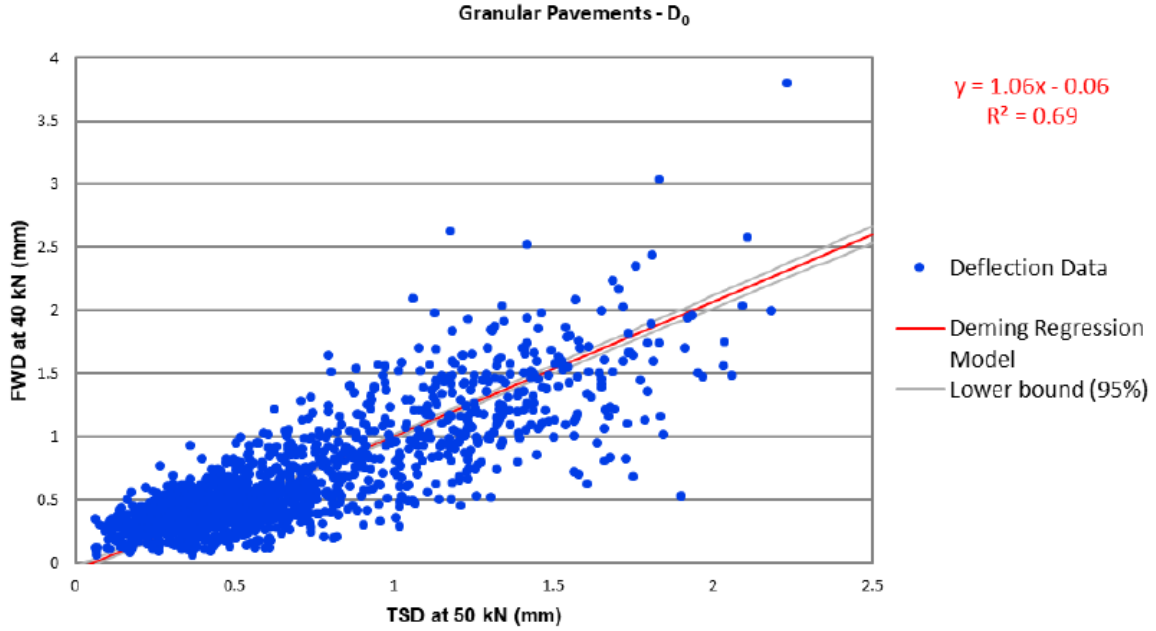

For asphalt pavements, the regression equation and statistical parameters are presented in. Data and the regression line are shown in Figure 2.20.

Table 2.3: Linear relationships between FWD and TSD maximum deflections for asphalt pavements

Offset	FWD vs TSD regression equation(1)	Pearson correlation coefficient R	Coefficient of Determination R^2	Standard error SE(2) mm
D_0	y = 0.93x – 0.04	0.78	0.60	0.14

1 y is the predicted 40 kN FWD value and x is representative of the 50 kN TSD data value, both in mm.
2 SE is the standard error of the estimate.
Source: Austroads 2019b.

The SE indicates less uncertainty in FWD D0 values for asphalt pavements than for sprayed seal surfaced granular pavements. However, the lower standard error is mainly due to the D_0 values being lowered for asphalt pavements. The coefficient of determination was smaller for asphalt pavement data with $R^2 = 0.6$ compared to 0.7 for sprayed seal granular pavements showing a linear regression of lesser quality.

Figure 2.20 Determining regression of FWD vs TSD for maximum deflection D_0 for asphalt pavements (Source: Austroads 2019b)

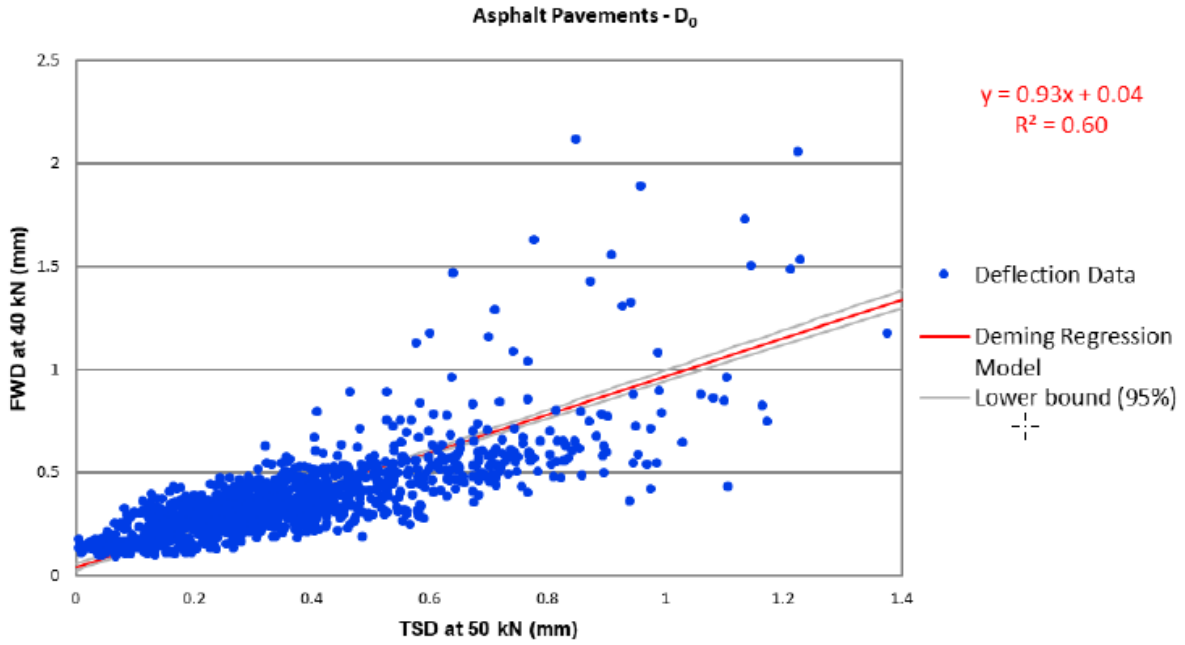

In terms of regression analysis, for FWD a weight falling on a rubber-coated metal plate generates the pavement deflection whereas for TSD it is moving load (dual-wheel). An important factor is the effect of gradient and crossfall which can lead to more variability when comparing TSD and FWD deflections. Another factor is the use of two initial seating drops with the FWD before the reported deflection drop, versus the configuration of TSD loading being behind a two-wheel assembly which creates a different loading history for the two measuring devices.

show Demming regression of FWD vs TSD using the maximum deflection (D_0) for combined data.

Figure 2.21 Determining regression of FWD vs TSD using D_0 for combined data (Source: Austroads 2019b)

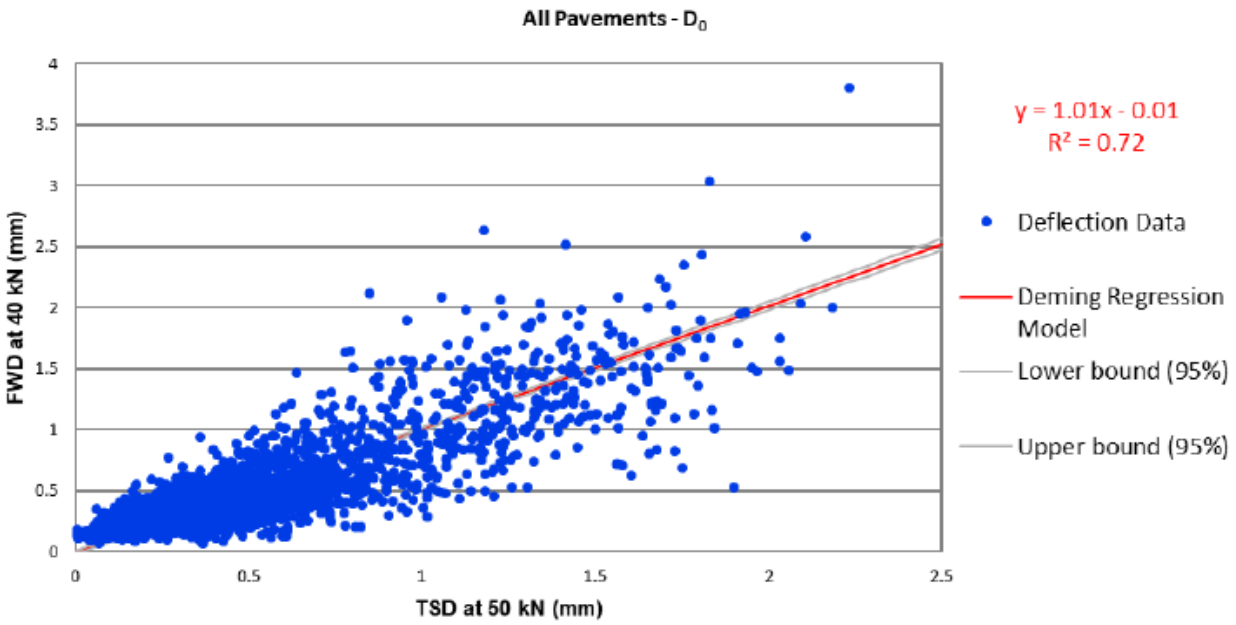

To assess the significance of the relative variance of the TSD and FWD measurements, the sensitivity of the fittest regression to the parameter λ was performed using the data related to sprayed seal surfaced granular pavements. Parameter λ values greater than 1.0 were considered, assuming that variance of TSD deflection could be up to two times larger than the variance of FWD deflection. Demming regression parameters obtained for three values are presented in Table 2.4

Table 2.4: Effect of the relative variance (parameter λ) between TSD and FWD deflection data

Parameter λ	FWD vs TSD regression equation	Standard error SE(1) mm
1.0	y = 1.06x – 0.06	0.25
1.5	y = 1.11x – 0.09	0.26
2.0	y = 1.14x – 0.11	0.26

1 SE is the standard error of the estimate.
Source: Austroads 2019b.

It should be noted that the increase of parameter λ affected the regression parameters and led to an increase of the slope and a reduction of the offset. The impact on the standard error was marginal. The increase of the slope suggests that larger TSD to FWD conversion factors would be obtained, when a higher variance of TSD data is considered compared with FWD data. High variance of FWD data compared with TSD would result in the opposite.

2.5 Use of TSD Data for Pavement Structural Evaluation

2.5.1 Project level treatment design

Austroads (2019b) described the use of TSD data to design granular overlays. To assess the structural adequacy of sprayed seal granular pavements and design granular overlays, the TSD D_0 values are adjusted to equivalent Benkelman Beam maximum deflections using a design standardisation factor (DSF) of 1.2.

To design strengthening treatments using bound materials (e.g asphalt overlays), Austroads (2019) uses a mechanistic-empirical design method which requires estimation of pavement layer and subgrade design modulus. One method of estimating these moduli is to back-calculate the moduli from measured FWD deflection bowls. Austroads (2019) does not yet provide a method of modulus back-calculation from measured TSD deflection bowls.

According to Austroads (2021), none of the Australian state road and transport agencies has implemented layer modulus back-calculation using TSD deflection bowls. Several methods have been published such as:

- Nielsen 2019 - Determining pavement and subgrade layer properties from the slope data from the TSD. This method is based on two parameters of a viscoelastic pavement materials model. The back-calculation algorithm includes a viscoelastic pavement response-to-load-model. This method was developed using data collected from a TSD fitted with 10 doppler lasers including lasers covering a range of offsets 750 mm, 1000 mm, 1500 mm and three lasers behind the rear loading axles. This method was applied to assess the practical applicability to a three-layer pavement (100 mm thick asphalt layer, 300 mm granular layer, semi-infinite subgrade) without any validation of moduli such as Young's modulus and damping parameters.
- Elbagalati et al. 2018 – An artificial neural network (ANN) based model to predict FWD equivalent deflection bowls from TSD measured bowls. This method has a major advantage that once transformed to an equivalent FWD bowl, existing modulus back-calculation methods could be used. The overall data showed scatter but the model was found to predict FWD equivalent deflection within 5% root mean square error (RMSE) for different offsets across the database used. The approach was validated based on back-calculation using ELMOD6 software using a circular load assumption for both TSD and FWD devices. Overall, there was a good agreement of the back-calculated moduli derived from TSD and FWD data. Figure 2.22 show comparison of FWD and TSD back-calculated moduli.

Figure 2.22 Comparison of FWD or TSD back-calculated moduli (Source: Austroads 2021, after Elbagalati et al. 2018)

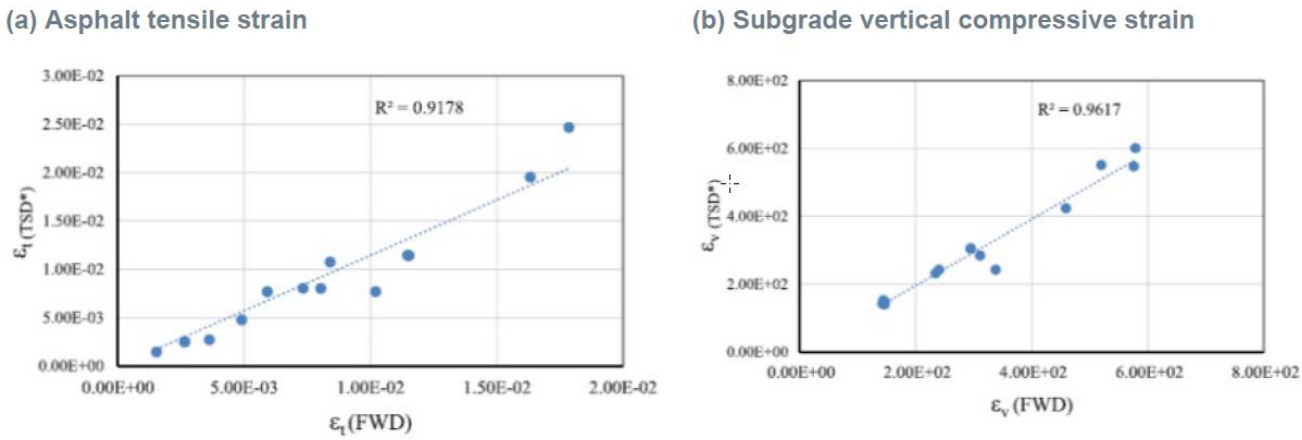

- Nasimifar, Thyagarajan & Sivaneswaran (2017) calculated layer moduli of a flexible pavement from TSD measurements. This study proposed two practical approaches to back-calculating pavement layer moduli from TSD data. In the velocity method, the 3D-Move program was identified as an efficient analytical tool for back-calculating layer moduli by directly using TSD-measured deflection velocities. The program can consider a moving load with nonuniform contact pressure and viscoelastic material properties and compute deflection velocities that can be matched with measured velocities. The approach was verified with TSD data at the MnRoad facility and results were compared with the conventional linear elastic analysis based (LEA-based) back-calculating results obtained

from the FWD test conducted on the same day. The deflection method used the Excel-based WESLEA analysis tool to back-calculate layer moduli with the TSD-computed deflections at the TSD sensor locations. The study showed the need to use TSD deflection data with dual uniform circular loads, which is the only difference from the conventional LEA-based FWD back-calculation approaches in which a single circular plate is used. The research findings ascertained that the velocity method has advantages over the deflection method as it uses measured deflection velocities directly and moving load, nonuniform contact pressure and viscoelastic properties during TSD measurements.

According to Austroads (2019a) Guide to Pavement Technology Part 5: Pavement Evaluation and Treatment Design (AGPT05-19), it is expected that the mechanistic-empirical procedure (MEP), previously known as a general mechanistic procedure (GMP), will be increasingly used for the design of structural treatments. Austroads (2019b) described the use of TSD deflection bowls for mechanistic-empirical treatment design. The regression analysis provides a relationship between maximum deflections measured using both the TSD and FWD. For both FWD and TSD data measurements, the D_0 values include measurement errors.

In terms of maximum deflection (D_0), the design deflections are based on values measured using a Benkelman Beam. Therefore, deflection values measured by other devices (Deflectograph, FWD, TSD) need to be converted to equivalent Benkelman Beam values. This conversion required a design standardisation factor (DSF). Austroads Guide to Pavement Technology Part 5 (Austroads 2019a) provides a DSF for this conversion as shown in Table 2.5.

Table 2.5: Deflection standardisation factors

Deflectograph measurement device	Deflection standardisation factor
Deflectograph. 80 kN single axle with dual tyres	1.2
TSD, 50 kN dual tyres	1.2
Falling Weight Deflectometer, 40 kN load	1.1

Source: Austroads 2019b.

Note that these DSF for TSD is 1.2 which is based on measurement speed of 40 to 80 km/h, relate to pavement deflections estimated by the AUTC method and are applicable deflections of thin bituminous surfaced granular pavements.

In AGPT05 layer moduli are back-calculated from FWD measured deflection bowls. However, use of TSD measured deflection bowls in the GMP would require a process to convert TSD measured deflection bowls into FWD equivalent bowls.

Based on difference in deflection bowls measured by FWD and derived from TSD, regression equations have been developed to predict maximum deflection from the TSD but could not be extended to a reliable prediction of the entire deflection bowl. More research is required (e.g. additional lasers) to predict more reliable deflection bowls from TSD measured responses. Currently the Australian road agencies (SRAs) have yet to implement modulus back-calculation from TSD deflection data. Some methods are of particular interest in this regard (e.g. Nielson 2019 & Elbagalati et al. 2018).

2.5.2 Network level use of deflection data

Australian state road agencies (SRAs) collect TSD data for network level use. The TSD measure pavement response virtually continuously at highway speed (usually at 80 km/h). Testing is reported at a 10 m or greater interval, with measurements being made in the outer wheelpath. Although procedures have yet to be developed to back-calculate pavement and subgrade moduli from the TSD responses, the TSD may assist in identifying homogeneous sections for use in the mechanistic-empirical procedure (Austroads 2019a). The TSD can be used as an asset management decision support tool and is capable of being used as network level screening tool, to identify suspect pavements within a survey run.

Virginia Transportation Research Council (2020) conducted research to incorporate TSD data into Virginia Transportation VDOT pavement management system. The distribution of effective structural number (SN_{eff}) calculated from the TSD measurements was found to be similar to that obtained from the FWD measurements. The relatively good consistency between TSD and FWD SN_{eff} and the similarities between the SN_{eff} distribution suggest that the structural information derived from the TSD can be successfully used as an alternative to similar data derived from the FWD for VDOT network level pavement management applications. All the indices investigated that could be used to replace the FWD-based subgrade resilient modulus (M_R) were also found to be highly correlated to the overall TSD-based structural properties of the pavement and not very highly correlated to the FWD-based M_R. Therefore, the research did not recommend the TSD-based measure of the subgrade strength.

2.6 TSD Deflection - iPAVE2 vs iPAVE3

The traffic speed deflectometer (TSD) is the core component of NTRO's intelligent pavement assessment vehicles (iPAVE) and is used to assess the structural condition of the pavement. The TSD was developed by Greenwood Engineering in the early 2000s and since then it has been upgraded over time.

Historically, NTRO has used iPAVE2 to survey the Western Australian road network for Main Roads Western Australia (Main Roads). This 2nd generation device has 6 doppler sensors positioned in the outer wheel path plus a reference sensor. The locations of the sensors in relation to the position of the rear axle, which is taken as the zero point, are shown in Table 2.6.

Table 2.6: iPAVE sensor positions

	iPAVE sensor positions (mm)										
	Behind load			In front of load							
iPAVE3	-450	-300	-200	130	215	300	450	600	900	1500	3080*
iPAVE2				100	200	300	450	600	900		3500*

* Reference sensor

The TSD measures the velocity of the pavement as it moves, or deflects, under the load at each of the sensor locations and the slope velocity is calculated at each of these points by dividing the velocity readings by the horizontal velocity of the iPAVE. A velocity slope curve is then generated which assumes the slope velocity is zero both directly under the nominal 5 ton load and at the location of the reference sensor. The area under this curve is then integrated to produce an estimate of the deflection bowl. This methodology is known as the area under the curve (AUTC) technique and is the Australian standard for estimating the deflection bowls from the iPAVE. An example of a slope velocity curve and the resultant deflection bowl is shown in Figure 2.23.

Figure 2.23 Velocity slope curve and resultant deflection bowl – iPAVE2

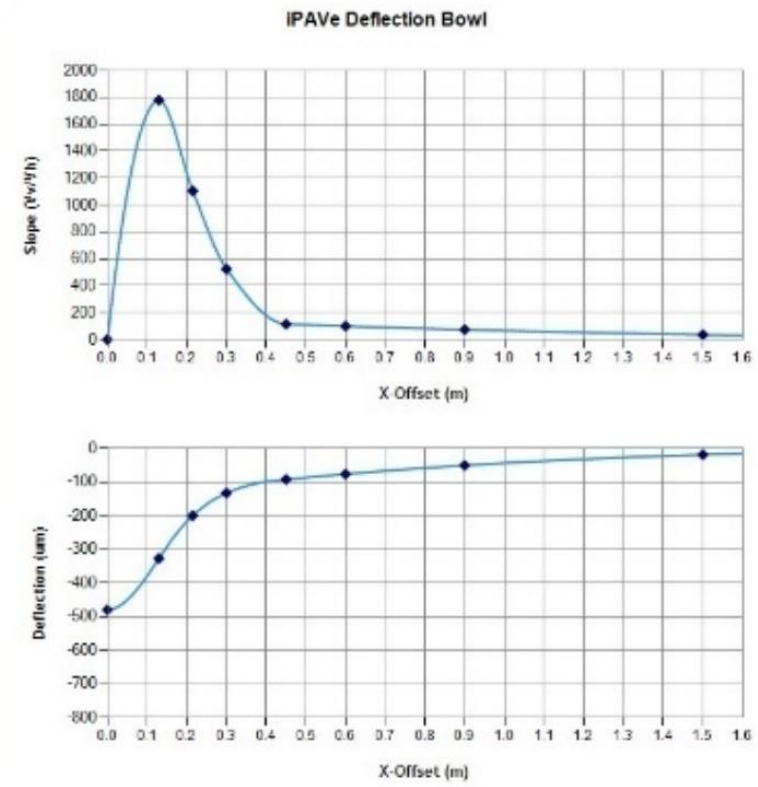

Whilst there is no sensor located at the 1500 mm position, the deflection at this location can be derived from the deflection bowl, as can the deflection at any point along the curve (not just at the corresponding sensor locations). The measurement at this location is key to determining the subgrade performance of the pavement.

In 2023, NTRO took delivery of its first 3rd generation TSD, iPAVE3, which has an increased number of doppler sensors to provide a more detailed coverage of the deflection bowl. The additional sensors are positioned in front of and behind the rear axle at the locations detailed in Table 1. iPAVE3 also measures the deflection in both wheel paths. (Please note there are also other differences between these two systems, but these fall outside the scope of this project).

The 3 sensors behind the load allow the system to measure the maximum load, D_{max} which occurs behind the rear axle and rather than estimating the deflection at the 1500 mm position, the additional sensor in front of the load can be used to measure the deflection at this point directly.

An example of a typical slope curve from iPAVE3, with its additional measurement points, and the resultant deflection curve is shown in Figure 2.24.

Figure 2.24 Velocity slope curve and resultant deflection bowl – iPAVE3

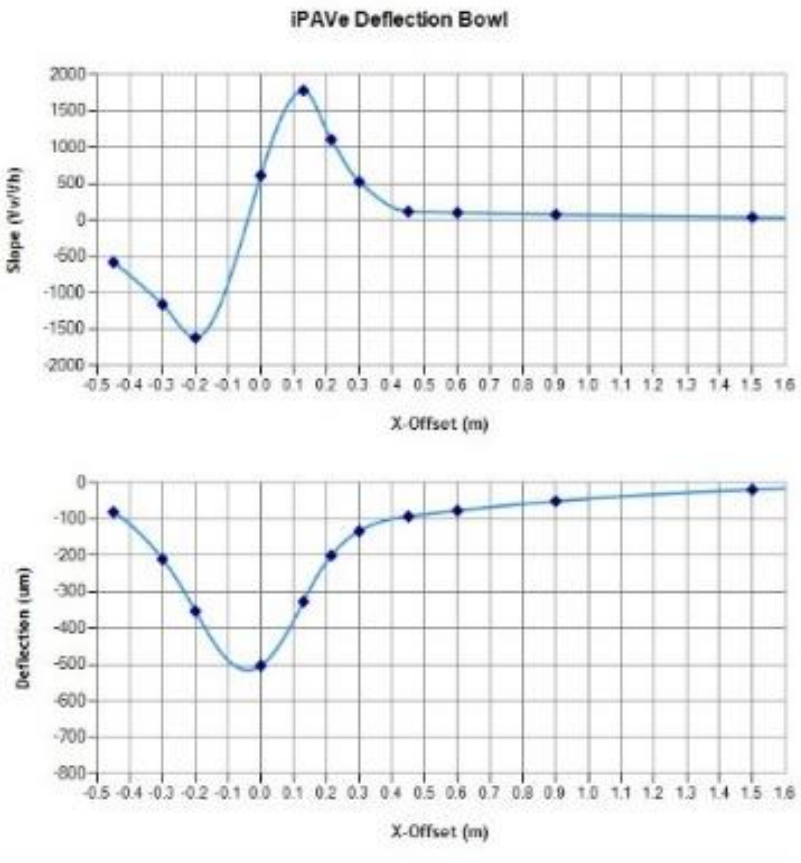

It should also be noted that the D_0 values produced by the two different configurations will often be different. With both systems, the slope velocity at the reference laser is assumed to be zero, however, this is not the case at the zero measurement point under the load. With iPAVE2, the slope velocity is assumed to be zero, however, the additional sensors behind the load in iPAVE3 result in the slope curve intersecting the y-axis above zero, resulting in an increased area under the curve and a potentially larger D_0 value. D_{max}, which occurs behind the load where the velocity slope curve crosses the x-axis, can also be measured using iPAVE3.

The other factor that should be taken into consideration is the length of the tail for each iPAVE configuration. The tail of the velocity slope curve for iPAVE3 is considerably shorter than iPAVE2 and this has the potential to introduce a difference in the resultant deflections.

Taking all the above into account, this project aims to determine how the measurements from the iPAVE compare with those from an FWD, whether there are any differences in the measurements reported using the 2 different iPAVE configurations and also whether the addition of a 1500 mm sensor improves the assessment of the subgrade condition using back calculation software. This is of significant interest as iPAVE2 has the capacity to be upgraded with additional sensors in front of and behind the load, especially if this upgrade allows additional insights into the condition of the subgrade.

3 Test Sections and Data Collection

3.1 Field Test Sections

3.1.1 Basis for Site Selection

The deflection field trial sites were selected to cover various pavement profiles and composition of different types of pavement materials, the following two pavement types were chosen to be investigated:

- Two sections of thick (>150 mm) asphalt on unbound granular pavements Sprayed seal surfaced unbound granular pavement.

The field trials were planned to be organised in Queensland. For this purpose, different sites around Brisbane were considered. Following factors were considered for the site selection:

- Fieldwork efficiency – optimisation of cost and mobilisation
- Road geometry – avoiding intersections and bends impacting speed and deflection readings
- Practicality of testing – traffic control, sufficient lead-in distance for TSD to attain the required speed and stop.

Based on existing data provided by the Queensland Department of Transport and Main Roads (TMR) and visual site inspection, two sections of Ipswich Rosewood Road in Amberley area and one on New England Highway were identified for the investigation and testing. Table 3.1 provides a summary of the selected sections.

Table 3.1: Summary of the selected sections

Sections	Chainage (km)		Road	Section Length (km)	Pavement type
	From	To			
Section 1	0.6	1.6	Ipswich Rosewood Road Amberley	1	Thick asphalt surfaced granular
Section 2	94.0	95.147	New England Highway	1	Sprayed seal surfaced granular
Section 3	5.3	6.3	Ipswich Rosewood Road Amberley	1	Thick asphalt surfaced granular

Each site was 1 km long in order to have enough data and include a range of weak to strong deflection readings particularly for different subgrade responses.

3.1.2 Sections 1 & 3 - Ipswich Rosewood Road

iPAVE3 deflection data was collected for two sections in both directions. Each section underwent 3 consecutive runs, with measurements taken along both wheelpaths. Figure 3.1 presents the naming codes used for these sections.

Figure 3.1 Runs and naming codes on Ipswich Rosewood Road sections

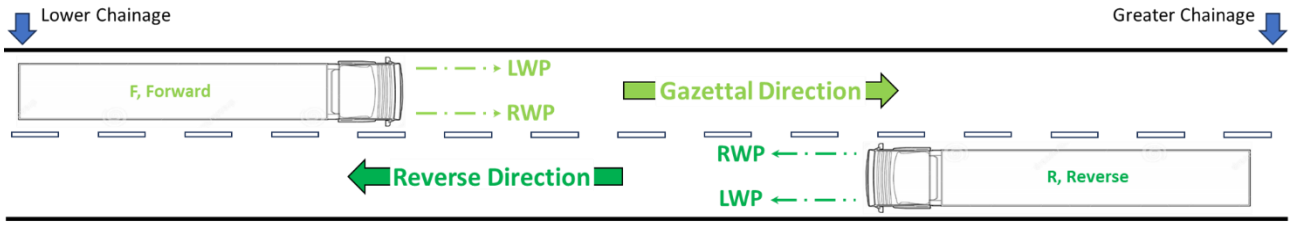

3.1.3 Section 2 – New England Highway

All standard runs were surveyed in this section. Additional runs were also conducted to evaluate the parameters such as bends, curves and IRI. These extra runs were intended to allow for further checks and analysis. These extra runs varied in terms of travel, direction, wheel path location, and exposure to different curves and surfaces roughness. Data analysis of these runs may provide valuable insights into the influence of various operational and road characteristic parameters on the deflection data. Figure 3.2 presents TSD runs on New England Highway and naming codes.

Figure 3.2 TSD runs on New England Highway and naming codes

a)

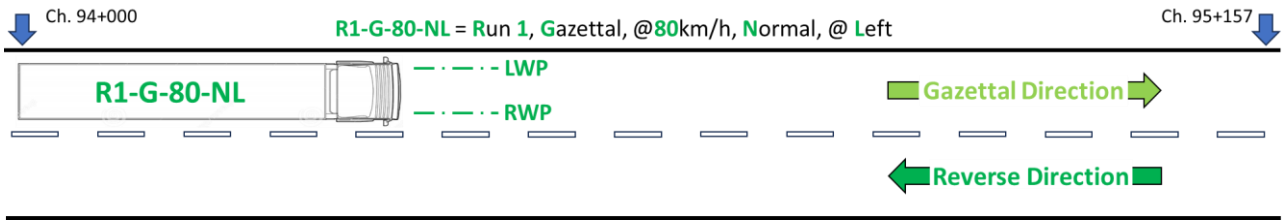

b)

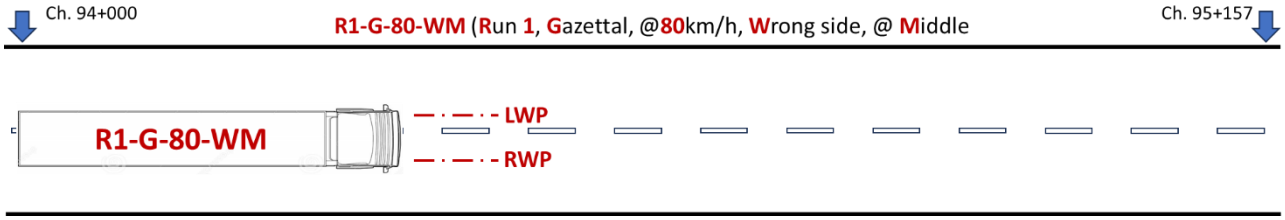

c)

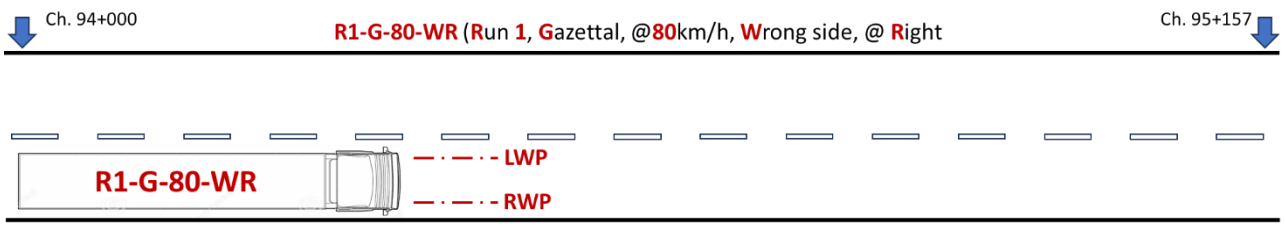

d)

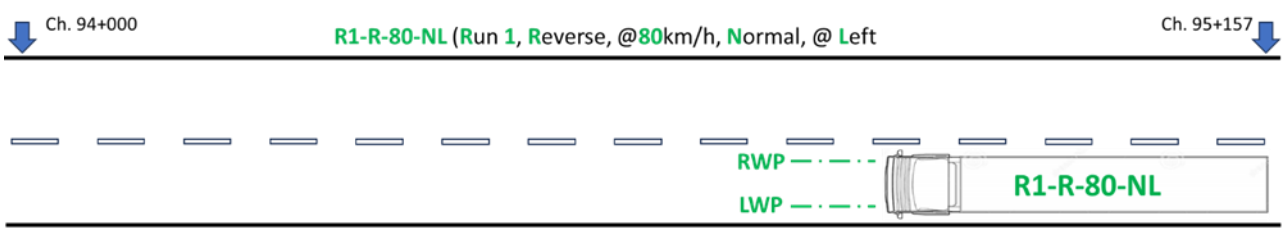

e)

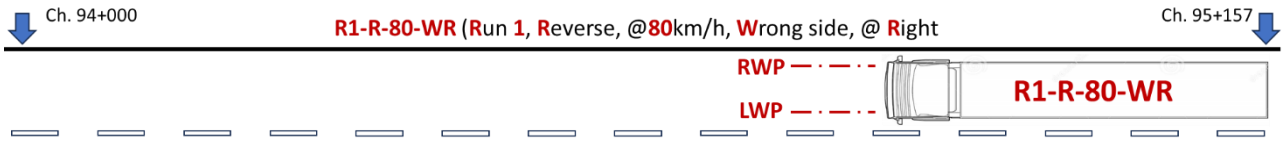

It should be noted that the Inner wheel path (IWP) deflections from R1-G-80-WM run (Figure 3.2b) should be comparable with outer wheel path (OWP) data from R1-G-80-WR survey (Figure 3.2c). Similarly, the OWP deflection data from R1-G-80-WR (Figure 3.2c), when aligning the changes, is comparable with the deflection on the IWP from data on R1-R-80-NL (Figure 3.2d)

3.2 Pavement Profiles

Table 3.1 to Table 3.4 list the existing pavement profiles for the trial sections. It should be noted that these pavement profiles are based on TMR Asset Roads Management Information System (ARMIS) data provided by TMR. Note that the Table 3.4 structure is not consistent with the field core data which indicated asphalt thicknesses in the range 140 mm to 270 mm.

Table 3.2: ARMIS pavement structure for Section 1 (Thick asphalt on granular)

Pavement layer	Material	Thickness (mm)
Surfacing	Dense graded asphalt (DGA)	65
Basecourse	Dense graded asphalt (DGA)	130
Sprayed seal		
Basecourse	Granular	150
Subbase	Granular	200
Subgrade	Subgrade	-

Source: ARMIS Data, TMR

Table 3.3: ARMIS pavement structure for Section 2 (Sprayed seal on granular)

Pavement layer	Material	Thickness (mm)
Sprayed seal (multiple)		
Basecourse	Granular	100
Subbase	Granular	125
Subgrade	Subgrade	-

Source: ARMIS Data, TMR

Table 3.4: ARMIS pavement structure for Section 3 (Thick asphalt on granular)

Pavement layer	Material	Thickness (mm)
Surfacing	Dense graded asphalt (DGA)	50
Surfacing	Dense graded asphalt (DGA)	20
Sprayed seal		

Basecourse	Granular	150
Subbase	Granular	280
Subgrade	Subgrade	-

Source: ARMIS Data, TMR

3.3 First Round of Data Collection

Field measurements were conducted in Queensland and supervised by NTRO team, which involved deflection measurements (FWD, iPAVE3) by NTRO as well as contractor engagement to conduct coring and push tube sampling. Note that the TSD data collected as part of first round of data collection cannot be used of analysis due to iPAVE3 technical problem .

Prior to the testing, based on the available information, a testing plan was prepared by the project team including number and location of the test points and the target depth for the core and push tube samples. However, it was decided to review and potentially alternate the test points if needed based on FWD results to maximise the information obtained from the coring and testing. Therefore, the coring and push tube sampling was planned to be carried out a couple of days after the FWD testing.

The FWD testing was conducted on 26th April 2023 on Section 1 and 27th April 2023 on Section 3 by NTRO Infrastructure Measurement team. The data was collected at 10 m intervals (no staggered) on the LWP in both gazettal and reverse directions with loads of 40 kN and 50 kN. However, measurements with 50 kN load were used in data analysis so that these measurements could be compared with TSD. Moreover, temperature measurements were carried out at the time of testing. Note that FWD and TSD measurements were done on similar time to avoid any variation in temperature. Figure 3.3 Shows the configuration of FWD testing on sections 1 and 3. FWD data is attached in Appendix A.

Figure 3.3 FWD testing configuration on Ipswich Rosewood Road, Amberley

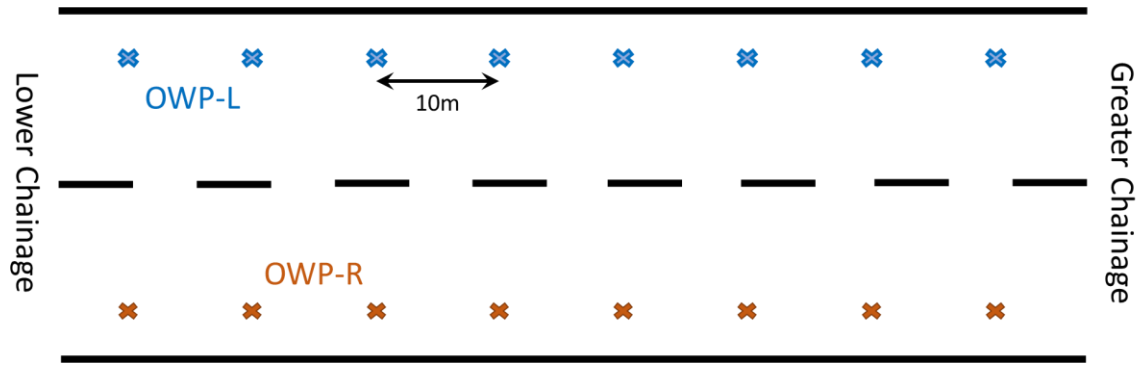

For the coring and push tube sampling and testing a contractor specialising in this field was engaged, and all the work was carried out in the presence of NTRO representative at the site.

Figure 3.4 shows the approach of using the accumulative difference from the mean for the maximum deflection (D_0) to define the homogeneous subsections on Section 1 to guide the selection of pavement investigation chainages.

Figure 3.4 Section 1 OWP 50 kN FWD Maximum Deflections (top figure) and pavement investigation sites selected within each homogeneous subsection(bottom figure)

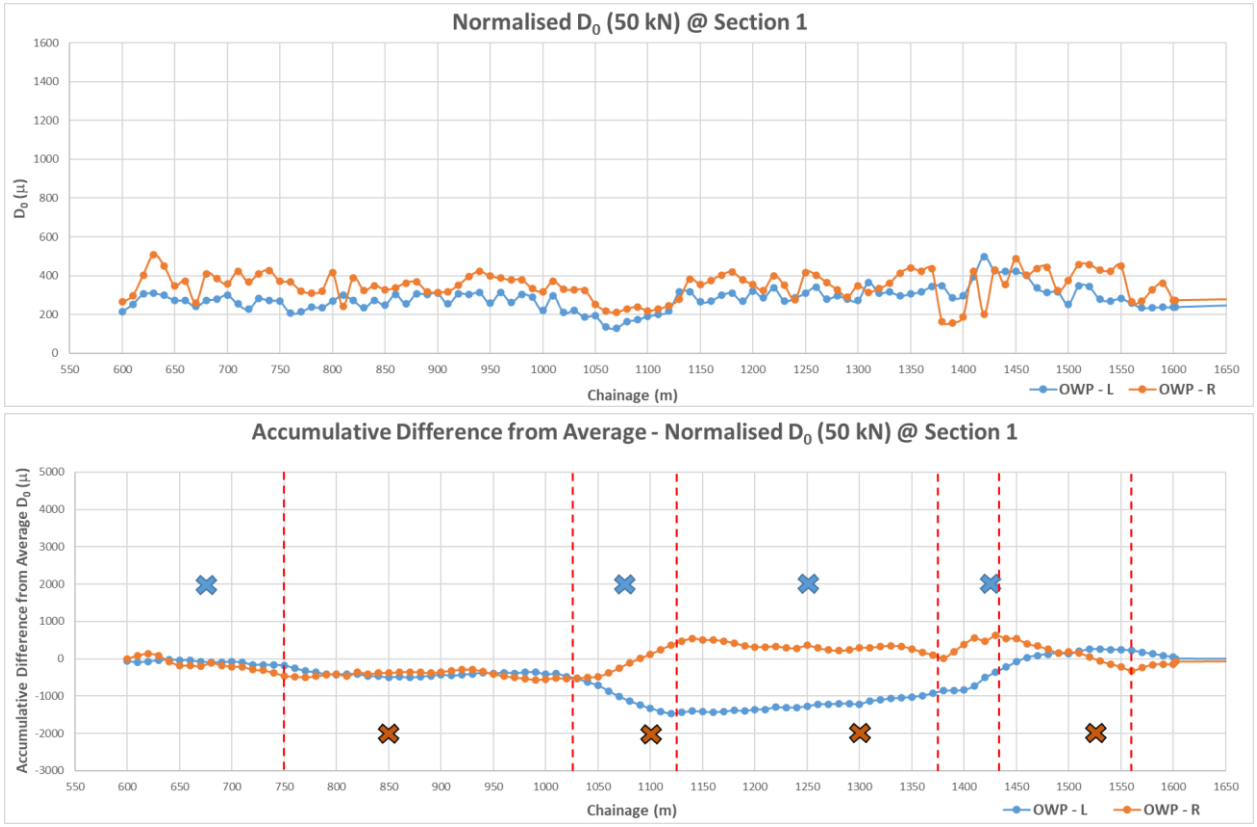

As FWD results demonstrated more uniformity than expected the number of pavement investigation sites on Section 1 was reduced the 10 originally planned to 8 sites. Figure 3.5 shows the pavement investigation locations for the identified homogeneous subsections.

Figure 3.5 Section 1 pavement investigation location and depth of coring

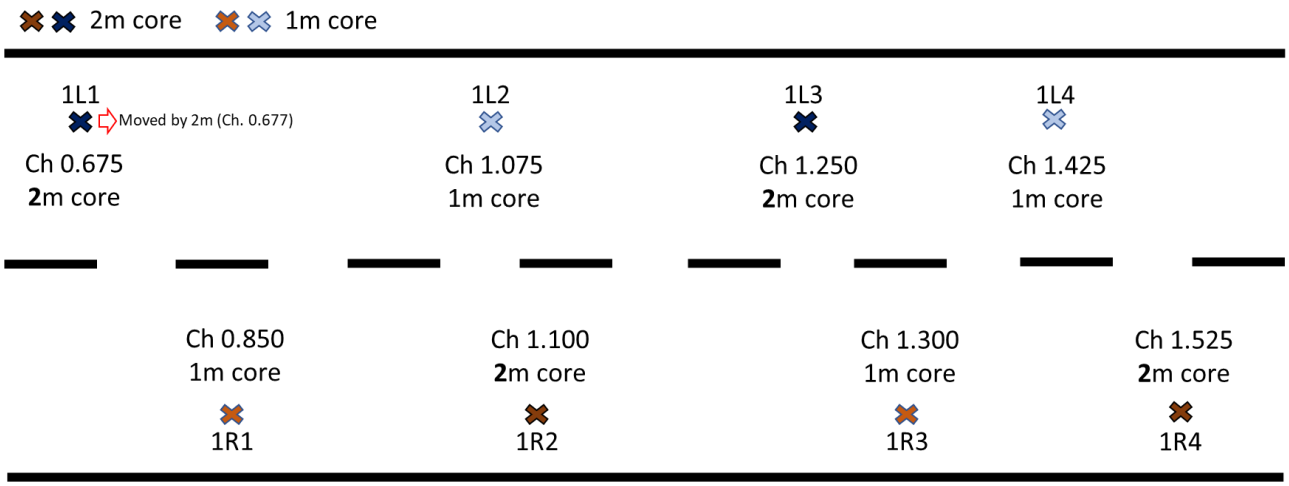

Due to presence of an abutment of a culvert, the 1L1 test point was shifted by 2 m (to Ch. 0.677).

Figure 3.6 shows the use of the same approach for defining the homogeneous sub-sections and locations of pavement investigation sites on Section 3. Consideration was also given to locations of construction joints in the site sections (Figure 3.7).

Figure 3.6 Section 3 OWP 50 kN FWD Maximum Deflections (top figure) and pavement investigation sites selected within each homogeneous subsection(bottom figure)

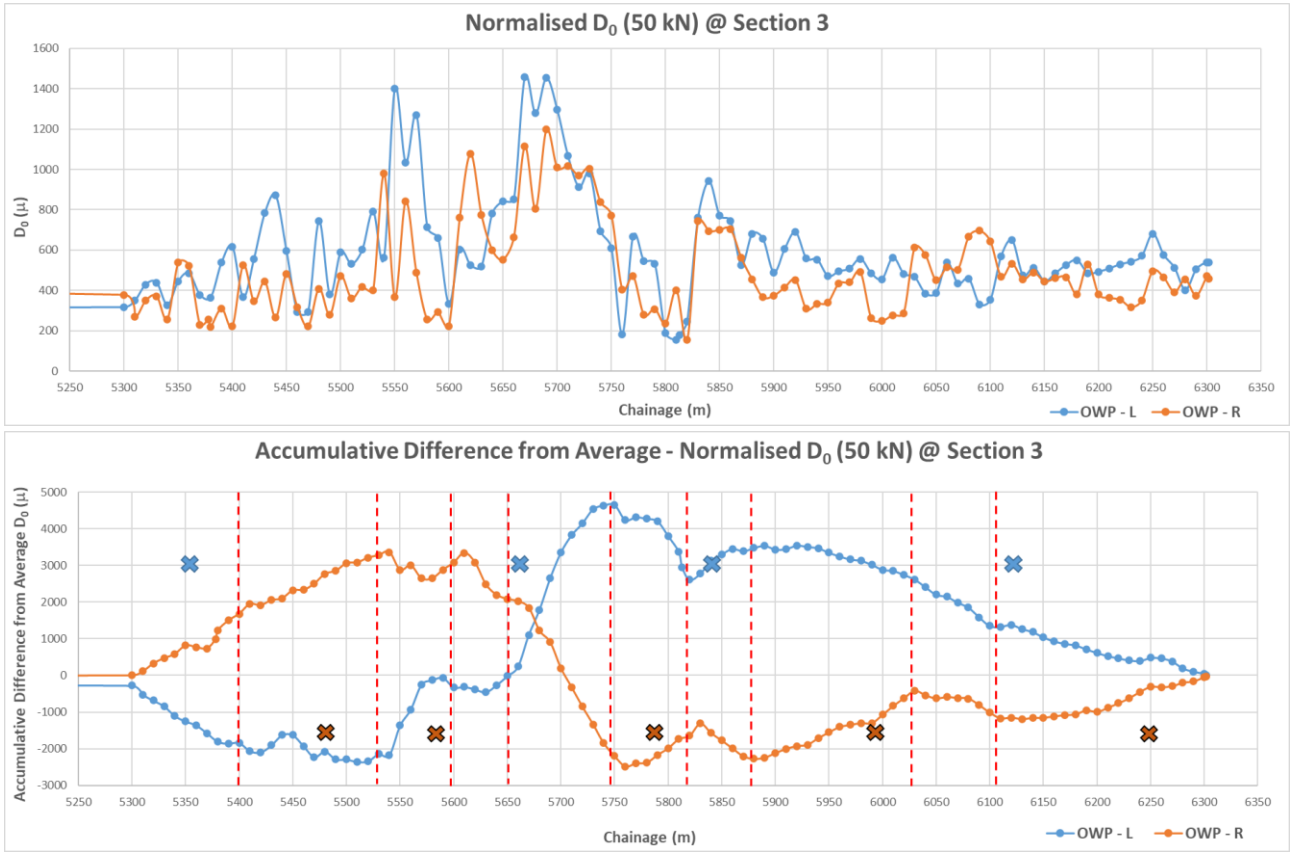

Figure 3.7 Consideration of high and low deflections in defining the test locations

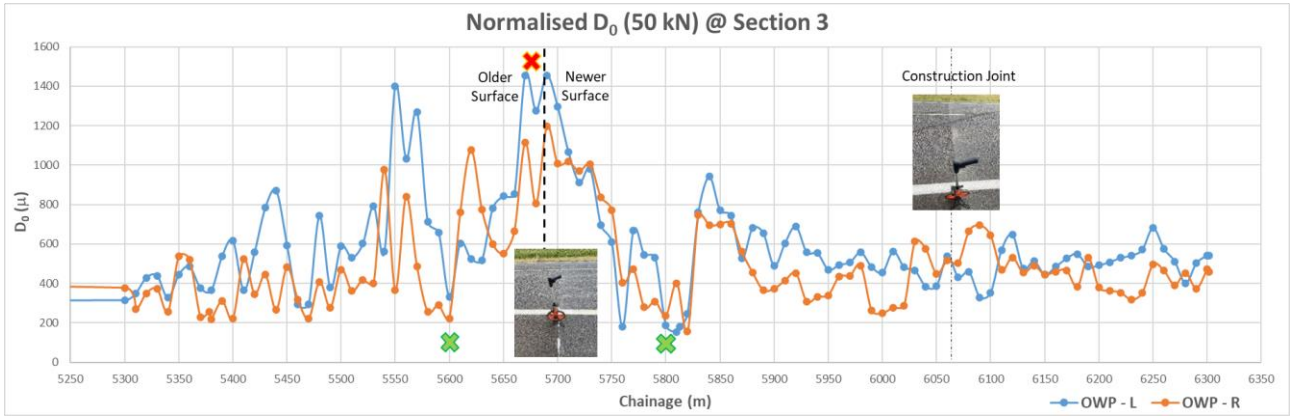

To investigate the lower subgrade , the original test plan was to have one core on each direction to be carried out to the depth of 2m. However, for Section 3 in right direction it was necessary to excavate to a 2 m depth at two sites to provide sufficient subgrade material for laboratory testing. Figure 3.8 illustrates the locations of the tests.

Figure 3.8 Section 3 pavement investigation locations and investigation depths

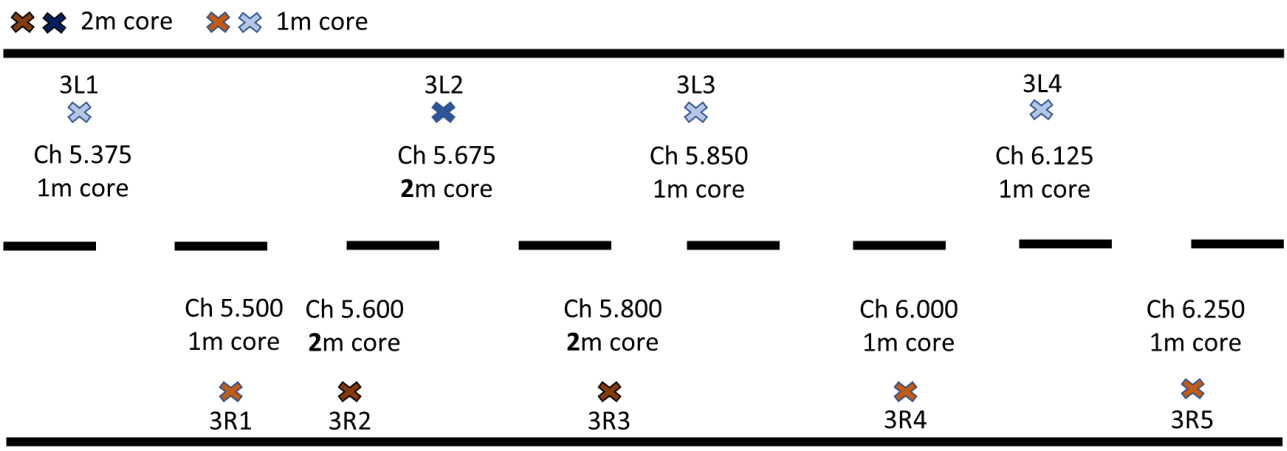

3.3.1 Field Sampling

The pavement investigations were conducted by the contractor according to the plan.

At each test site, the thick asphalt layer was firstly cored and the push tube sampling method was used to sample the granular materials and subgrade as demonstrated in Figure 3.9 and Figure 3.10.

Figure 3.9 Push tube sampling through hammering and core sampling with diamond coring

The samples collected were carefully packed and sealed to prevent change in moisture within the tubes. The documentation including field sheets and photographs were maintained to cover all field activities and details of the operation.

Figure 3.10 Sampling (depth of 1m & 2m), packing the pushed tubes and documenting the samples

The field data sheets and geotechnical logs for the first round of data collection are provided in Appendix A.

3.3.2 In situ Testing

Dynamic Cone Penetrometer Test

DCP test was carried out on each test site on the top of subgrade. Figure 3.11 shows the DCP testing at the site.

Figure 3.11 DCP test on each test point

Subgrade Temperature and Moisture Content

The temperature and moisture content at different depths in the subgrade were measured and recorded for each test point by using the prob as demonstrated in Figure 3.12,

Figure 3.12 On site measurements of temperature and moisture content

In situ testing details and results were recorded in the field data sheets which are provided in Appendix A.

Pavement Reinstatement

Upon completion of the sampling and testing at each test location, certified road base material and cold mix asphalt were utilised for the reinstatement of the sampled boreholes. As illustrated in Figure 3.13, backfill materials were compacted in layers using manual and hydraulic compactor.

Figure 3.13 Reinstating using certified road base and cold mix AC

3.3.3 Laboratory Testing

All samples collected at the site were sent to the laboratory in Brisbane, Queensland for further investigations and testing. Figure 3.14 provides an overview of samples in the laboratory.

Figure 3.14 All samples in the laboratory

Following laboratory tests were performed.

- Atterberg Limits (PL, LL & PI)
- Linear Shrinkage (LS)

- Particle Size Distribution (PSD)
- California Bearing Ratio (CBR)
- Field Moisture Content (FMC)
- Maximum Dry Density (MDD)
- Unconfined Compressive Strength (UCS).

Table 3.5 provides an overview of the laboratory testing program.

Table 3.5: Test arrangements for sections 1 and 3

Sample ID	AS1289.03.1.1, 3.2.1,3.3.1 – Atterberg's Limit	AS1289.3.6.1 – PSD	AS1289.6.1.1 – CBR (includes MDD) - 4day soaked	Comment
BH 1L1 (1.27-2.47m)			Y	
BH 1L1 (0.89-1.27m)	Y	Y		
BH 1L3 (1.25-2.21m)			Y	
BH 1L3 (0.77-1.04m)	Y	Y		
BH 1R2 (0.51-1.55m) + (1.58-2.180m)			Y	BH 1R2 (0.51-1.55m) + (1.58-2.180m)
BH 1R2 (0.51-0.80)	Y	Y		
BH 1R4 (1.260-2.220m)			Y	
BH 1R4 (0.84-1.23m)	Y	Y		
BH 3L3 (0.40-1.05m) + BH 3L4 (0.8-1.07m) + BH3L1 (0.51-0.56m) + (0.70-1.00m)	Y	Y	Y	BH 3L3 + BH3L4 + BH3L1
BH 3R2 (0.58-1.08m) + (1.50-2.09m)			Y	BH 3R2 (0.58-1.08m) + (1.50-2.09m)
BH 3R2 (1.10-1.14m)	Y	Y		
BH 3R4 (0.73-1.03m) + BH 3R5 (0.93-1.05m) + BH 3R1 (0.83-1.10m)			Y	BH 3R4 + BH 3R5 + BH 3R1
BH3R1 (0.50-055m) + (0.60-0.83m)	Y	Y		BH 3R1 (0.50-055m) + (0.60-0.83m)

The laboratory test results for the first round of data collection are presented in Appendix A.

3.4 Second Round of Data Collection

The data collection exercise was repeated on 7 to 10 December 2023. The data was collected all three sections. Push tube and core samples were reduced based on the available data. The laboratory testing was not conducted except moisture testing in accordance with AS1289.2.1.1. In situ moisture and field density testing was also performed. Figure 3.15 shows core and push tube sampling locations. The data collection in the second round including FWD, geotechnical logs and testing details are provided in Appendix B. Note that the TSD data collected during this round is not valid due to technical issues with iPAVE3 and cannot be used for analysis.

Figure 3.15 Coring and boring and documenting the samples for second round of data collection

3.5 Third Round of Data Collection

The final round of field data collection was carried out on 29 April to 1 May 2024. The data was collected from all three sections. FWD and TSD data was collected on similar times to avoid any variation due to change in temperature and moisture. Push tube and core samples were reduced based on the available data. The laboratory testing was not conducted except moisture testing in accordance with AS 1289.2.1.1. Figure 3.16 shows cores and push tube sampling locations. In situ moisture and density testing was performed. The data collection in the third round including FWD and TSD data, geotechnical logs and testing details are provided in Appendix C.

Note that the TSD data collected during third round is valid and used for data analysis and interpretations.

Figure 3.16 Coring and boring and documenting the samples for third round of data collection

3.6 Overview of Data Collection

Table 3.6 provides an overview of the data collected as a part of this project for al three sections.

Table 3.6: Overview of data collected as a part of this project

Data	First data collection	Second Data collection	Third data collection	Comment
FWD	✓	✓	✓	
TSD	x	x	✓	First and second TSD dada collections are not valid due to technical problem in iPAVE3
Coring/Puch Tube Sampling	✓	✓	✓	Second and third data collections has limited core and push tube test points
In situ moisture testing	✓	✓	✓	
Laboratory testing (Atterberg limits, MDD, CBR)	✓	x	x	

4 Pavement and Geotechnical Interpretations

4.1 Pavement Structure and Materials

Table 4.1shows a typical pavement structure based on pavement cores and push tube samples and geotechnical logs of Section 1 – full depth asphalt pavement.

Table 4.1: Typical pavement structure and materials – Section 1 (Thick asphalt on Granular)

Type of Material	Material Description	Estimated Thickness (mm)	Condition
Asphalt	Asphalt surfacing, 7 – 10 mm aggregate	30	Very dense
Asphalt	Asphalt intermediate course, 10 – 14 mm aggregate	100-240	Very dense
Granular (Fill)	Silty sandy gravel Fine to coarse subangular gravel, fine to course low plasticity sand	340-450	Dense to very dense
Natural	Silty sandy clay Low to medium plasticity	80-320	Stiff to very stiff
	Silty sand Fine to medium sand, medium to high plastic fines	100-420	Medium dense
	Clay Highly plastic	1150	Stiff to hard

Table 4.2 shows a typical pavement structure based on pavement cores and push tube samples and geotechnical logs of Section 3 – granular with thin asphalt surfacing.

Table 4.2: Typical pavement structure and materials – Section 3 (Thick asphalt on Granular)

Type of Material	Material Description		Estimated Thickness (mm)	Condition
Asphalt	Asphalt surfacing, 7 – 10 mm aggregate		150-200	Dense/very dense
Granular (Fill)	Silty Sandy Gravel Fine to coarse subangular gravel, fine to course low plasticity sand		220-580	Very dense
Natural	Silty sandy clay		150-600	Very stiff to hard

Table 4.3 shows a typical pavement structure based on pavement cores and push tube samples and geotechnical logs of Section 2 – granular with sprayed seal.

Table 4.3: Typical pavement structure and materials – Section 2 (granular with sprayed seal)

Type of Material	Material Description	Estimated Thickness (mm)	Condition
Seal	Sprayed seal, 14 mm aggregate	20-35	Dense/very dense
Granular (Fill)	Silty Sandy Gravel/ Fine to coarse subangular gravel, fine to course low plasticity sand	320	Very dense

	Silty sandy clay Alternate layers of sandy silt and silty sandy gravel	180	Very stiff to hard
Natural	Silty clay/clayey silt	850	Stiff to hard

4.2 Laboratory Testing

Table 4.4 summarises the laboratory test results of moisture and CBR for the field trial sections at Ipswich Rosewood Road and New England Highway.

Table 4.4: Summary of laboratory test results – Moisture and CBR

Trial Section	Road/Pavement	Sample ID	Depth (m)	FMC (%)	CBR[1] (%)	MDD (t/m^3)	OMC (%)	Swell (%)
1	Ipswich Rosewood Road (Full depth asphalt)	BH 1L1	1.27-2.47	19.8	7.0	1.66	22.0	1.0
		BH 1L3	1.25-2.21	17.6	7.0	1.75	18.5	1.0
		BH 1R2	0.51-2.18	12.6	3.0	1.81	16.0	3.0
		BH 1R4	1.26-2.22	21.3	2.0	1.59	23.5	4.5
2	New England Highway (Granular with sprayed seal)	BHS SL1	1.03-2.21	16.3	7.0	1.33	33.5	0.5
		BHS SR5	0.71-1.20[2]	12.4	4.5	1.52	28.0	1.0
		BHS SL3	1.10-1.72[3]	14.3	14.0	1.66	21.5	0.5
		BHS SR2	1.58-1.98[4]	27.6	4.0	1.43	33.5	1.5
3	Ipswich Rosewood Road (granular with thin asphalt surfacing)	BH 3L3	0.40-1.05[5]	22.4	5.0	1.61	22.0	1.5
		BH 3R2	0.58-2.09[6]	15.4	3.0	1.67	16.0	3.5
		BH 3R4	0.73-1.03[7]	20.4	3.5	1.57	21.5	3.0

Notes

1. 4 days soaked, standard compaction
2. + BHS SR5, 1.21-1.59 m+1.6-2.03 m
3. + BHS SR3, 0.425-1.030 m
4. + BHS SL2, 0.515-0.950 m
5. + BH 3L4, 0.80-1.07 m + BH 3L1, 0.51-0.56 m + 0.7-1.0 m
6. Exclude 1.08-1.05 m
7. + BH 3R5, 0.93-1.05 m + BH 3R1, 0.83-1.10 m

Table 4.5 summarises the laboratory test results of PSD and Atterberg Limits.

Table 4.5: Summary of laboratory test results – PSD and Atterberg Limits

Trial Section	Road/Pavement	Sample ID	Depth (m)	Particle Size Distribution (%)											Linear Shrinkage (%)	Atterberg Limits (%)			
				13.2 mm	9.5 mm	6.7 mm	4.75 mm	2.36 mm	1.18 mm	0.6 mm	0.425 mm	0.3 mm	0.15 mm	0.075 mm		LL	PL	PI	Weighted PI
1	Ipswich Rosewood Road (Full depth asphalt)	BH 1L1	0.89-1.27	100	100	100	100	99	98	96	93	85	65	54	6.0	23	12	11	1021
		BH 1L3	0.77-1.04	100	99	97	97	93	90	88	86	83	73	65	11.0	49	12	37	3193
		BH 1R2	0.51-0.80	100	100	100	100	100	100	99	99	99	97	86	11.5	37	15	22	2185
		BH 1R4	0.84-1.23	100	100	100	100	100	100	100	99	99	97	96	16.5	80	22	58	5763
2	New England Highway (Granular with sprayed seal)	BHS SL1	1.03-2.21	100	100	100	99	94	93	89	85	81	72	62	Not Reported	69	36	33	2819
		BHS SR5	0.71-1.20[1]	100	99	97	95	89	81	73	70	67	62	58	Not Reported	61	25	36	2507
		BHS SL3	1.11-1.72	100	100	100	100	100	97	77	67	55	37	27	No Reported	38	28	10	666
		BHS SR2	1.58-1.98	100	100	100	100	100	98	95	94	92	88	83	Not Reported	63	32	31	2900
3	Ipswich Rosewood Road (granular with thin asphalt surfacing)	BH 3L3[3]	0.40-1.05[2]	93	88	84	80	70	67	66	66	65	59	53	14.0	61	17	44	2884
		BH 3R2[4]	1.10-1.14	97	95	92	88	81	75	66	62	58	43	34	11.0	41	14	27	1678
		BH 3R4[6]	0.73-1.03[5]	94	93	92	91	88	86	84	84	82	74	60	11.0	35	12	23	1921

Notes

1. + BHS SR5, 1.21-1.59 m+1.60-2.03 m
2. + BH 3L4, 0.80-1.07 m + BH 3L1, 0.51-0.56 m+0.70-1.0 m
3. Sieve 53mm, 100% passing & 37.5mm, 97% passing & Sieve 26.5 & 19mm, 96% passing
4. Sieve 26.5, 100% passing
5. BH 3R5, 0.93-1.05 m + BH 3R1, 0.83-1.10 m
6. Sieve 53mm, 100% passing & 37.5mm, 98% passing & Sieve 26.5mm, 97% passing, Sieve 19mm, 95% passing

5 Pavement Deflection Analysis

5.1 Comparison of iPAVE3 TSD Outer and Inner Wheel Paths

Traditionally, pavement engineers have generally assumed that the OWP deflections are higher than the IWP values when using the FWD. However, the new data reveals a different trend: in many parts of road sections, the IWP deflections are greater than those on the OWP. In several cases, up to 50% of a road segment exhibited higher deflections on the IWP compared to the OWP. This finding challenges the conventional understanding and has significant implications for pavement design and asset management practices, indicating a potential need to revise current assumptions and design methodologies.

With the introduction of the new generation of the Traffic Speed Deflectometer (TSD), there have been significant advancements in both technology and data collection capabilities. The latest TSD models (e.g iPAVE3) are equipped with additional sensors, including those positioned behind the wheel, allowing for precise measurements and the right beam to measure deflection on the Inner wheel path (IWP). This new capability offers a more comprehensive assessment of pavement structural conditions, as it eliminates the need to rely solely on the OWP deflections, which were previously assumed to represent the critical values when using the FWD.

The data collected from the OWP and IWP for 3 trial sections have been plotted for comparison.

5.1.1 Section 1 – Ipswich-Rosewood Road

Figure 5.1 illustrates the TSD deflection for both OWP and IWP for Section 1.

Figure 5.1 TSD deflection (D_0) on OWP and IWP - Section 1 – Ipswich Rosewood Road

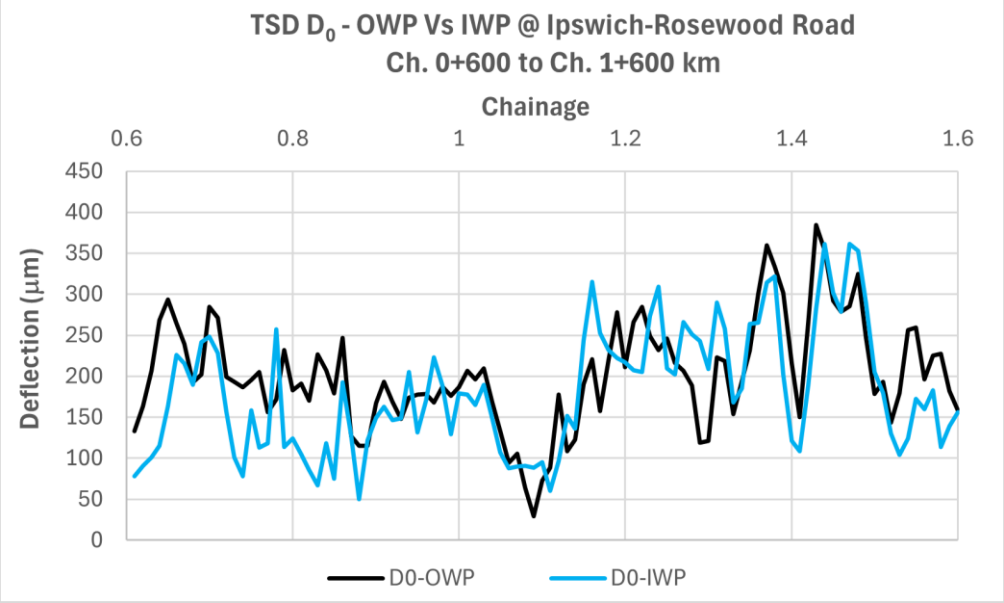

Detailed statistical data for Section 1 is presented in Table **Table 5.1**.

Table 5.1: Deflection statistics for Section 1 – Ipswich Rosewood Road

	TSD D_0 – OWP	TSD D_0 – IWP	TSD D_0 – Max (OWP, IWP)
Mean maximum deflection (mm)	202	181	216
Standard deviation (SD) of D0 (mm)	64	74	65

	TSD D_0 – OWP	TSD D_0 – IWP	TSD D_0 – Max (OWP, IWP)
Coefficient of variation (CoV) (%)	32	41	30
Characteristic variation (CD) (mm)	286	278	302

Note

* Considered coefficient of 1.3 for CD calculation.

Figure 5.2 shows the FWD results for this section.

Figure 5.2 FWD deflection (D_0) on OWP and IWP - Section 1 – Ipswich-Rosewood Road

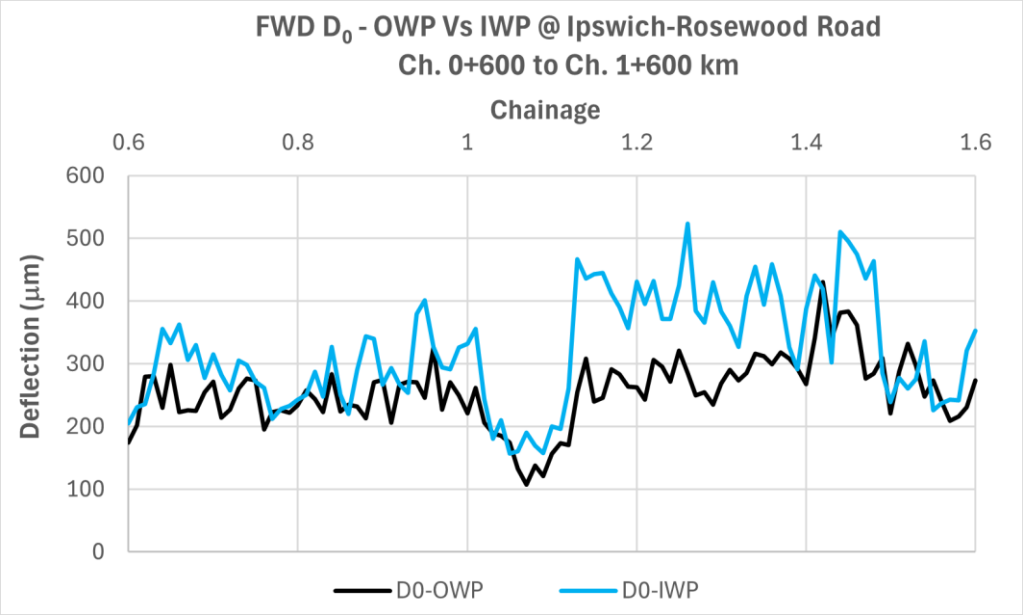

For Section 1, the iPAVE3 OWP D_0 values exceeded the IWP values but the reverse occurred with the FWD measured D_0 values for Section 2 – New England Highway.

Figure 5.3 illustrates the TSD deflection for both OWP and IWP.

Figure 5.3 TSD deflection (D_0) on OWP and IWP - Section 2 – New England Highway

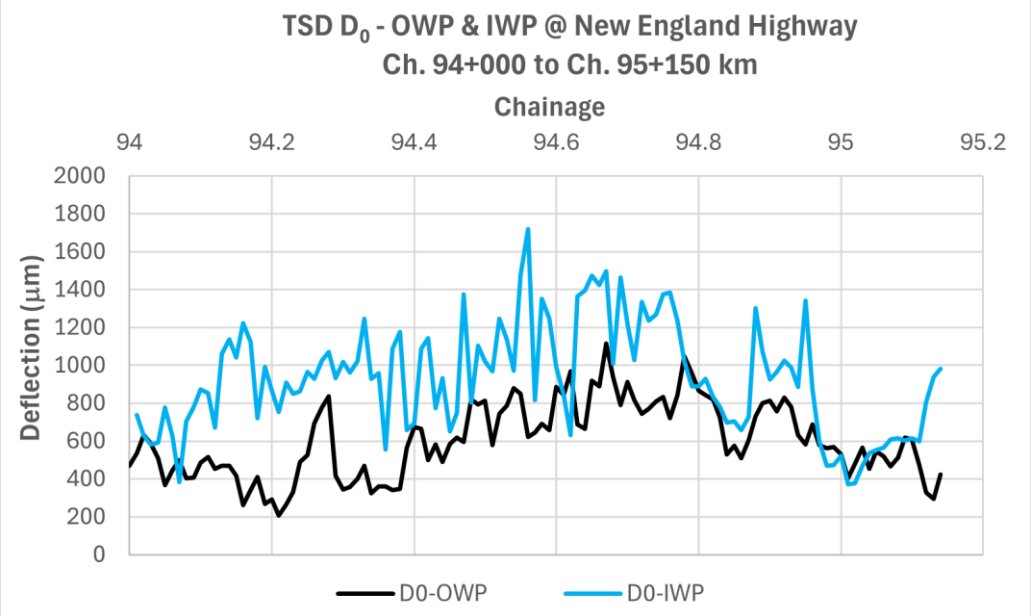

Detailed statistical data for Section 2 is presented in Table 5.2

Table 5.2: Deflection statistics for Section 2 – New England Highway

	TSD D_0 – OWP	TSD D_0 – IWP	TSD D_0 – Max (OWP, IWP)
Average deflection (mm)	604	929	934
Standard deviation (SD) (mm)	196	285	278
Coefficient of variation (CoV) (%)	33	31	30
Characteristic variation (CD) (mm)	863	1305	1301

Note

* Considered coefficient of 1.3 for CD calculation.

A comparison of TSD deflection values revealed that 86% of the test points in this section showed higher deflections on the IWP than on the OWP. This observation contradicts the typical assumption in pavement design that the OWP deflection is critical. As a result, the CD magnitude increased by 51% when the IWP deflections were considered, highlighting the potential risks of underestimating deflections in current road management practices. Such discrepancies could lead to inaccurate estimates of remaining pavement life and an increased likelihood of premature failures.

To further verify these findings and determine whether they are specific to TSD data, FWD data for the same road section were analysed. Figure 5.4 shows the FWD results for this section. The FWD Do values in the OWP and IWP were similar contrary to the iPAVE3 findings.

Figure 5.4 FWD deflection (D_0) on OWP and IWP - Section 2 – New England Highway

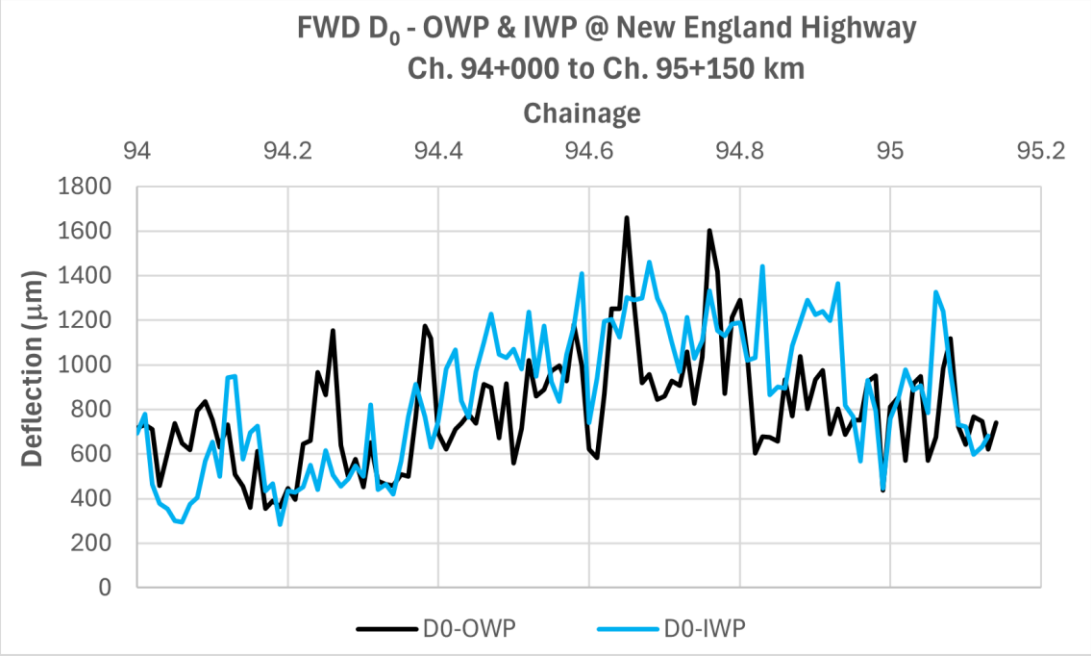

5.1.2 Section 3 – Ipswich-Rosewood Road

The data analysis for Section 3 (Figure 5.5) revealed that the OWP was the critical side for most of the segment (86% of the test points).

For Section 3 the OWP characteristic maximum deflection exceeded the IWP value.

Figure 5.5 TSD deflection (D_0) on OWP and IWP - Section 3 – Ipswich Rosewood Road

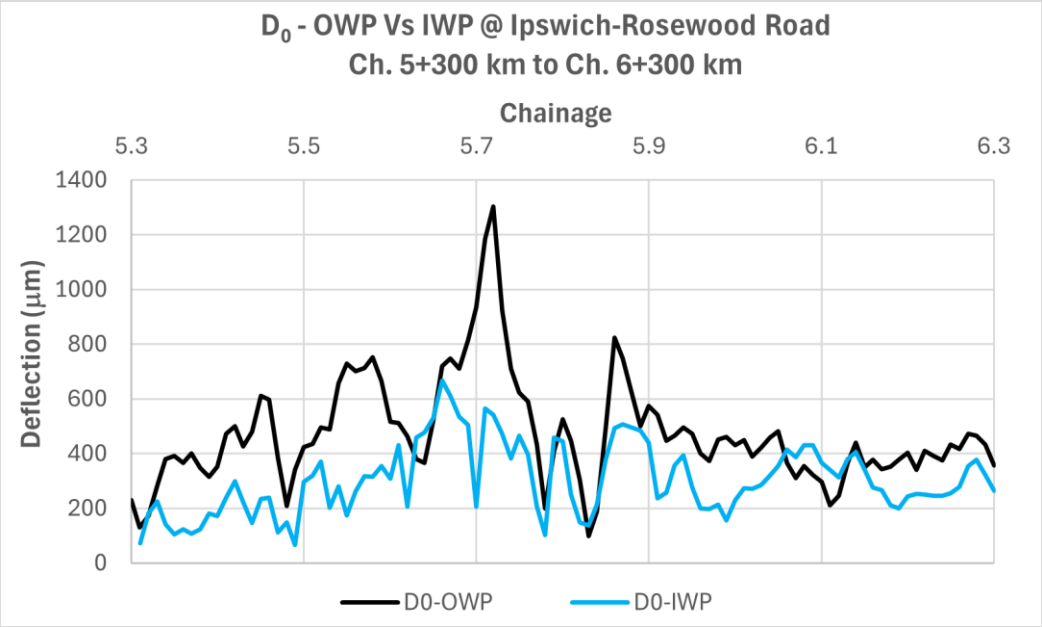

The findings from the comparison of the deflection values on outer and inner wheel paths highlight the importance of incorporating deflection measurements from both wheel paths (OWP and IWP) in pavement assessments. Traditional assumptions in FWD testing that prioritise the OWP as the critical path may overlook significant risks associated with the higher deflections on the IWP. At one test section (Section 1) this assumption was not valid as the IWP characteristic deflection exceeded the OWP value.

The inclusion of IWP data enables asset managers to develop a more accurate understanding of pavement conditions, leading to better-informed design decisions and more reliable estimates of remaining pavement life. Moreover, these insights suggest a need for a revised guideline and methodology in pavement design and asset management practices. Moving forward, the consideration of both wheel paths in deflection analysis should become a standard practice to improve the accuracy of structural evaluations and minimise the risk of unexpected and premature pavement distress.

5.2 Repeatability of iPAVE3 TSD and Comparison of D_0 Results from iPAVE3 with FWD

Since its introduction to Australia in 2014, there has been several exercises aimed at developing a correlation between the deflections measured by the iPAVE with those measured by a falling weight deflectometer (FWD). However, as previously mentioned in this report there are some differences because the FWD is a static measurement that attempts to simulate the response from the moving wheel whilst the iPAVE measurement is a rolling wheel measurement.

Many TSD data users have come to accept that the measurements from the 2 devices do not always have a high correlation but that they can both accurately locate and identify pavement strength trends. This has also been shown in the previously documented literature search. Any linear correlation should be utilized with care, as the correlation may only be applicable to the road or roads that were used to develop the relationship.

Figure 5.6 to Figure 5.23 demonstrate the repeatability of the D_0 measurements made by the iPAVE at each of the 3 test sites and how they compare to the measurements made by an FWD. Only the lefthand wheel path results that were surveyed in the forward (gazettal) direction are shown but it should be noted that they are representative of all the results.

Note that this data was collected using iPAVE3 and that these D_0 values shown in the plots were calculated using the full deflection bowl. Additionally, the FWD D_0 values were not corrected for temperature.

Figure 5.6 Section 2 – New England Highway Chainage 94000m: TSD, Forward Direction, OWP

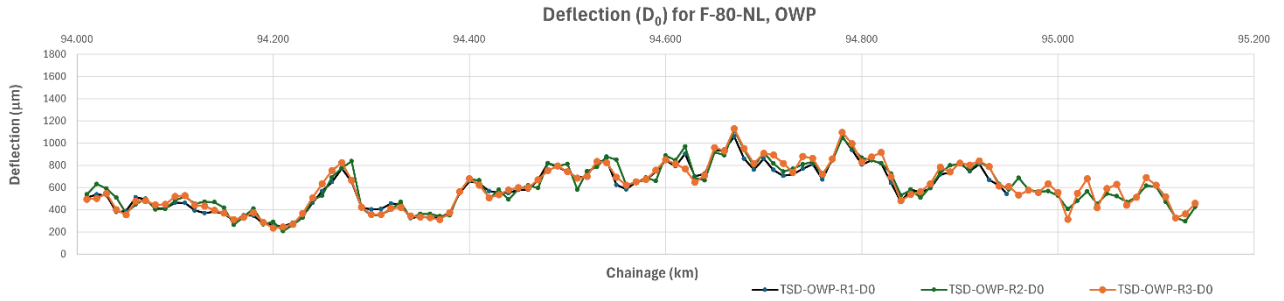

Figure 5.7 Section 2 – New England Highway Chainage 94000m: FWD and TSD, Forward Direction, OWP

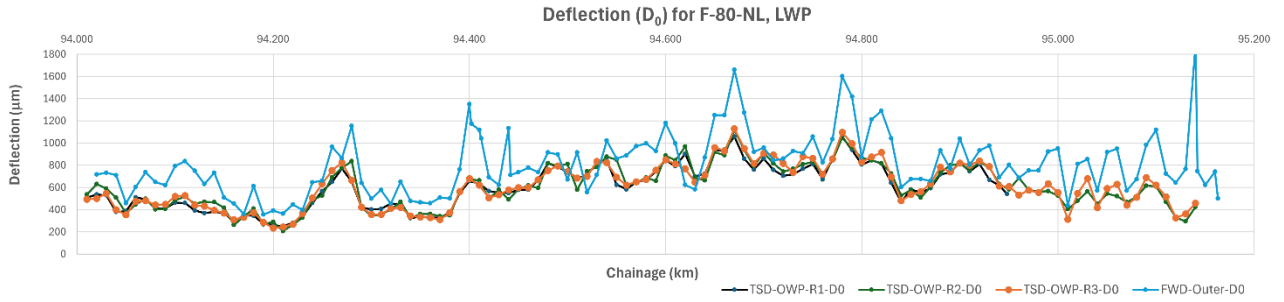

Figure 5.8 Section 2 – New England Highway Chainage 94000m: TSD, Forward Direction, IWP

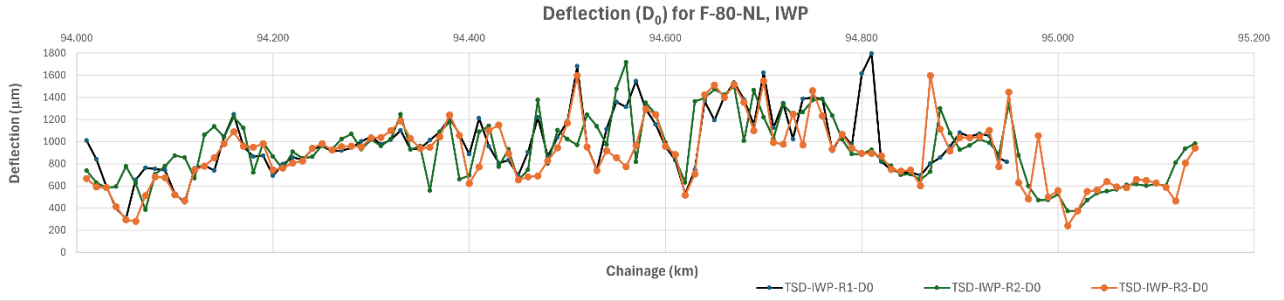

Figure 5.9 Section 2 – New England Highway Chainage 94000m: FWD and TSD, Forward Direction, IWP

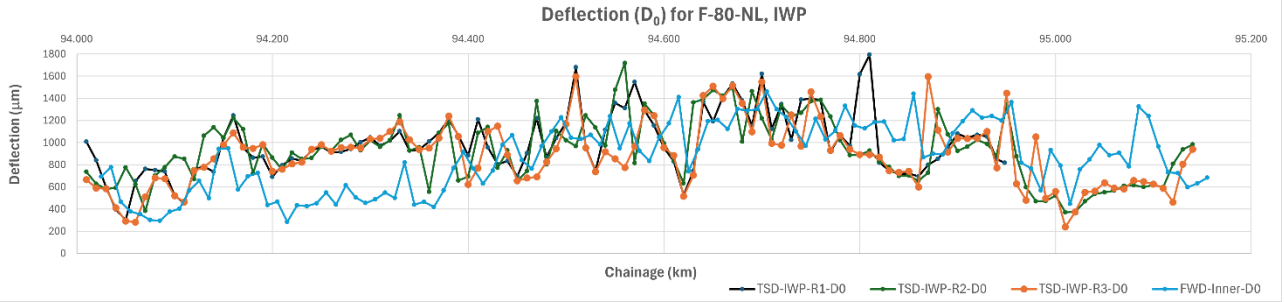

Figure 5.10 Section 2 – New England Highway Chainage 94000m: TSD, Reverse Direction, OWP

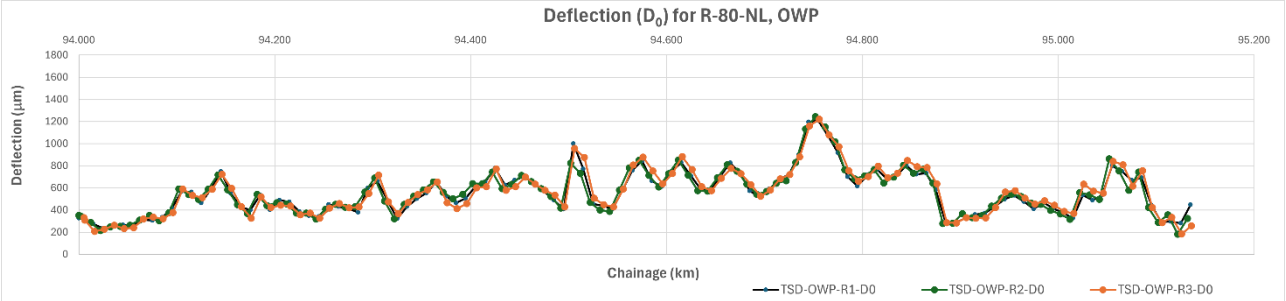

Figure 5.11 Section 2 – New England Highway Chainage 94000m: FWD and TSD, Reverse Direction, OWP

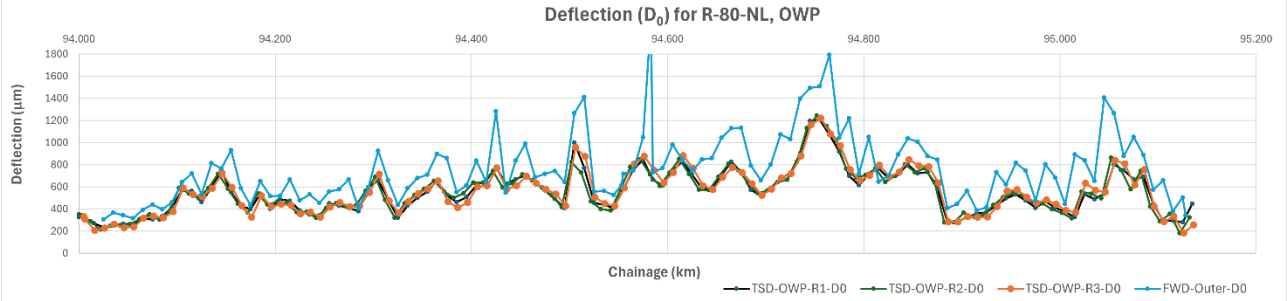

Figure 5.12 Section 1 – Ipswich-Rosewood Road chainage 600m: TSD, Forward Direction, OWP

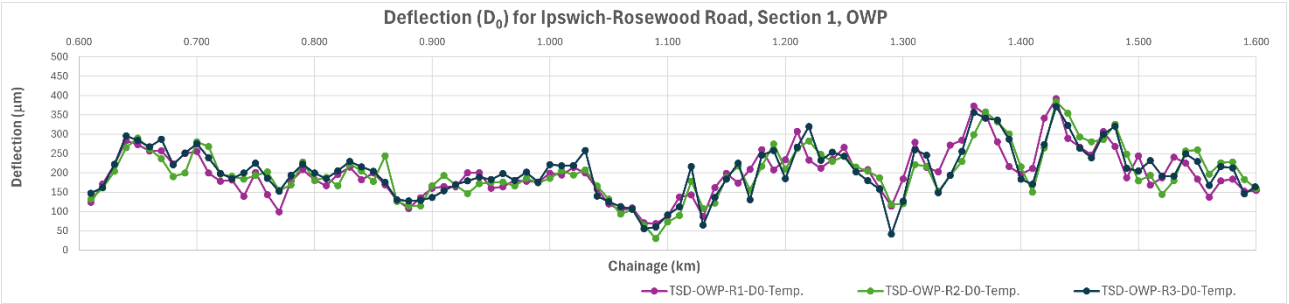

Figure 5.13 Section 1 – Ipswich-Rosewood Road chainage 600m: TSD and FWD, Forward Direction, OWP

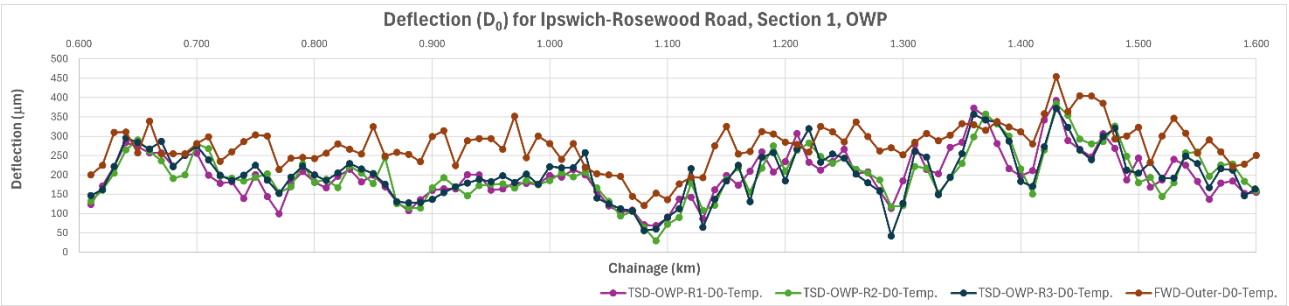

Figure 5.14 Section 1 – Ipswich-Rosewood Road chainage 600m: TSD, Forward Direction, IWP

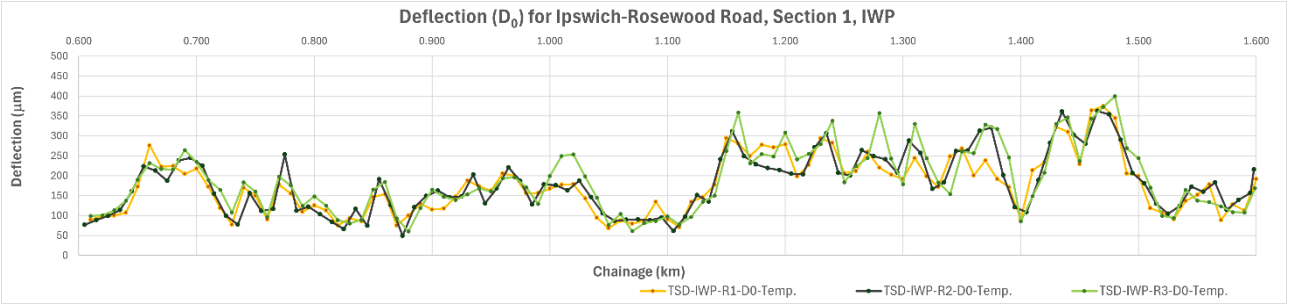

Figure 5.15 Section 1 – Ipswich-Rosewood Road chainage 600m: TSD and FWD, Forward Direction, IWP

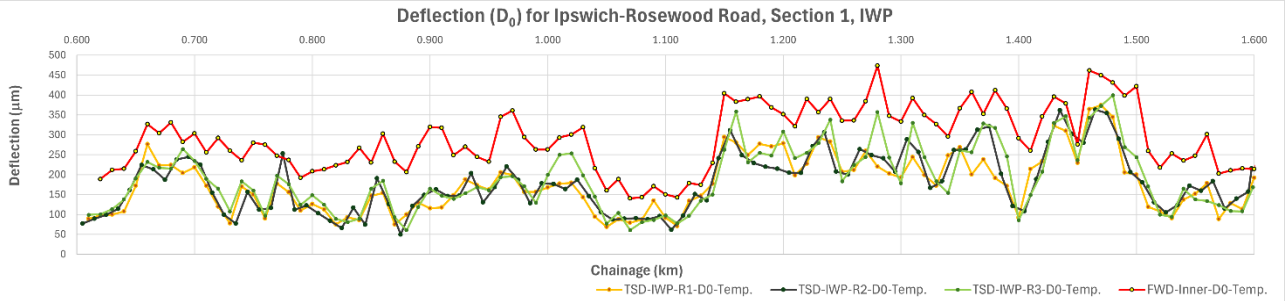

Figure 5.16 Section 1 – Ipswich-Rosewood Road chainage 600m: TSD and FWD, Reverse Direction, OWP

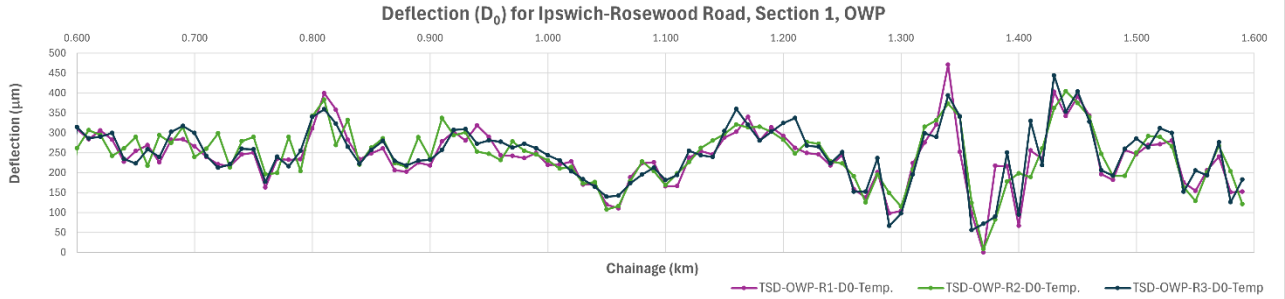

Figure 5.17 Section 1 – Ipswich-Rosewood Road chainage 600m: TSD and FWD, Reverse Direction, OWP

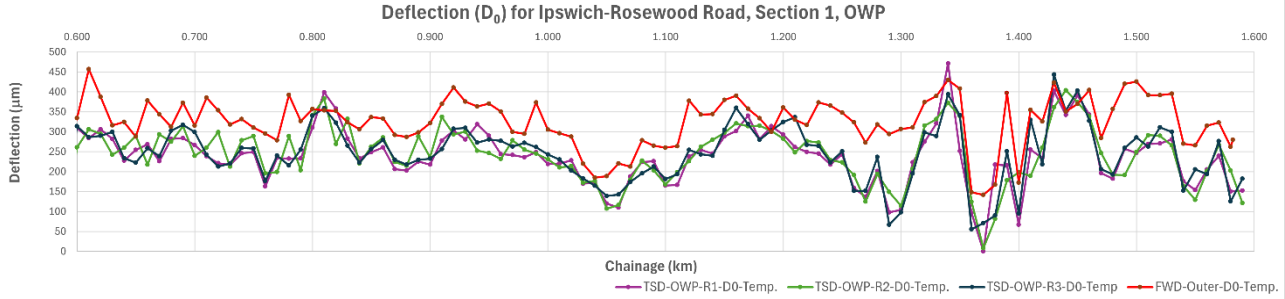

Figure 5.18 Section 3 – Ipswich-Rosewood Road chainage 5300m: TSD, Forward Direction, OWP

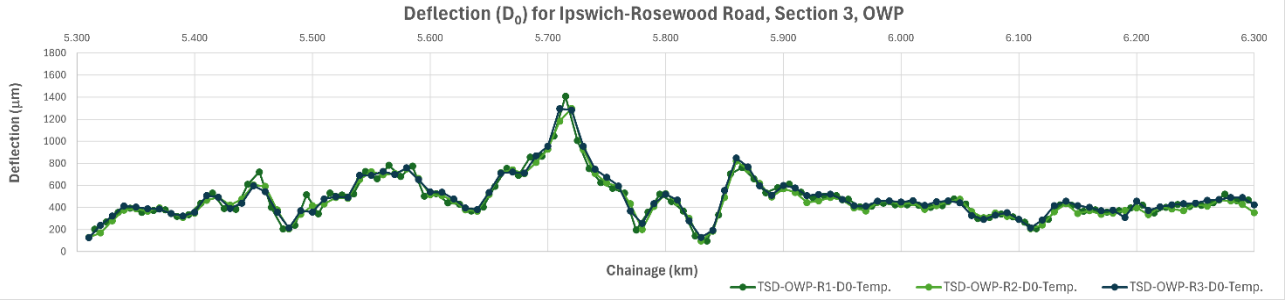

Figure 5.19 Section 3 – Ipswich-Rosewood Road chainage 5300m: TSD and FWD, Forward Direction, OWP

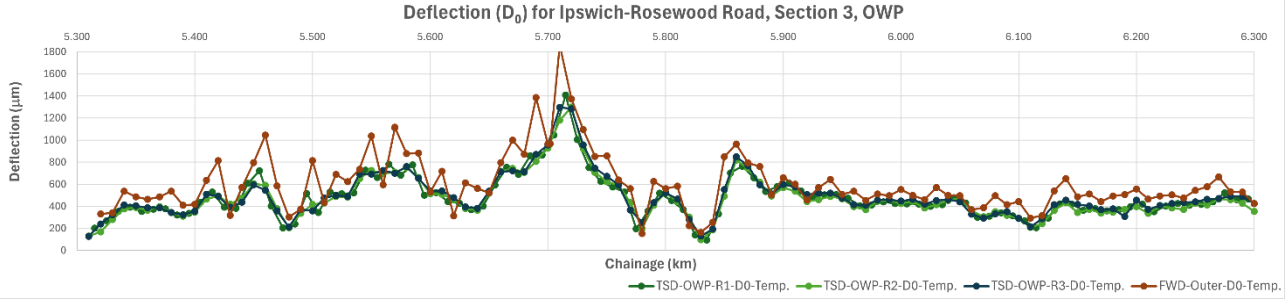

Figure 5.20 Section 3 – Ipswich-Rosewood Road chainage 5300m: TSD, Forward Direction, IWP

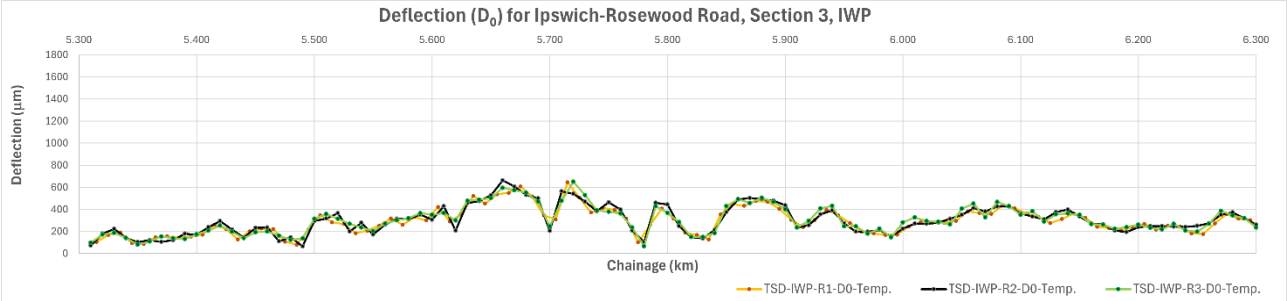

Figure 5.21 Section 3 – Ipswich-Rosewood Road chainage 5300m: TSD and FWD, Forward Direction, IWP

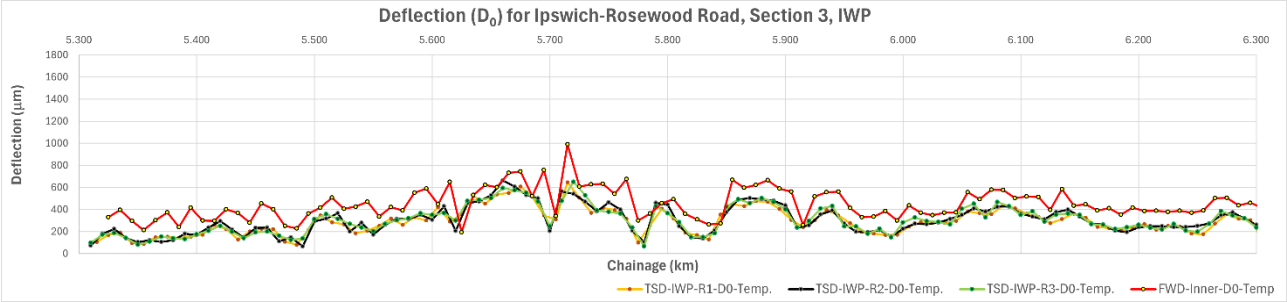

Figure 5.22 Section 3 – Ipswich-Rosewood Road chainage 5300m: TSD, Reverse Direction, OWP

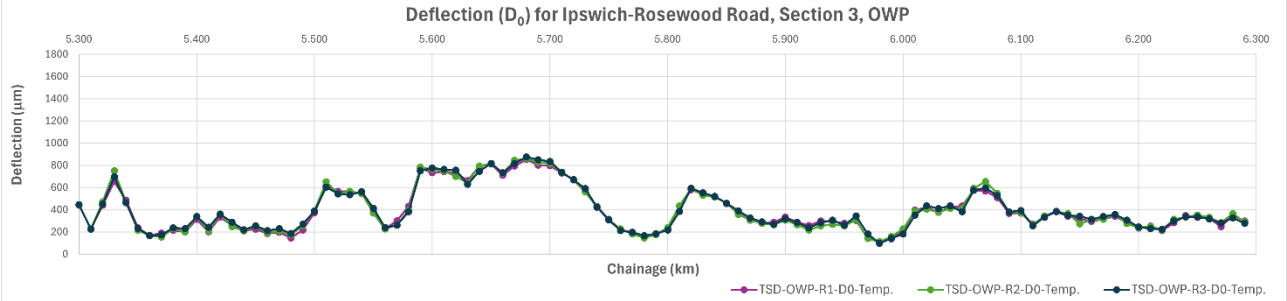

Figure 5.23 Section 3 – Ipswich-Rosewood Road chainage 5300m: TSD and FWD, Reverse Direction, OWP

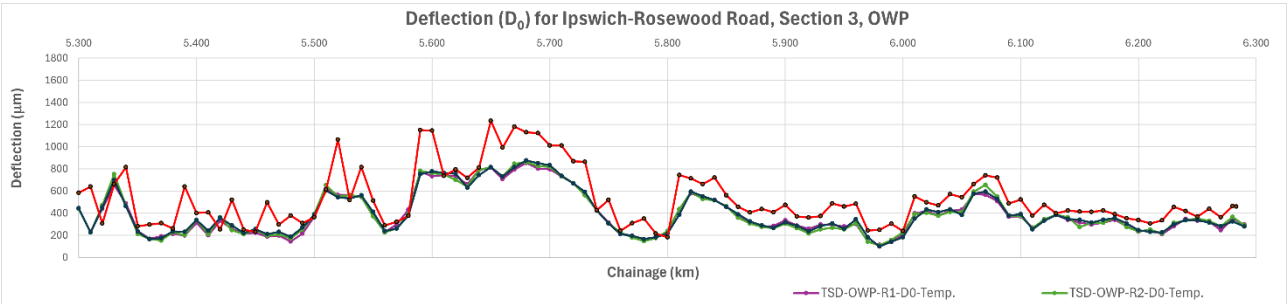

The results from all the test sites exhibited the following features:

- iPAVE3 demonstrated a high level of repeatability
- iPAVE3 and the FWD showed the same pavement strength trends
- the D_0 values measured by the iPAVE3 were lower than those measured by the FWD. The differences were most noticeable at Sites 1 and 2, whereas the iPAVE3 results from Site 3 were still lower, but a lot closer the FWD measurements, particularly for the second half of the site.
- the spikes in the FWD results may be the result of localized defects and are not as noticeable in the iPAVE3 data where the deflection is an average value calculated over the entire 10 m length rather than at a particular point like the FWD.

5.3 Comparison of iPAVE3 deflections with Simulated iPAVE 2 values

To better understand the effect of the extra lasers behind the load and the additional laser located at the 1500 mm position on the deflection measurements, the data from iPAVE3 was analyzed in two different ways and the results were compared.

- The data was processed using the full suite of sensors behind and in front of the load consistent with iPAVE3 , and
- The data was reprocessed excluding the lasers behind the load and setting the slope velocity to zero at the zero location point under the load, thus emulating the way iPAVE2 collects and processes data.

The two methodologies, known as the full bowl and front of load configurations, are shown in Figure 5.24.

Figure 5.24 Measurements configurations – full bowl (left) and front of load (right)

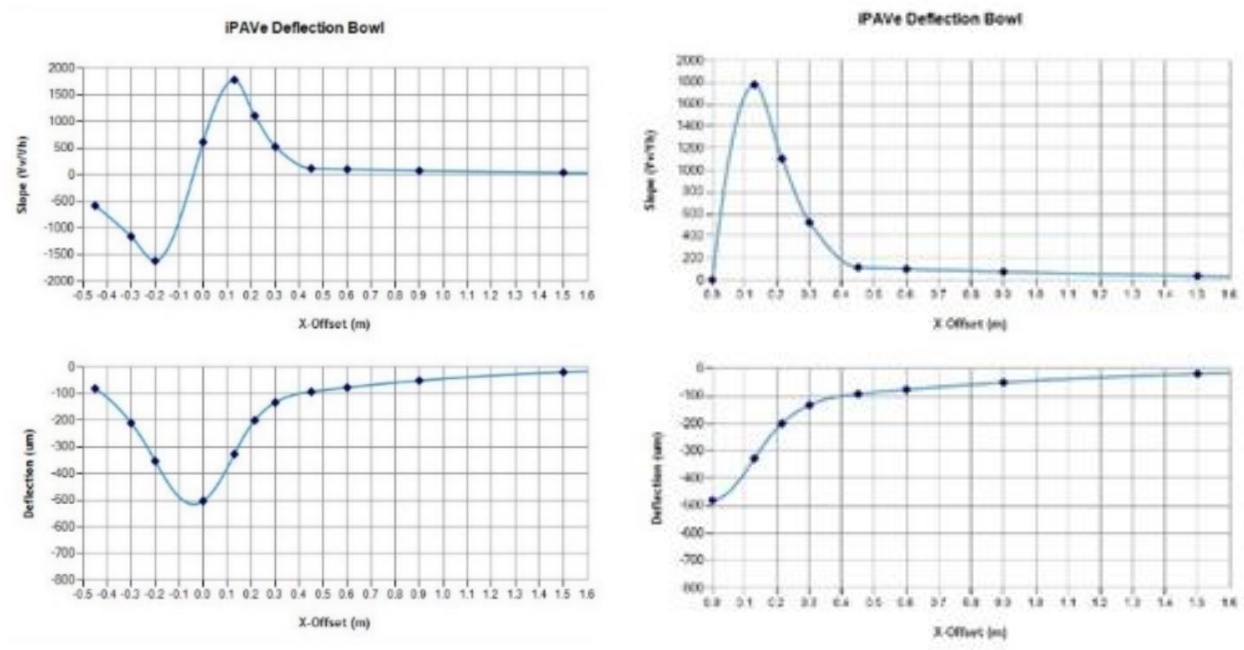

In both instances, the effect of 1500 mm sensor on the results was also investigated by removing it from the analysis for both above configurations.

The data used for the comparisons is from *Section 3 - Ipswich-Rosewood Road Chainage 5300m* and the results are presented in Figures Figure 5.25 to Figure 5.28.

Figure 5.25 highlights the difference in the D_0 values measured when only the sensors in front of the load are used compared to the full sensor configuration. As discussed, the deflection measurements calculated using the full deflection bowl should be larger than those produced using the front of load methodology and this is what the results show.

Figure 5.25 Comparison of D_0 values; front of load versus full bowl and excluding 1500mm sensor

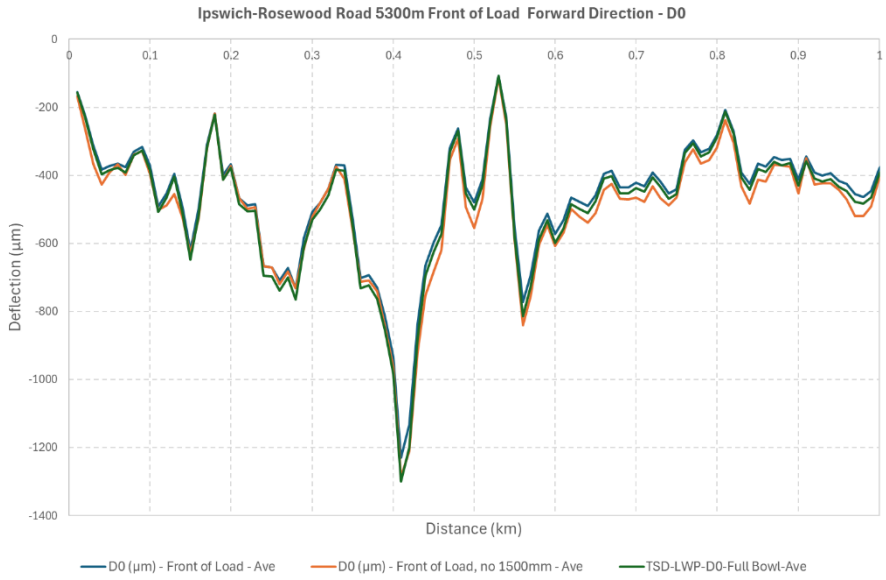

It is also interesting to note that the exclusion of the sensor at 1500 mm position results in an increase in deflection. This indicates that the curve fitting algorithm used to join the individual points of the velocity slope curve increases the area under the curve compared to when the slope velocity measured by the 1500 mm sensor is included (which means the line of the curve between the 900 and 3500 mm sensors generated by the algorithm passes at a higher point than when the 1500 mm sensor is included).

SCISUB, or the subgrade SCI, is defined as the deflection at the 900 mm location minus the deflection at the 1500 mm position (D900-D1500) . Figure 5.26 shows that there is a difference in this value when the 1500 mm sensor is excluded from the analysis, and this could have potential ramifications for subgrade assessments. Additionally, there is no difference in the SCISUB values measured using the front of load and full bowl configurations as the sensor positions are the same for the two configurations. Therefore, only one of these plots is visible in Figure 5.26, this case it is the SCISUB line plot sing the full bowl configuration, as two plots overlay each other perfectly.

Figure 5.26 Comparison of SCISUB values; front of load only

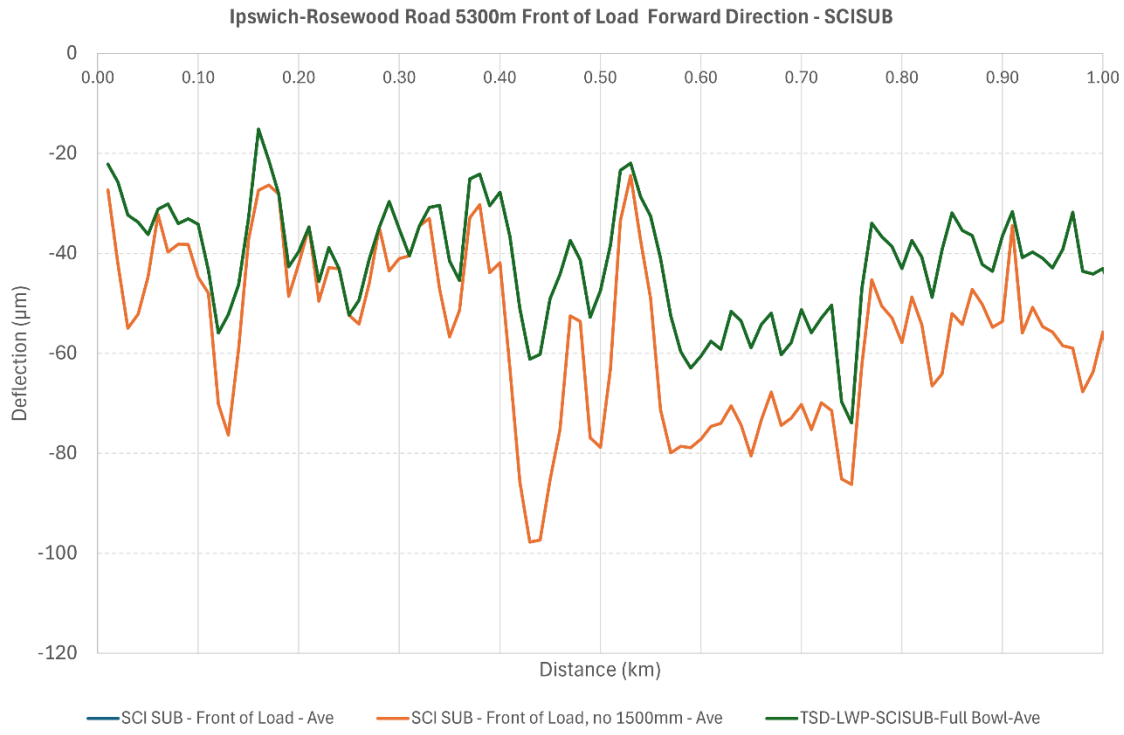

Figure 5.27 further highlights the difference in the SCISUB measurements by making a direct comparison of the deflection measurements at 1500 mm position for the front of load configuration.

Figure 5.27 Comparison of D_{1500} values; front of load only

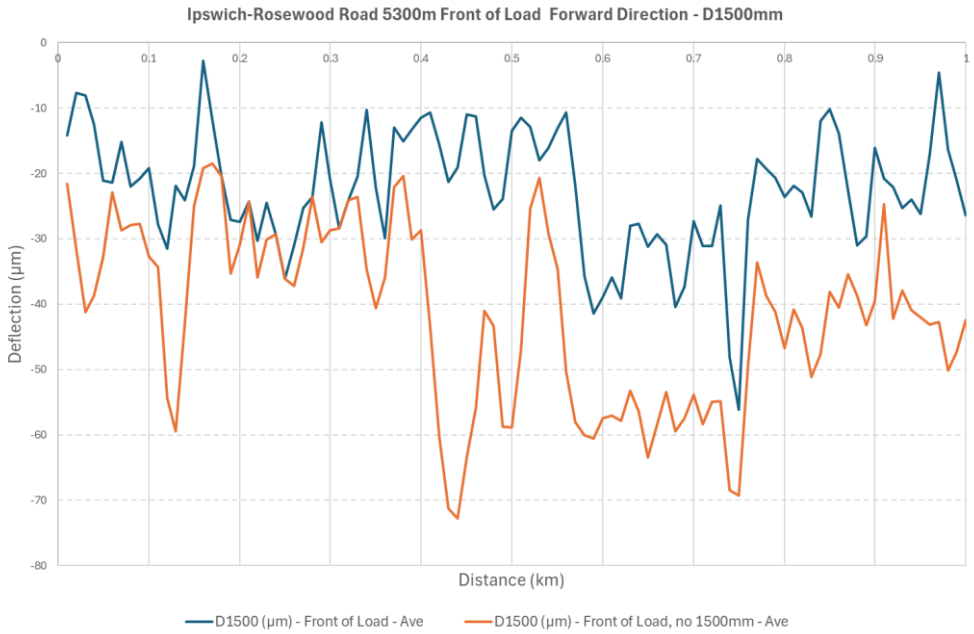

Finally, Figure 5.28 demonstrates the effect of excluding the 1500 mm sensor from the full bowl configuration. Once again, it follows the same pattern as was seen with the front of load sensor configuration.

Figure 5.28 Comparison of D_0 values; full bowl, with and without D_{1500} sensor

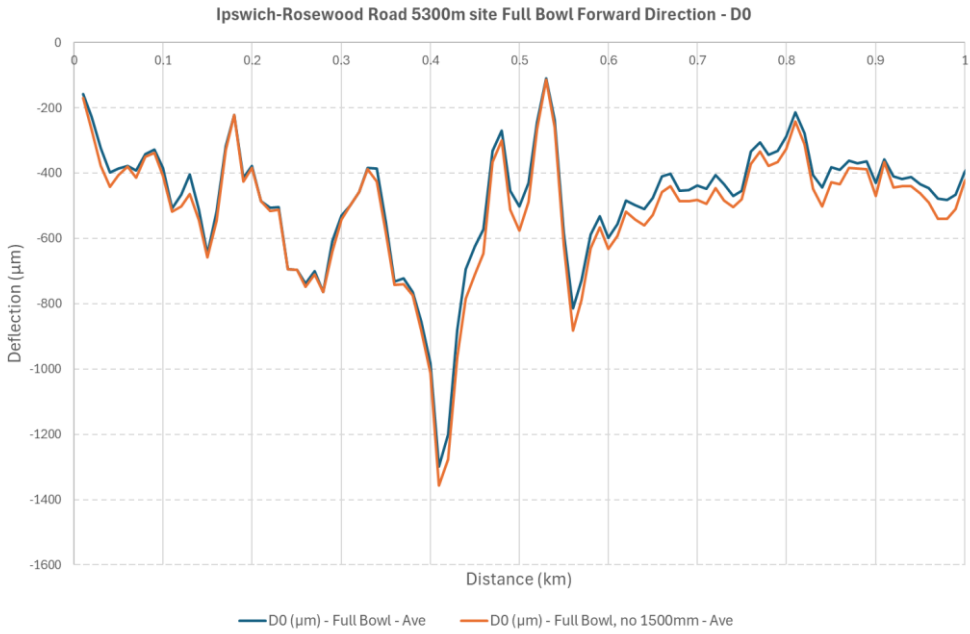

From the information above there is a high likelihood that the D_0 values produced by iPAVE2 and iPAVE3 will be different. The analysis showed that the D_0 values from iPAVE3 were larger than those from iPAVE2. However, the comparison methodology did not consider the longer length of the slope velocity curve exhibited by iPAVE2. Additionally, the inclusion/exclusion of the 1500 mm sensor can change the SCISUB and D_{1500} measurements. Further research be considered to develop a reliable relationship between iPAVE3 D_0 and iPAVE2 D_0 as follows:

D_0 (iPAVE3) = a x D_0 (iPAVE2)

5.4 Curvature Results

In pavement terminology, curvature or the structural condition index (SCI200), is defined as being the difference between the pavement deflection measured directly under the load and 200 mm in front of the load. Curvature is an important measurement for pavement management engineers who use this statistic to assess the structural capacity of the road to help determine whether the pavement can support expected traffic loads without failure.

5.4.1 FWD versus iPAVE3

A direct comparison was made between the curvature values obtained from the FWD (single survey) and the average of 3 runs from the iPAVE3 at each of the 3 test sites in the forward direction of travel. The results for both wheel paths are highlighted in Figure 5.29 through Figure 5.34. Whilst only the average curvature values are shown in the plots, it should be noted that at all sites there was good repeatability between the individual iPAVE3 runs. Both the iPAVE3 and FWD data was collected in April 2024.

Figure 5.29 Outer wheel path curvature Ipswich-Rosewood Road Section 1 – FWD v iPAVE3

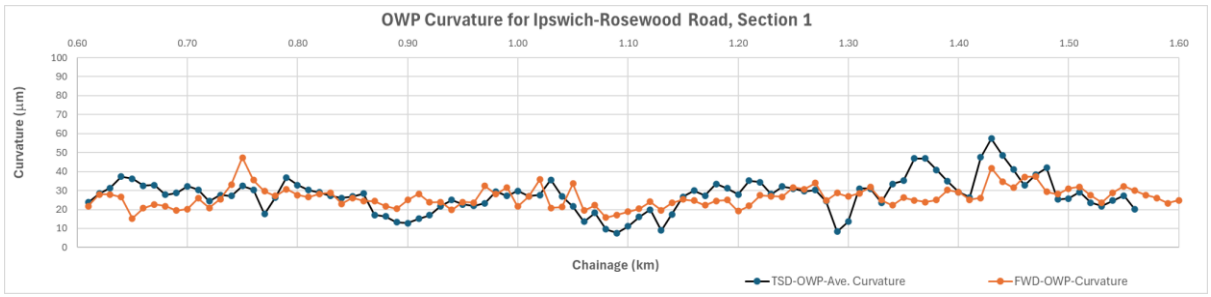

Figure 5.30 Inner wheel path curvature Ipswich-Rosewood Road Section 1 – FWD v iPAVE3

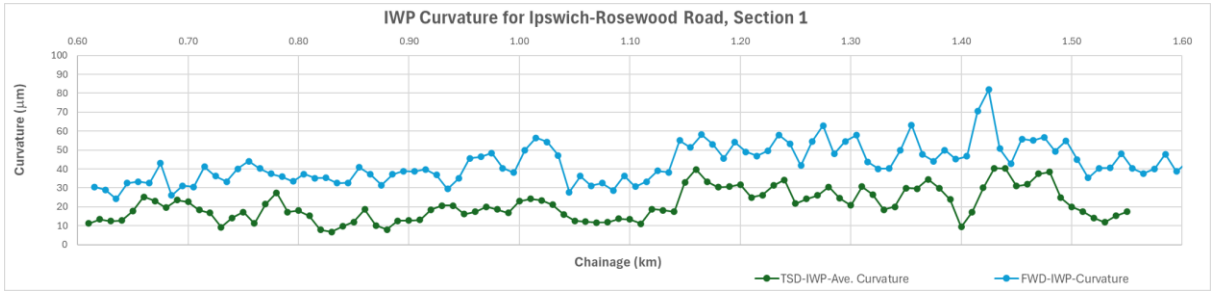

Figure 5.31 Outer wheel path curvature Ipswich-Rosewood Road Section 3 – FWD v iPAVE3

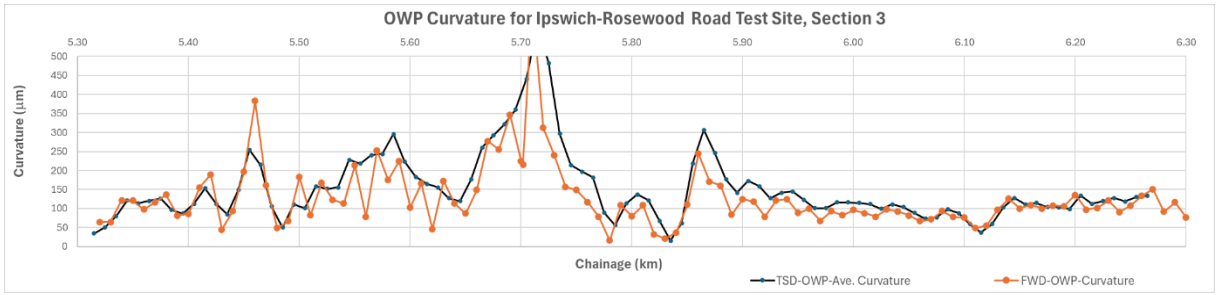

Figure 5.32 Inner wheel path curvature Ipswich-Rosewood Road Section 3 – FWD v iPAVE3

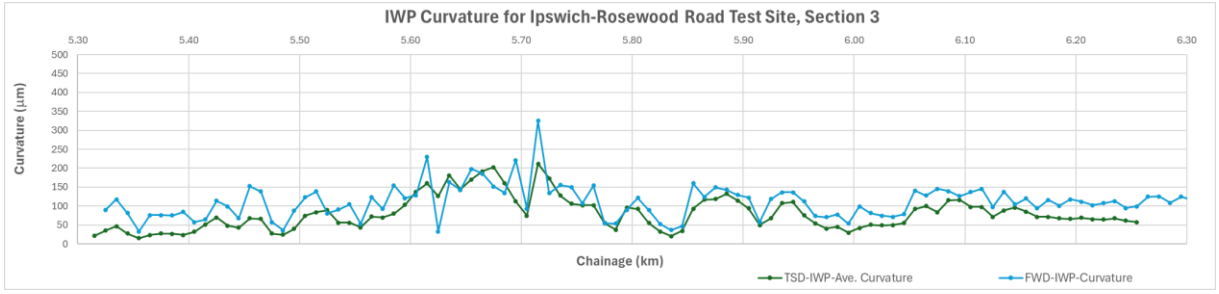

Figure 5.33 Outer wheel path curvature New England Highway Section 2 – FWD v iPAVE3

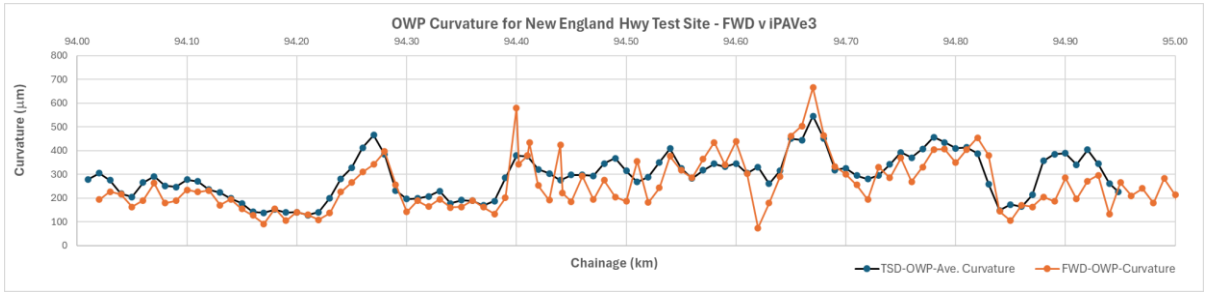

Figure 5.34 Inner wheel path curvature New England Highway Section 2 – FWD v iPAVE3

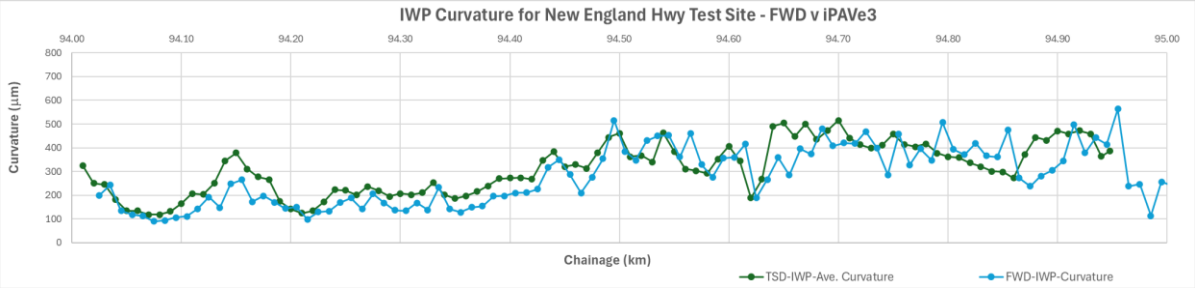

As shown in the above figures, there was good agreement in general between the FWD and iPAVE curvature values in both wheel paths at all 3 test sites, with the line plots from both devices showing the same trends and often intersecting each other. The 2 exceptions were in the inner wheel path of Sections 1 and 3 on the Ipswich-Rosewood Road where the FWD curvature values were higher than those from the iPAVE. However, as can be seen in Table 5.3, the magnitude of the difference in the average curvature value for each wheel path for each device was similar for the other paired results.

It was also interesting to note the much lower curvature values measured along Section 1 of the Ipswich Rosewood Road test site. This likely due to the pavement type which is a spray seal over full depth asphalt.

Table 5.3: Curvature statistics for test sections

Location	Statistics	iPAVE-Outer-Curvature (µm)	FWD-Outer-Curvature (µm)	iPAVE3-Inner-Curvature (µm)	FWD-Inner-Curvature (µm)
Ipswood Road – Section 1	Average	28	26	21	43
	Stdev	9	5	8	10
Ipswood Road – Section 3	Average	152	131	79	111
	Stdev	93	87	44	45
New England Highway – Section 2	Average	292	261	312	282
	Stdev	91	114	109	124

5.4.2 Variation in Curvature Values Over Time

FWD testing was performed 3 times across each of the test sites over a 12-month period from April 2023 to April 2024 thus providing an opportunity to determine the magnitude of any potential seasonal variation in the curvature readings. Only the outer wheel path results are shown as this was the only wheel path that was tested on all 3 occasions.

As can be seen in Figure 5.35, Figure 5.36 and Figure 5.37 there is generally good agreement between the curvature results that were measured in April in both years at all 3 sites. However, there was an increase in December 2023 curvature values at the 2 asphalt test sites on the Ipswich-Rosewood Road. As October to March is generally rainy season in Queensland and April starts to dry out till October. The testing was performed in the wet season, so this result is not unexpected. Contrastingly, the New England Highway spray sealed site did not show the same trend with the curvature values being similar to those measured in April 2023 and April 2024.

Figure 5.35 FWD outer wheel path curvature Ipswich-Rosewood Road Section 1 - variation with time

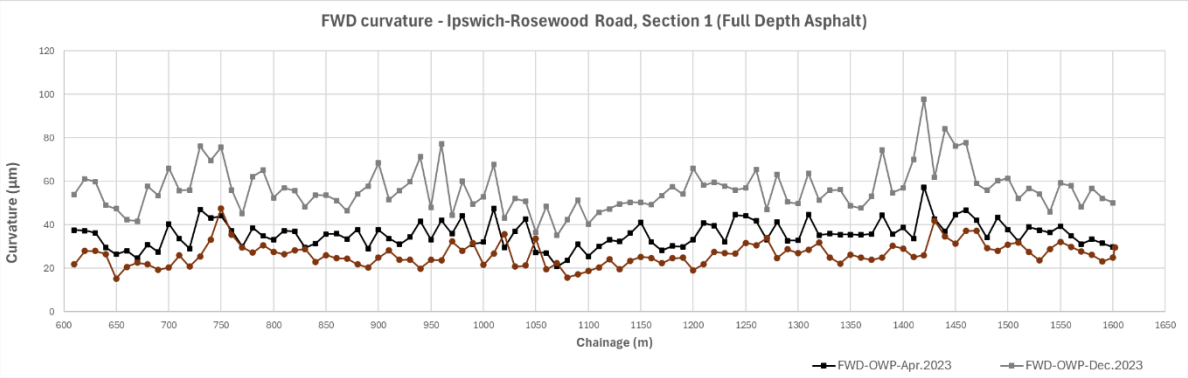

Figure 5.36 FWD outer wheel path curvature Ipswich-Rosewood Road Section 3 - variation with time

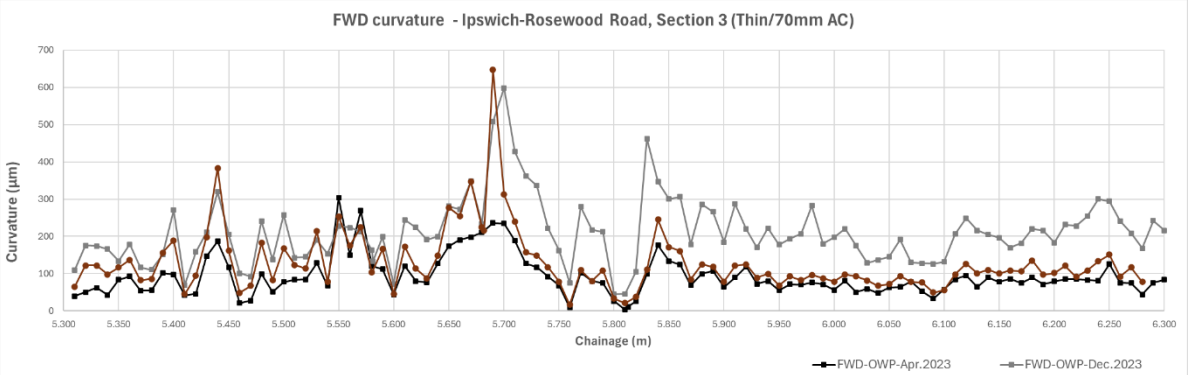

Figure 5.37 FWD outer wheel path curvature New England Highway Section 2 - variation with time

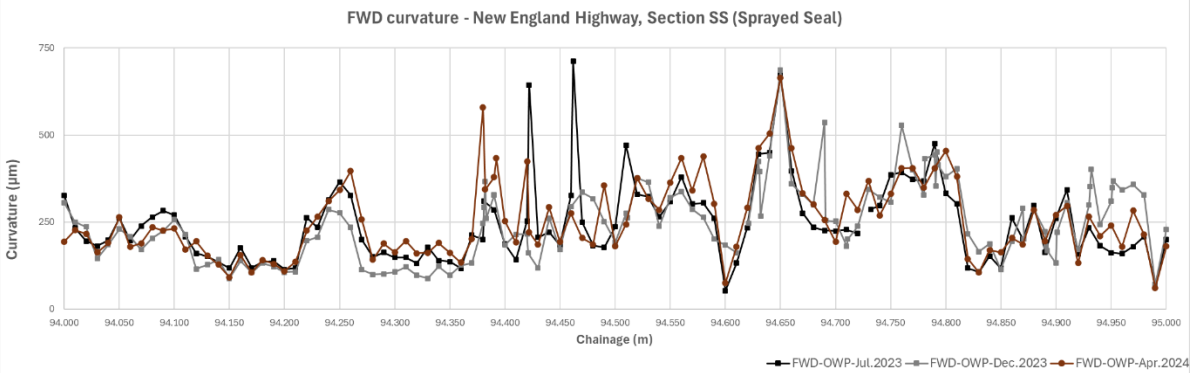

The results shown in Table 5.4 also reconfirm the above observations. However, it should be noted that there appears to be several outliers in the New England Highway test site data but the removal of these values will not drastically change the trends. Additionally, the scale and size of the curvature values for this site are considerably higher than the Ipswich-Rosewood Road sites.

Table 5.4: FWD curvature statistics over time for each test section

Location	Statistics	Curvature April 2023 (µm)	Curvature December 2023 (µm)	Curvature April 2024 (µm)
Ipswood Road – Section 1	Average	36	56	26
	Stdev	6	10	5
Ipswood Road – Section 3	Average	92	210	130
	Stdev	54	90	85
New England Highway – Section 2	Average	245	249	255
	Stdev	117	113	112

5.4.3 Variation in Curvature Values – Full Bowl and Excluding Rear Sensors

As mentioned previously, one of the key differences between iPAVE2 and iPAVE3 is the number and location of the test sensors used to assess the bearing capacity of the pavement (Section 5.1). iPAVE3 has an additional 3 sensors behind the rear axle which allows the modelling of the full deflection instead of assuming the deflection velocity is zero directly under the load (as is the case when determining the deflection bowl with iPAVE2 (**Error! Reference source not found.** and **Error! Reference source not found.**). Using the full bowl, typically always results in larger D_0 values, whilst the D_{200} is essentially the same which subsequently results in larger curvature values as in shown in Figure 5.38, Figure 5.39 and Figure 5.40. For the purpose of this comparison, the same slope velocities were used to generate both data sets, one including the values behind the load and the other only using the forward sensor values and mimicking the iPAVE2 processing algorithm.

Figure 5.38 iPAVE outer wheel path curvature Ipswich-Rosewood Road Section 1 – full bowl versus no rear sensors

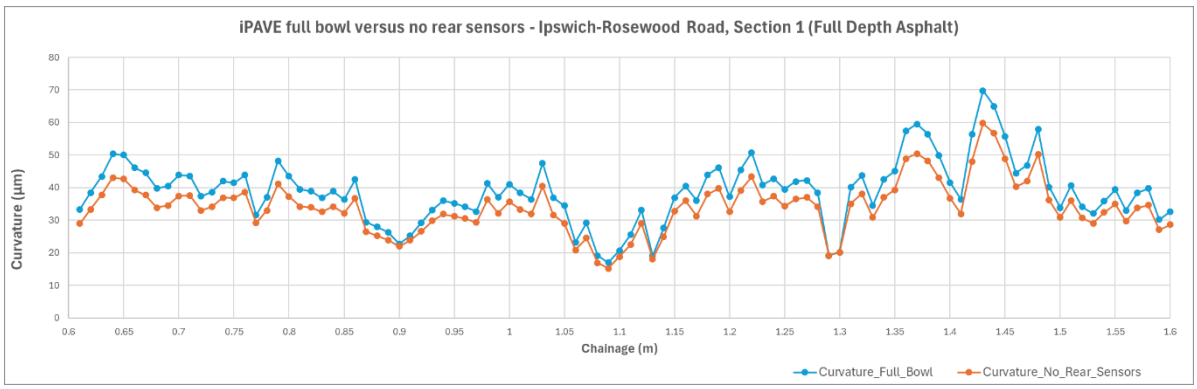

Figure 5.39 iPAVE outer wheel path curvature Ipswich-Rosewood Road Section 3 – full bowl versus no rear sensors

Figure 5.40 iPAVE outer wheel path curvature New England Highway Section 2 – full bowl versus no rear sensors

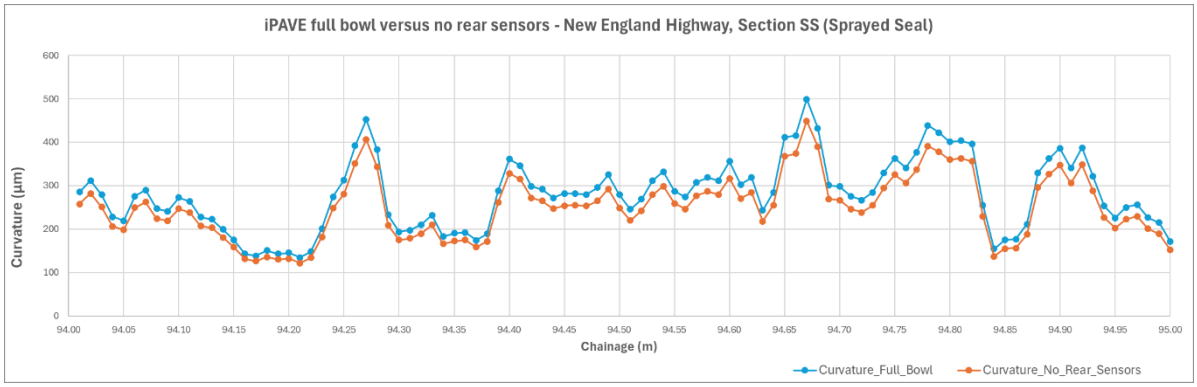

The difference in the curvature values is also highlighted in Table 5.5 where the difference between the 2 outputs increases with the magnitude of the curvature.

Table 5.5: iPAVE curvature statistics – full bowl versus no rear sensors

Location	Statistics	Curvature – full bowl (µm)	Curvature – excluding rear sensors (µm)
Ipswood Road – Section 1	Average	39	34
	Stdev	10	8
Ipswood Road – Section 3	Average	167	144
	Stdev	95	84
New England Highway – Section 2	Average	282	254
	Stdev	82	73

5.5 SCISUB Results

While curvature provides a good estimate of the bearing capacity of the upper layers, pavement engineers may use a parameter called SCISUB, which is the subgrade structural condition index, to provide an indication of the strength of the pavement's subgrade. Knowing the strength of the subgrade is important, as the subgrade rests upon the natural soils or earth that supports the upper layers. When measured with an FWD or iPAVE, SCISUB is defined as the difference in the deflection values measured at the 900 and 1500 mm (D_{900}-D_{1500}) positions in front of the load.

A direct comparison was made between the SCISUB values obtained from the FWD (single survey) and the average of 3 runs from the iPAVE at each of the 3 test sites in the forward direction of travel. The results are shown in Figure 5.41 through Figure 5.46.

Figure 5.41 Outer wheel path SCISUB Ipswich-Rosewood Road Section 1 – FWD v iPAVE3

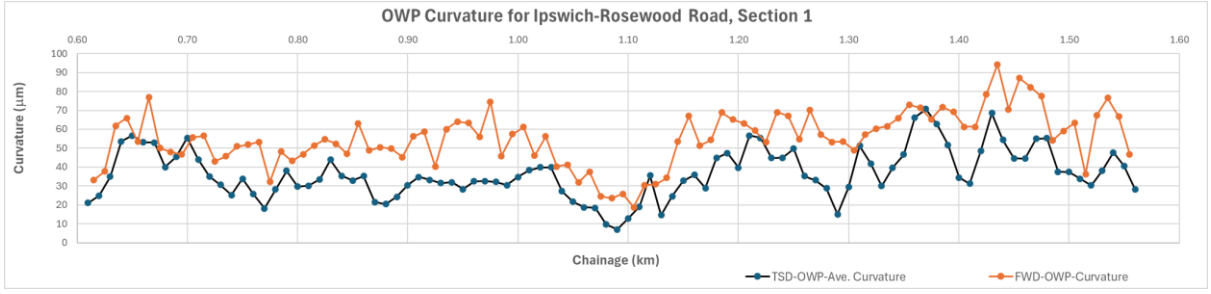

Figure 5.42 Inner wheel path SCISUB Ipswich-Rosewood Road Section 1 – FWD v iPAVE3

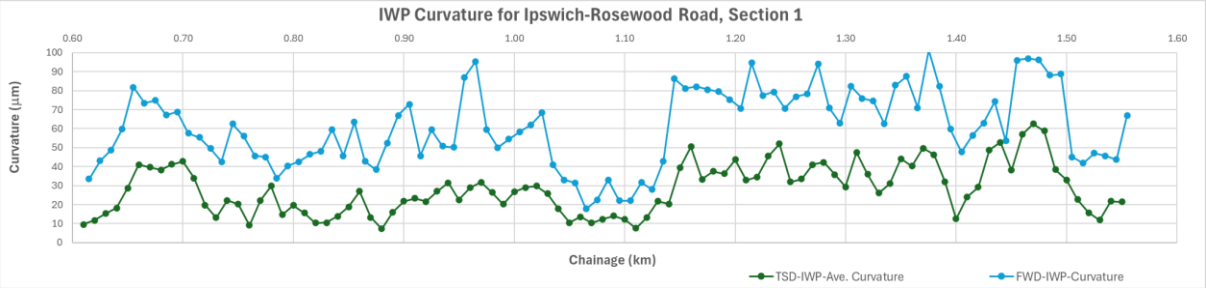

Figure 5.43 Outer wheel path SCISUB Ipswich-Rosewood Road Section 3 – FWD v iPAVE3

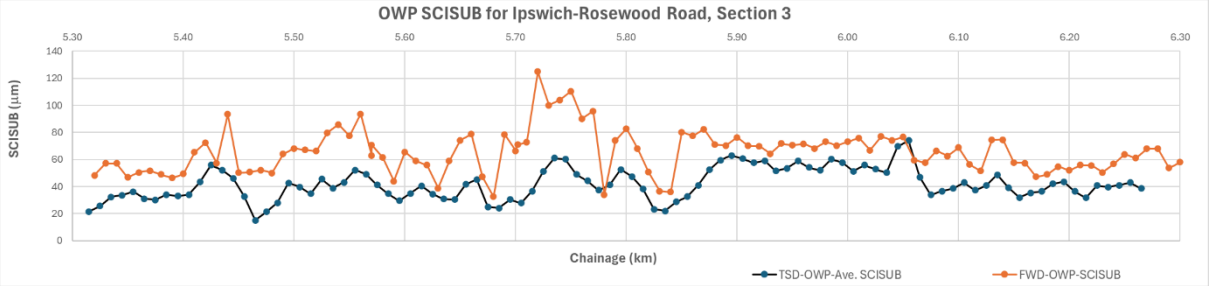

Figure 5.44 Inner wheel path SCISUB Ipswich-Rosewood Road Section 3 – FWD v iPAVE3

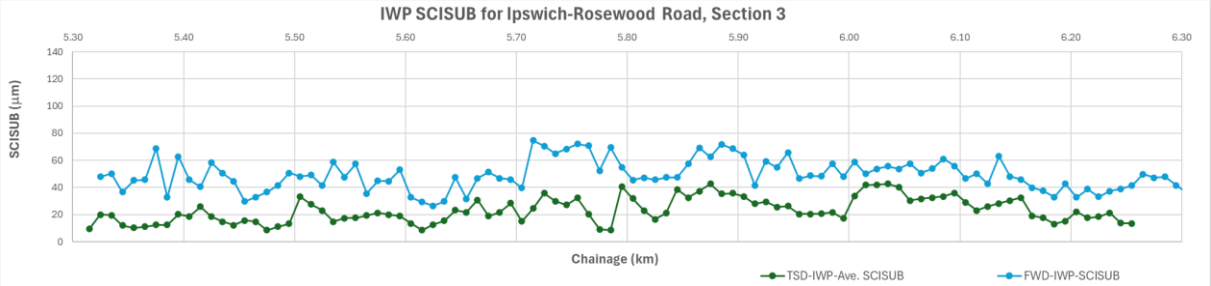

Figure 5.45 Outer wheel path SCISUB New England Highway Section 2– FWD v iPAVE3

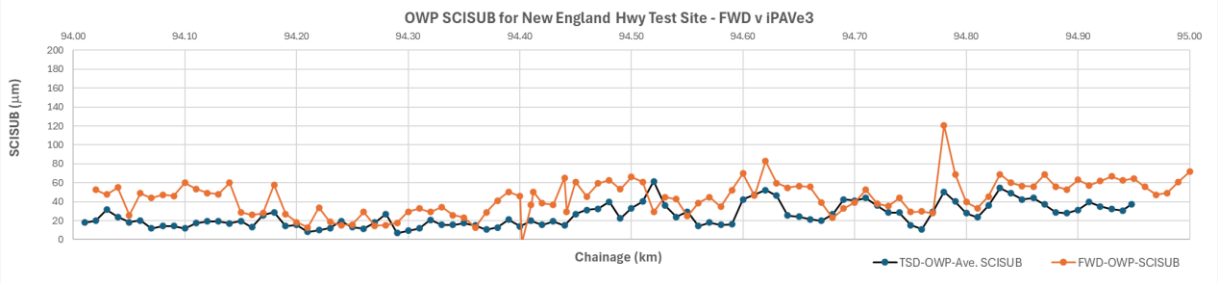

Figure 5.46 Inner wheel path SCISUB New England Highway Section 2 – FWD v iPAVE3

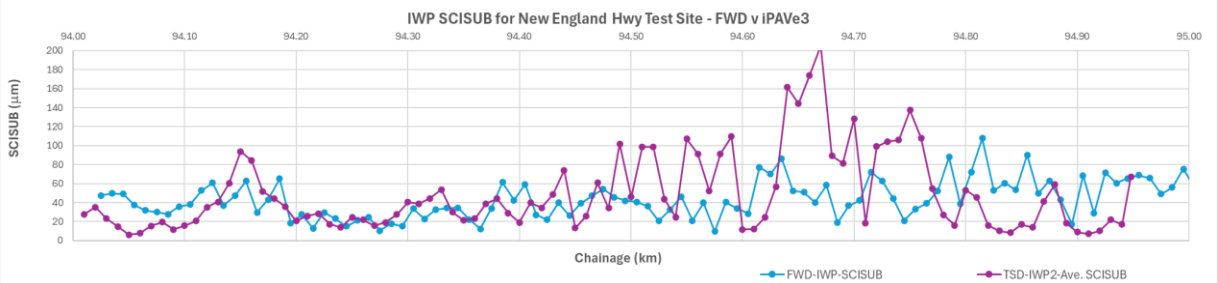

As highlighted in the above figures and in Table 5.6, the SCISUB values measured by the FWD were higher than those from the iPAVE by an average of 24 µm, which is consistent across the test sites, the only exception being the inner wheel path at the New England Highway test site (granular with sprayed seal) where the iPAVE SCISUB readings are higher than the FWD. However, as can

be seen in Figure 5.46, there is a section of pavement from chainage 94.4 to 94.8 km where the iPAVE results are significantly higher than those measured by the FWD which is biasing the average.

Table 5.6: SCISUB results for the 3 test sections

Location	Statistics	iPAVE-Outer-SCISUB (µm)	FWD-Outer-SCISUB (µm)	iPAVE3-Inner-SCISUB (µm)	FWD-Inner-SCISUB (µm)
Ipswood Road – Section 1	Average	37	55	28	61
	Stdev	13	14	13	20
Ipswood Road – Section 3	Average	42	66	23	50
	Stdev	12	16	9	11
New England Highway – Section 2	Average	26	43	49	43
	Stdev	12	18	41	20

Spreadsheets containing all plots presented in this report has been provided in Appendix D.

6 Key Findings and Conclusions

Traffic Speed Deflectometer (TSD) differs from other deflection measuring devices in terms of its mechanism for data collection. Unlike Falling Weight Deflectometer (FWD) which directly measures pavement deflection, the TSD measures surface deflection velocity resulting from a rolling wheel. The velocity data is then converted to deflection data using different methods. Historically, TSD vehicles in Australia were equipped with seven doppler lasers with iPAVE2, however, NTRO's new iPAVE (iPAVE3) is equipped with eleven lasers. The data analysis leads to following key findings:

- iPAVE3 deflection data indicate high level of repeatability for all 3 trial sites.
- A comparison of iPAVE3 maximum deflection (D_0) values on the OWP and IWP show higher deflection on the IWP at on one of the three test sections which is not in line with the prevailing assumption among pavement engineers that the OWP deflections are generally higher and should be used to determine the adequacy for pavement structural strength. FWD data also show the similar trends (higher deflections on IWP). This finding highlights the need of incorporating deflections from both wheel paths (OWP & IWP) for improved pavement assessment. This practice will help avoid inaccurate estimates of pavement remaining life.
- Research findings indicate that the deflection measurements from TSD and FWD do not always show high correlation mainly due to different deflection measurement mechanisms of both devices. It should be noted that the TSD and FWD both can accurately identify pavement strength and condition trends. For a linear correlation between TSD and FWD should be utilised with care as it may only be applicable to the road sections used to develop the relationship. The data analysis as part of this project from 3 trial sites indicate that the TSD maximum deflection (D_0) values are lower than the FWD deflection values. However, TSD and FWD deflection data mostly show similar pavement strength trends.
- For curvature results, all sites showed a good repeatability between the individual iPAVE runs. In general, there was a high correlation between the TSD and FWD curvature values in both wheel paths at all trial sites. However, there were a couple of exceptions (IWP of Sections 1 and 3 where the FWD curvature values were higher than those from the TSD). Moreover, the full depth asphalt pavement (Section 1) showed much lower curvature values.
- There is generally a good agreement between FWD curvature results that were measured in April 2023 and 2024 at all 3 sites. However, the curvature values measured in December 2023 were higher at the 2 sites on Ipswich-Rosewood Road (with asphalt surfacing) possibly due to rainy season in Queensland (November to March) or differences in asphalt temperature. The New England Highway test section (sprayed seal surfaced granular pavement) showed contrasting results (similar curvature values measured in April 2023 and 2024). As expected , curvature values for this section were higher than the Ipswich-Rosewood Road sections.
- NTRO's iPAVE3 has 3 additional lasers behind the rear axle enabling it modelling the full deflection instead of assuming the zero deflection velocity directly under the load. Using the full bowl typically results in larger D_0 values which subsequently results in larger curvature values (as D_{200} is essentially the same). The comparison of curvature values calculated by using values behind the load (iPAVE3) and only forward sensors (iPAVE2) processing algorithm. In all 3 sites, curvature values with full bowl measurements were higher than the curvature values determined by excluding rear sensors. Further analysis of iPAVE3 data of this type is recommended so that a reliable method of adjusting between iPAVE3 and iPAVE2 Do values is derived.

- Based on the project findings, it is suggested that Austroads consider revising design standardisation factors (Table 9.2 of Austroads Guide to Pavement Technology Part 5) by providing separate DSF factors for iPAVE2 and iPAVE3.
- It is also suggested that further research be undertaken by analysing iPAVE3 and iPAVE2 measured responses to provide a reliable relationship to convert iPAVE3 D_0 to Benkelman Beam D_0 across a wide range of sprayed seal surfaced granular pavements.
- Direct comparison between the SCISUB (D_{900}-D_{1500}) obtained by FWD (single survey) and the average of 3 runs from the iPAVE3 at each of the 3 test sites in the forward direction of travel. The results indicate that the SCISUB values measured by FWD were higher by an average of 24 µm across all the test sites. However, there is only exception is the IWP at Section 2 (granular with sprayed seal) where iPAVE3 SCISUB values are higher than the FWD. In addition, the SCISUB values measured using iPAVE3 tended to be higher than iPAVE2 reflecting a more reliable estimate of upper subgrade modulus provided by iPAVE3 due to the inclusion of additional lasers.The TSD is relatively a new technology and use of TSD measured deflection data needs more improvement in its utilisation for pavement structural evaluation and rehabilitation design. Austroads (2021) highlighted future research directions for maximising the use of TSD deflection data in back-calculation of pavement layer and subgrade moduli. In Australasia, methods have been developed to predict equivalent FWD maximum deflections and implemented those in the design of granular overlays using the empirical approach (Austroads 2019b). There is a need to develop a method to estimate pavement and subgrade moduli from TSD deflections to assist in the design of a wider range of treatments.

7 Future Research Direction

To use the Austroads Guide to Pavement Technology Part 5 (Austroads 2019b) method for the design of granular overlays, a method is required to estimate Benkelman Beam D_0 values from iPAVE3 D_0 values. Austroads AGPT05 has an adjustment factor for iPAVE2. As iPAVE3 D_0 values exceed iPAVE2 D_0 values, a critical immediate need is to derive the correlation Do(iPAVE3) = a x Do(IPAVE2). This will enable the derivation of an iPAVE3 to DSF for inclusion in AGPT05.

Following key research areas are suggested to be focused and investigated in the future.

- Continue comparison of FWD vs iPAVE3 on a range of asphalt pavements including (probe in pavement) the asphalt temperature during FWD and iPAVE3 measurements. The field trial sites should be 100 mm or more asphalt thickness so most sites in Western Australia will not be suitable (BC of moduli cannot reliably be obtained for layer thickness less than 100 mm).
- Take asphalt field cores at a large number of sites and measure indirect tensile modulus of these field core to compare to BC asphalt moduli from FWD and iPAVE3 (need also research to develop this BC method).
- Take DCP results of the subgrade and correlate these with BC moduli of top (300 mm) of subgrade from FWD and iPAVE3 moduli.

References

Austroads 2012a, *Review of the traffic speed deflectograph – Final project report*, AP-R395-12, Austroads, Sydney, New South Wales.

Austroads 2012b, *Benefits and Risks of investing in network level deflection data collection*, AP-T217-12, Austroads, Sydney, New South Wales.

Austroads 2013, *State-of-the-art traffic speed deflectometer practice*, AP-T246-13, Austroads, Sydney, New South Wales.

Austroads 2014a, *Traffic speed deflectometer – Data review and lessons learnt*, AP-T279-14, Austroads, Sydney, New South Wales.

Austroads 2014b, *Traffic speed deflectometer – data analysis approaches in Europe and USA compared with ARRB analysis approach*, AP-T280-14, Austroads, Sydney, New South Wales.

Austroads 2015, *A common data output specification for texture, cracking, strength and skid resistance*, AP-T290-15, Austroads, Sydney, New South Wales.

Austroads 2019a, *Guide to pavement technology part-5: Pavement evaluation and treatment design,* AGPT05-19, Austroads, Sydney, New South Wales.

Austroads 2019b, *Improved methods of using pavement deflection data in the design of rehabilitation treatments*, AP-T350-19, Austroads, Sydney, New South Wales.

Austroads 2021, *Strategy for an improved mechanistic-empirical flexible pavement treatment design*, AP-R650-21, Austroads, Sydney, New South Wales.

Baltzer, S 2009, *Three years of high speed deflectograph measurements of the Danish State Road Network*, 8th International Conference on Bearing Capacity of Roads, Railways and Airfields, Illinois, USA.

Brezina, I, Stryk, J & Grosek, J, 2017, *Using traffic speed deflectometer to measure deflections and evaluate bearing capacity of asphalt road pavements at network level*, Material Science and Engineering, vol. 236.

Chai, G, Manoharan, S, Golding, A, Kelly, G & Chowdhury, S, 2016, *Evaluation of the traffic speed deflectometer data using simplified deflection model*, Transportation Research Procedia, vol. 14, pp. 3031-3039.

Elbagalati, O, Mousa, M, Elseifi, M, Gaspard, K & Zhang, Z 2018, *Development of a methodology to backcalculate pavement layer moduli using the traffic speed deflectometer,* Canadian Journal of Civil Engineering, vol. 45, pp. 377-385.

Elseifi, M, Zihan, Z & Icenogle, P 2019, *A mechanistic approach to utilize traffic speed deflectometer (TSD) measurements into backcalculation analysis*, Final Report 612, Louisiana Transportation Research Center, Baton Rouge, Louisiana.

Lee, J 2019, *Ground instrumentation for traffic speed deflectometer (TSD)*, contract report PRP17037-02, ARRB Group, Vermont South, Vic.

Lee, J and Conaghan, A 2016, P40 *Benefits of traffic speed deflectometer data in pavement analysis (TSD and FWD correlation study and investigation to ground truth instrumentation) (year 2 – 2015/2016)*, contract report 010554, ARRB Group, Vermont South, Vic.

Muller, W & Roberts, J, 2013, *Revised approach to assessing traffic speed deflectometer data and field validation of deflection bowl predictions*, International Journal of Pavement Engineering, vol. 14, no. 4, pp. 388-402.

Nasimifar, M, Thyagarajan, S & Sivaneswaran, N 2017, *Backcalculation of flexible pavement layer moduli from traffic speed deflectometer data*, Transportation Research Record: Journal of the Transportation Research Board, No. 2641, pp. 66-74.

New Zealand Transport Agency, 2016, *Traffic speed deflectometer – The application of TSD data in New Zealand for asset management and design.*

Nielsen, C, 2019, *Visco-elastic back-calculation of traffic speed deflectometer measurements*, Transportation Research Record: Journal of the Transportation Research Board, vol. 2673, no. 12, pp. 439-448.

Pedersen, L 2013, *Viscoelastic modelling of road deflections for use with the traffic speed deflectometer*, PhD thesis, Technical University Denmark, Lyngby, Denmark.

Rasmussen, S, Aagaard, L, Baltzer, S & Krarup, J 2008, *A comparison of two years network level measurements with the traffic speed deflectometer*, Transport Research Arena Europe, pp. 8, Ljublijana, Slovenia.

Triplow, C 2017, *An evaluation of the traffic speed deflectometer for Main Roads Western Australia*, contract report PSS16174-1, ARRB Group, Vermont South, Vic.

Virginia Department of Transportation, 2020, *Network level pavement structural testing with the traffic speed deflectometer*, Final Report VTRC 21-R4, Virginia Transportation Research Council, Charlottesville, Virginia, USA.

Virginia Transportation Research Council, 2020, Network level pavement structural testing with the traffic speed deflectometer, Final Report VTRC 21-R4, Virginia Transportation Research Council, VA, USA.

Wix, R, Murnane & Moffatt, M, 2016, *Experience gained investigating, acquiring and operating the first traffic speed deflectometer in Australia*, Transportation Research Procedia, vol. 14, pp. 3060-3069.

Zofka, A, Sudyka, J, Maliszewski, M, Harasim, P & Sybilski, D 2014, *Alternative approach for interpreting traffic speed deflectometer results*, Transportation Research Record, no. 2457, pp. 12-8.

Appendix A Data Collected During First Round

- FWD data
- Geotechnical Logs
- Lab Test Results

To request appendix data please contact info@warrip.com.au.

Appendix B Data Collected During Second Round

- FWD data
- Geotechnical Logs
- Lab Test Results

To request appendix data please contact info@warrip.com.au.

Appendix C Data Collected During Third Round

- TSD data
- FWD data (Spreadsheets)
- Geotechnical Logs
- Deflection Plots (Spreadsheets)

To request appendix data please contact info@warrip.com.au.

Appendix D Spreadsheets

- Deflection Plots (Spreadsheets)

To request appendix data please contact info@warrip.com.au.

WARRIP

WESTERN AUSTRALIAN
ROAD RESEARCH &
INNOVATION PROGRAM

www.warrip.com.au | info@warrip.com.au | Perth, Western Australia